Ubiquitination and proteasomal regulation of Pannexin 1 and Pannexin 3

Anna Blinder

A thesis submitted in partial fulfillment of the requirements for the
Master's degree in Cellular and Molecular Medicine

Department of Cellular and Molecular Medicine
Faculty of Medicine
University of Ottawa

ABSTRACT

Pannexin 1 (PANX1) and Pannexin 3 (PANX3) are single-membrane channel glycoproteins that allow for communication between the cell and its environment to regulate cellular differentiation, proliferation, and apoptosis. Their expression is regulated through post-translational modifications, however, their regulation by ubiquitination and the ubiquitin proteasome pathway (UPP) has not been examined. Here, I show that PANX1 is monoubiquitinated and K48- and K63-polyubiquitinated, and PANX3 is polyubiquitinated. While treatment with MG132 altered the banding profile and subcellular distribution of both pannexins, data suggested that only PANX3 is degraded by the UPP. To study the purpose of PANX1 ubiquitination, a PANX1 mutant bearing nine lysine mutations was engineered. Results revealed increased cell surface expression of the mutant, suggesting that ubiquitination may regulate trafficking. I thus demonstrated for the first time that PANX1 and PANX3 are polyubiquitinated and differentially regulated by ubiquitin and by the proteasome, indicating distinct mechanisms that stringently regulate pannexin expression.

TABLE OF CONTENTS

LIST OF TABLES

LIST OF FIGURES

LIST OF ABBREVIATIONS

AMSH – Associated molecule with the SH3 domain of STAM

Ankrd13 – Ankyrin repeat domain-containing protein 13

AP2 – Clathrin adaptor protein 2

ATF6 – Activating transcription factor 6

ATG5 – Autophagy-related protein 5

ATG8 – Autophagy-related protein 8

ATG12 – Autophagy-related protein 12

ATL3 – Atlasin 3

ATP – Adenosine triphosphate

BAG1 – BCL2-associated athanogene 1

BAG3 – BCL2-associated athanogene 3

BCA – Bicinchoninic acid assay

BiP – Binding immunoglobulin protein

BNIP3 – BCL2/adenovirus E1B 19 kDa protein-interacting protein 3

BRCC36 – BRCA1/BRCA2-containing complex subunit 36

BSA – Bovine serum albumin

CCPG1 – Cell cycle progression protein 1

CHX – Cycloheximide

CME – Clathrin-mediated endocytosis

CNX – Calnexin

Co-IP – Co-immunoprecipitation

CRT – Calreticulin

CTF – C-terminal fragment

Cx43 – Connexin43

DDI1 – DNA damage-inducible protein 1

DMEM – Dulbecco Modified Eagle's medium

DMSO – Dimethyl sulfoxide

DNA – Deoxyribonucleic acid

DUB – Deubiquitinating enzyme

E1 – Ubiquitin-activating enzyme

E2 – Ubiquitin-conjugating enzyme

E3 – Ubiquitin ligase

EDEM1 – ER degradation enhancing mannosidase 1

EGF – Epidermal growth factor

eGFP – Enhanced green fluorescent protein

EGFR – Epidermal growth factor receptor

ER – Endoplasmic reticulum

ERAD – Endoplasmic reticulum-associated degradation

ERdj5 – Endoplasmic reticulum DNA J domain-containing protein 5

ERLAD – Endoplasmic reticulum-to-lysosome-associated degradation

ESCRT – Endosomal sorting complex required for transport

EV – Empty vector

FBS – Fetal bovine serum

FBXO4 – F-box only protein 4

FUNDC1 – FUN14 domain containing 1 protein

GABARAP – Gamma-aminobutyric acid receptor-associated protein

GAPDH – Glyceraldehyde 3-phosphate dehydrogenase

GFP – Green fluorescent protein

GIM – GABARAP-interacting motif

Gly0 – Pannexin un-glycosylated core

Gly1 – Pannexin high mannose species

Gly2 – Pannexin complex glycosylated species

H2A – Histone 2A

H2B – Histone 2B

HA – Human influenza hemagglutinin

HECT – Homologous to E6-AP carboxyl terminus

HEK – Human embryonic kidney

HERC – Homologous to the E6AP carboxyl terminus (HECT) and regulator of chromosome condensation 1 (RCC1)-like domain-containing proteins

HERP – Homocysteine-responsive ER-resident ubiquitin-like domain member protein 1

HRP – Horseradish peroxidase

Hrs – Hepatocyte growth factor-regulated tyrosine kinase substrate

HSC70 – Heat shock cognate 71 kDa protein

Hsp40 – Heat shock protein 40

Hsp70 – Heat shock protein 70

ILV – Intraluminal vesicle

IP – Immunoprecipitation

IRE1 – Inositol-requiring enzyme 1

ISG15 – Interferon-stimulated gene 15

JAMM – JAB1/MPN/Mov34

K6 – Lysine-6

K11 – Lysine-11

K27 – Lysine-27

K29 – Lysine-29

K33 – Lysine-33

K48 – Lysine-48

K63 – Lysine-63

kDa – Kilodaltons

LC3 – Microtubule-associated protein 1A/1B-light chain 3

LIR – LC3-interacting motif

LMW – Lower molecular weight

MARCH – Membrane-associated RING-CH finger

MARCH6 – Membrane-associated RING-CH finger protein 6

Met/cys – Methionine/cysteine

mg – Milligrams

MINDY – Motif interacting with ubiquitin-containing novel DUB family

MJD – Machado-Joseph disease

mM – Millimoles

MVB – Multivesicular body

MW – Molecular weight

MYSM1 – Myb Like, SWIRM and MPN domains 1

NDP52 – Nuclear dot protein 52 kDa

NEDD4 – Neural precursor cell expressed developmentally down-regulated protein 4

NEDD4-2 – Neural precursor cell expressed developmentally down-regulated protein 4-2

NEDD8 – Neural precursor cell expressed developmentally down-regulated 8

NEM – N-ethylmaleimide

NGF – Neuronal growth factor

OS-9 – Osteosarcoma-9

OTU – Ovarian tumor

PANX/Panx – Pannexin

PANX1/Panx1 – Pannexin 1

PANX2/Panx2 – Pannexin 2

PANX3/Panx3 – Pannexin 3

PBS – Phosphate-buffered saline

PDCD6IP – Programmed cell death 6-interacting protein

PDI – Protein disulfide isomerase

PE – Phosphatidylethanolamine

PERK – PRKR-like endoplasmic reticulum kinase

PINK1 – PTEN-induced kinase 1

PIP – Phosphatidylinositol phospholipid

PLEKHM1 – Pleckstrin homology domain-containing family M member 1

PSMD14 – 26S proteasome non-ATPase regulatory subunit 14

PTM – Post-translational modification

pUb – Polyubiquitin

PVDF – Polyvinylidene fluoride

RBR – RING-in between RING-RING

RETREG1 – Reticulophagy regulator 1

RIG-I – Retinoic-acid inducible gene I

RING – Really interesting new gene

RLD – RCC1-like domain

RNF5 – Ring finger protein 5

RNF139 – Ring finger protein 139

RNF170 – Ring finger protein 170

RNF185 – Ring finger protein 185

RPMI – Roswell Park Memorial Institute

RTN3 – Reticulon 3

SDS – Sodium dodecyl sulfate

SDS-PAGE – Sodium dodecyl sulfate-polyacrylamide gel electrophoresis

Sho – Shadoo

SMURF2 – SMAD-specific E3 ubiquitin protein ligase 2

SQSTM1 – Sequestosome 1 (also known as p62)

STAM1 – Signal-transducing adaptor molecule 1

SUMO – Small ubiquitin-like modifier

TOLLIP – Toll-interacting protein

TPA – 12-O-tetradecanoylphorbol 13-acetate

TRAF4 – TNF receptor-associated factor 4

TRAF6 – TNF receptor-associated factor 6

TRF1 – Telomeric repeat-binding factor 1

TRFH – Telomeric repeat factors homolog

TRIM – Tripartite motif

TRIM13 – Tripartite motif-containing protein 13

TrkA – Tropomyosin-related kinase A

TRPV5 – Transient receptor potential cation channel subfamily V member 5

TSG101 – Tumor susceptibility gene 101

ub – Ubiquitin

UBA – Ubiquitin-associated domain

UBAP1 – Ubiquitin-associated protein 1

UBD – Ubiquitin-binding domain

UbL – Ubiquitin-like protein

UBQLN2 – Ubiquilin 2

UCH – Ubiquitin carboxyl-terminal hydrolase

UCHL5 – Ubiquitin carboxyl-terminal hydrolase isozyme L5

Ufd1 – Ubiquitin recognition factor in ER-associated degradation protein 1

Ufd2 – Ubiquitin recognition factor in ER-associated degradation protein 2

UIM – Ubiquitin-interacting motif

UPP – Ubiquitin proteasome pathway

USP – Ubiquitin-specific protease

USP3 – Ubiquitin-specific protease 3

USP8 – Ubiquitin-specific protease 8

USP14 – Ubiquitin-specific protease 14

USP19 – Ubiquitin-specific protease 19

USP30 – Ubiquitin-specific protease 30

USP36 – Ubiquitin-specific protease 36

VCP – Valosin-containing protein (also known as p97)

WT – Wild type

WWP1 – WW domain-containing E3 ubiquitin protein ligase 1

ZUP1 – Zinc finger-containing ubiquitin peptidase 1

µg – Micrograms

µL – Microlitres

µm – Micrometers

µM – Micromoles

ACKNOWLEDGEMENTS

This thesis was accomplished through the support and encouragement of many individuals. First and foremost, I would like to give the sincerest of thanks to my supervisor, Dr. Kyle Cowan, as well as Dr. Stephanie Langlois, for the opportunity to work in their laboratory and share in their enthusiasm for research and for pannexins. It is through their mentorship, patience, and support, that I learned a broad range of techniques and was able to grow as a scientist. I would further like to thank my thesis advisors, Dr. Douglas Gray, Dr. Laura Trinkle-Mulcahy, and Dr. David Park, for their continued guidance and constructive feedback during this process.

A huge thanks to Dr. Bruno Fonseca, a scientist whose skills for western blotting I can only aspire to achieve one day, who took the time to train me to use the radioactive facility and imparted his western blotting wisdom upon me. Another huge thanks to Martine St. Jean, who helped me to find appropriate controls for my experiments, and supplied the plasmids, cells, and reagents to do so.

I couldn't have done this without all of my fellow colleagues and peers in the CHEO Research Institute, who helped me to brainstorm and troubleshoot, provided perspective, and showed me how enjoyable exercise can be – motivating me to run my first 5k. Going through the struggles of research and relishing in the small successes alongside them made all the difference.

Finally, I would like to give the biggest of thanks to my sister, Genya, who was my biggest supporter during my masters and helped keep me accountable. I never forget how fortunate I am to have a sister like her.

1.0 INTRODUCTION

1.1 An overview of pannexins

Pannexins are single-membrane channel glycoproteins which allow for the communication between the cell and the extracellular environment [1]. They act as conduits to release ATP from the cytosol to the extracellular environment, act as calcium channels between the endoplasmic reticulum (ER) and the cytoplasm [2], and are permeable to other small molecules and anions [3]. They were initially discovered through sequence homology to the invertebrate gap junctions, innexins [4], and were shown to share a similar topology to the vertebrate gap junctions, connexins [1]. Despite the initial assumption that pannexins form hemichannels destined to become gap junctions based on their similarity to connexins, research strongly suggests that pannexins only readily form single membrane channels [5]. This is likely due to the steric hindrance imposed by their extracellular N-glycan chains which obstructs docking of appositional pannexon channels [5]. There are three members in the mammalian pannexin family: PANX1, PANX2, and PANX3 (known as Panx1, Panx2, and Panx3 in rodents) [1]. While all pannexins are composed of four transmembrane domains, two extracellular loops, one intracellular loop, and amino and carboxyl terminals both located on the cytoplasmic face of the membrane, Panx1 and Panx3 are more similar to one another than to Panx2, which contains a larger carboxyl terminal domain [1]. Similarly, Panx1 and Panx3 channels are predicted to oligomerize into hexamers, whereas Panx2 is assembled into heptamers or octamers [1].

All three pannexins have been identified in numerous vertebrates, including rats, dogs, cows, zebrafish, and humans [6]. Their expression levels between tissues are highly regulated, with *Panx1* transcripts being more ubiquitously expressed, *Panx3* transcripts restricted to the skin, cartilage, bone, and skeletal muscle, and *Panx2* expression limited to the brain [7,8]. Functionally, pannexins are implicated in a wide array of cellular processes including cellular differentiation, proliferation, and apoptosis, and their dysregulation has been associated with numerous pathologies [8,9]. Studies have shown that Panx1 plays a role in the differentiation of myoblasts and keratinocytes, and Panx3 is involved in both the regulation of

differentiation and proliferation of myoblasts, chondrocytes, osteoprogenitor cells, and keratinocytes [10–14]. Panx2 has been shown to modulate the commitment of neural progenitor cells to the neuronal lineage [15,16].

In mature cells not capitalizing on Panx1 for proliferative or apoptotic purposes, pannexins are exploited for other physiological ends. In neuronal subpopulations, Panx1 is thought to contribute to synaptic plasticity through its activity at the synaptic cleft [2]. Panx1's involvement in purinergic receptor signaling also helps to foster long range calcium wave propagation in the brain and thus mediates communication between neighboring neural cells [1]. On a larger scale, blocking cerebral Panx1 channels confers a neuroprotective effect following a stroke, as channel activity under anoxic conditions promotes cell death [17], underscoring the importance of channel activity in maintaining an organ's functional integrity, or, in enhancing dysregulation. Panx1 plays an appreciable role in immune and inflammatory signaling, with this activity also being intimately linked with the activity of P_2X_7 purinergic receptors [18]. Panx1 activity directly recruits macrophages to apoptotic cells, and its activity stimulates downstream inflammasome activation and inflammatory cytokine release [19], a function also attributed to astrocytes in the brain [17]. More recently, a role for PANX3 in inflammatory signaling was also established, where it may act in a defensive capacity against inflammation in human dental pulp cells [20]. Interest in pannexin activity in muscles is gaining momentum, where not only are Panx1 and Panx3 modulated during both initial muscle development and muscle regeneration following trauma [21], but Panx1 is involved in regulating internal calcium transients following membrane depolarization [22] and mediates muscle potentiation [23]. Panx1 activity is not limited to just striated muscle, it is also detected in the smooth muscles (and endothelial cells) of small arteries and contributes to the maintenance of vascular tone [19]. This process can be dysregulated, where continuous sympathetic arousal promotes the development of hypertension through its stimulation of PANX1 channel activity [24]. Thus, it is evident that pannexins have pronounced roles in maintaining cellular and organismal integrity, and their activity can be capitalized on for either protective or for maladaptive purposes.

1.1.1 Pannexin post-translational modifications and life cycle

Post-translational modifications (PTMs) are important regulators pannexin expression and function [7]. Pannexins begin their life cycle in the ER, where they are proposed to be co-translationally inserted into

the ER membrane and are subject to their most notorious modification: glycosylation [8]. Both human and rodent Panx1 and Panx3 have three species with distinct patterns of glycosylation: the un-glycosylated Panx core (Gly0), the high mannose species (Gly1) which is often found in the endoplasmic reticulum, and the complex glycosylated species (Gly2) which has been associated with expression on the cell surface [7,9]. From the ER, Panx1 and Panx3 traffic to the Golgi apparatus by CopII vesicles [25], for maturation into the Gly2 species, en route to the plasma membrane [2]. While glycosylation null Panx1 and Panx3 mutants are capable of forming functional channels at the cell surface [26], they do display increased intracellular expression compared to their native counterparts [27].

The glycosylation status of pannexins is closely related to their cellular function, as their ability to form channels and traffic to the plasma membrane is essential for channel activity [7]. In addition, recent studies uncovered a leucine-rich repeat motif between residues S328-K348 of the Panx1 C-terminus vital for trafficking to the cell surface, where deletion of this motif drastically impaired both maturation to the Gly2 species and expression at the plasma membrane [28]. The importance of the C-terminus in Panx1 trafficking becomes more evident when considering it mediates binding to actin [25] and actin-related protein 3 [29], and that Panx1 and Panx3 trafficking is contingent on microfilament polymerization [25]. Interestingly, pannexins are also capable of intermixing to form heteromeric channels, with combinations of Panx1/2, and Panx1/3, being detected [26]. Heteromeric oligomerization, however, impedes channel activity, as Panx1/2 intermixing reduces the currents generated by the channels [30] and, in fact, decreases channel stability [31]. Moving forward, only PANX1 and PANX3 will be discussed as they are the focus of this thesis.

In addition to glycosylation, pannexins incur other PTMs. Rat and human Pannexin 1 are phosphorylated by Src kinases on tyrosines 308 [32] and 198 [24], respectively, and high throughput screens identified numerous other human phosphorylation sites [33]. Phosphorylation at Y198 was specifically detected on cell surface PANX1 and is correlated to its role in ATP release [24]. Panx1 is the subject of S-nitrosylation, which regulates its channel activity [34], and human PANX1 is further acetylated [33] and is a known target of Caspase-3/7 cleavage, which is important for its channel activation during apoptosis [35]. PANX1 caspase cleavage is predicted to occur at residues 164-167 of the intracellular loop, and residues

376–379 in the C-terminus, ultimately fragmenting PANX1 into three pieces of approximately 19 kDa (N-terminal fragment), 24 kDa (central fragment), and 6 kDa (C-terminal fragment), when both sites have been cleaved [35]. Additionally, PANX1 has been shown to be ubiquitinated on lysine residues 201, 307, 343, 355, 381, and 409 [33]. The functional relevance of acetylation and ubiquitination on PANX1 regulation is lacking, though these PTMs could affect channel gating, channel permeability, protein localization, and protein degradation [36]. Panx3 has only additionally been shown to be S-nitrosylated in HEK293T cells [37], and phosphorylated (in human samples) as per high throughput screens [33], although their effects on Pannexin 3 regulation have not yet been examined.

While the function of Panx1 and Panx3 as channels is unequivocal, their activity is not necessarily limited to the plasma membrane. As mentioned prior, these proteins can also to function as calcium leak channels within the ER [2,38]. Our lab also demonstrated for the first time that PANX1 may mediate its effects independently of its canonical channel function, as evidenced by its anti-tumorigenic properties in rhabdomyosarcoma cell lines, an effect which is not reversed by treatment with PANX1 channel blockers [39]. With this in mind, it is not surprising that pannexins have been detected in a wide variety of cellular compartments, including the cell surface, the ER, the Golgi, and the cytoplasm, with distinct labelling patterns among different cell types [40].

Few studies have investigated pannexin degradation, and those that have specifically focused on the cell surface population [41]. The mechanism of Panx1 internalization remains unclear as cells do not enlist the canonical endocytic pathways involving clathrin, caveolin, and dynamin [2], although some suspect that actin microfilaments may be involved [9]. Research suggests that cell surface Panx1 is relatively stable and may remain there for days a time [2], and once internalized, Panx1 is shunted to endolysosomes for degradation [41]. However, others suspect that pannexins may also be degraded via the UPP [42]. While the full length Panx1 protein has only been confirmed to be degraded by the lysosomal pathway, a Panx1 mutant with a truncated C-terminus is indeed degraded by the proteasome [43].

1.2 Ubiquitination

Ubiquitination is a dynamic PTM involved in numerous cellular processes [44], and is being likened to phosphorylation in its complexity and versatility [45]. Ubiquitination occurs through the concerted action of three groups of enzymes which covalently conjugate ubiquitin (ub), a 76 amino acid polypeptide, to a target protein [46]. The process begins with the activation of ub by an E1 ub-activating enzyme, which hydrolyzes ATP and uses the energy to generate a thioester bond between the C-terminus of ub and a cysteine residue of the E1 enzyme [47,48]. Ub is then transferred to a cysteine residue in the active site of an E2 ub-conjugating enzyme [48]. The E2~Ub conjugate is recognized by E3 ubiquitin ligases, which mediate the transfer of ub to the target protein via an isopeptide bond between ubiquitin and the ε-amino group of a lysine residue [48], or, less frequently, to a cysteine, serine, threonine, or N-terminal methionine [49].

The 3 groups of catalysts exist in a hierarchy in mammalian cells, with two E1's identified [47], ~40 E2s [48], and over 600 E3s [47] which confer substrate specificity [50], although recent advances have found that E2s also contribute to substrate specificity [48]. The E3s are grouped into 3 families – RING, HECT, or RBR- according to shared domains and mechanism of ub transfer [50]. The RING E3s possess a zinc-binding RING (Really Interesting New Gene) domain or a U-box domain and mediate the direct transfer of ub from the E2 to the substrate, and includes the Cullin-RING ligases, the anaphase promoting complex/ cyclosome [50], and the tripartite motif (TRIM)-containing family of proteins [51]. The HECT (Homologous to E6-AP Carboxyl Terminus) family, which includes the NEDD4 (neural precursor cell expressed developmentally down-regulated protein 4) and the HERC (homologous to the E6AP carboxyl terminus (HECT) and regulator of chromosome condensation 1 (RCC1)-like domain-containing) family of ligases, catalyzes the transfer of ub first to an internal catalytic cysteine residue, and then transfers it to a substrate [50]. Finally, the RBR (RING-IBR-RING) ligases contain a RING1 domain, an in-between RING (IBR) zinc-binding domain, and a RING2 domain, and also form a Ub~E3 intermediate using a conserved cysteine residue in the RING2 domain prior to transferring it to the substrate [50,52]. While many E3s possess the ability to recognize both the E2~Ub conjugate and the target substrate singlehandedly, some E3s, notably the Cullin-RING ligases, work in conjunction with adaptors and substrate receptors to bring the two into proximity [50].

Following ub conjugation to the substrate, ub will either remain as a single moiety or will be extended to form a polyubiquitin (pUb) chain through any of ubiquitin's seven internal lysine residues (K6, K11, K27, K29, K33, K48, K63) or its N-terminal methionine [53]. The growing chain is described as homotypic or heterotypic, according to whether the branches consist of a single linkage type or a mixed composition of linkages, respectively [54]. The degree to which the E3 ligase contributes to governing the ub chain topology, from conjugating a single ub molecule to catalyzing chain elongation, depends on the family that the E3 pertains to [52]. HECT E3s are generally responsible for establishing the chain initiation, elongation, and ub chain specificity [52]. Similarly, the RBR ligases also confer chain linkage specificity [52]. For RING E3s, the propensity for chain elongation and the specificity of linkage type is largely dictated by their cognate E2s and therefore utilize different E2s accordingly [52]. For example, the E2 UBE2G2 catalyzes K48 ub chain polymerization, whereas the E2 UBE2N/UBEV1 dimer shows preference for K63 pUb chain formation [47].

1.2.1 Substrate recognition for ubiquitination

Target proteins may be recognized by their respective E3 ligases by short linear sequences in the substrate, called degrons [52]. PTMs on the substrate may enhance or obstruct this interaction, ensuring substrate ubiquitination only occurs in the correct context [52,55]. For instance, phosphorylation of a degron (ie a phoshodegron) is recognized by Cbl and F-box E3 ubiquitin ligases to target proteins for degradation [52]. E3 ligases containing multiple degron-binding domains or that are capable of dimerization may use those capacities to enhance ubiquitination efficiency of substrates with weak degrons, or target ubiquitination to specific lysine residues [52]. In addition to recognizing primary sequences and their PTMs, E3 can also recognize more general structures, like hydrophobic patches exposed on misfolded proteins, high mannose oligosaccharides on glycosylated proteins, or specific amino acids flanking the N-terminus of polypeptides [52] in a process termed the N-end rule pathway [52,56].

The N-end rule pathway is distinguished by its ability to recognize substrates expressing N-terminal degradation signals by E3s known as "N-recognins," and target them for proteolytic degradation [56]. N-recognins all share a UBR box, which binds to destabilizing N-terminal basic residues (arginine, lysine and histidine) or large, hydrophobic residues (leucine, isoleucine, tryptophan, tyrosine, and phenylalanine)

which are produced by removal of the N-terminal methionine or by endoproteolytic cleavage [56]. UBR box-containing ligases have therefore been proposed to mediate the clearance of C-terminal fragments of cleaved proteins [52]. The N-recognin family consists of 7 enzymes, UBR1 through UBR7, and all but UBR4 possess either a RING, HECT, or F-box domain [56]. UBR4 is still considered an E3 ligase, despite the lack of conclusive evidence supporting ubiquitylating activity, as additional data indicates it possesses a RING finger-like structure which may carry out substrate ubiquitination through the auxiliary action of other E3 ligases [57]. UBR4 has been shown to mediate ub-dependent proteasomal degradation of PINK1 (PTEN-induced kinase 1), the calcium channel TRPV5 (transient receptor potential cation channel subfamily V member 5), the metabolic enzyme ATP citrate lyase , and podocin [57] possibly through the assembly of K11/K48 heterotypic ub linkages [58].

Larger protein domain interfaces or higher order protein assemblies may also act as recognition modules for identification by E3 ligases [52]. This type of recognition more directly links a protein's functional state with its ubiquitination status as substantiated by cases like the telomere repeat binding factor, TRF1. When actively bound to telomeres, the TRFH domain of TRF1 is inaccessible for recognition by the E3 ligase FBXO4 (F-box only protein 4) as it overlaps with the domain which mediates TRF1's interaction with telomeric complexes, and therefore only unengaged TRFH is subject to ubiquitination [52]. Similarly, the Ring1b-Bmi E3 heterodimer only recognizes H2A when the histone is integrated into a higher order nucleosome core, as the ligase interfaces with four histones simultaneously to orient itself to monoubiquitinate K119 of H2A [52]. In summary, E3 ligases mediate substrate specificity through recognition of short linear polypeptide sequences, PTMs, or protein domain interfaces, with variable efficiency, using one or more degron binding domains [52].

1.2.2 Ubiquitin chain diversity

The diversity in ub chains created by adjusting chain linkage, length, and overall topology, allows ub to accomplish various roles according to the "ubiquitin code" [53]. Substrate ub chains are "decoded" by proteins containing ubiquitin-binding domains (UBDs) to mediate the execution of the role associated with the ub chain [59]. Over 20 UBDs exist [59], including ubiquitin-interacting motifs (UIMs) and ubiquitin-

associated domains (UBAs) [60]. According to the subset of UBDs present in a protein, the protein will have preferential binding to ub chains of specific linkages and lengths [53]. This provides additional layers of regulation as a protein is not regulated solely by the mere presence of a ub chain, but also by its necessary interaction with a particular ub-binding protein, which is contingent on spatial and temporal overlap between the two proteins [53,61].

While K48 is the most abundant linkage type found in cells [62] and is considered the "canonical" signal for proteasomal degradation, more ub chains have since emerged which can also serve as proteasomal signals, albeit with varying efficiencies [53], including K11 and K63 linkages [63]. K11 is further implicated in ER-associated degradation (ERAD), a subdivision of proteasomal degradation [64]. Recently, several substrates were discovered for which monoubiquitination and multi-monoubiquitination can adequately bind to 26S proteasomes to serve as a degradation signal, although this appears to only be effective for substrates smaller than 150 amino acids [63]. Monoubiquitination, multi-monoubiquitination, and K63 polyubiquitination have repetitively been shown to mediate endocytosis, act as sorting signals in multivesicular bodies (MVBs) for ensuing lysosomal degradation, modulate protein-protein interactions, and regulate DNA repair and replication [63–65]. Monoubiquitination has a salient role in managing gene transcription by modulating chromatin scaffolding and gene accessibility through the modification of nucleosome histone tails [52,64], as well as regulating cytoskeletal structure [63]. Other linkages (K6, K11, K27, K33) are also implicated in proteasomal degradation, ERAD, protein trafficking, protein interactions, mitochondrial quality control, and the DNA damage response [53,64].

1.2.3 Deubiquitinating enzymes

E3 ligases often work in concert with deubiquitinating enzymes (DUBs) to edit or remove ub chains, as needed [64]. However, while hundreds of E3 ligases execute the ubiquitination of substrates, only ~90 DUBs exist in opposition. DUBs are primarily cysteine proteases, with a few comprising metalloproteases, and are categorized into 5 groups according to catalytic domain similarity: the ubiquitin C-terminal hydrolases (UCH), the ubiquitin-specific proteases (USP), the ovarian tumor (OTU) group, the Machado-Joseph disease (MJD) family, and the JAB1/MPN/Mov34 (JAMM) family [49]. DUBs serve several purposes:

on the one hand, deubiquitination of substrates is used to liberate ub prior to protein degradation to replenish the cytosolic free ub pool [49]. On the other hand, DUBs are vital to remodeling ub chains to direct substrates to their appropriate fates and moderate their activity, and may act directly in complex with E3 ligases to modulate ubiquitination *of* or ubiquitination *by* the E3 ligase [49]. According to their overarching function, DUBs confer specificity for either the linkage type or to the substrate itself, and may function exclusively in association with the 26S proteasome, or execute their functions independently [61]. Most ub-specific proteases confer substrate specificity via either target protein interaction domains or adaptor proteins, but lack specificity for chain linkage type [61]. Many DUBs are associated with specific cellular pathways [49]. Three DUBs, the 26S proteasome non-ATPase regulatory subunit 14 (PSMD14), UCHL5, and USP14, are associated with the 26S proteasome [61]. Two DUBs, AMSH (associated molecule with the SH3 domain of STAM) and USP8, associate with the endosomal sorting complexes required for transport (ESCRT) complexes within the endolysosomal sorting pathway [49]. USP30 antagonizes Parkin during mitochondrial dysregulation, USP19 targets ERAD-destined substrates when anchored to the ER membrane, and MYSM1 (Myb Like, SWIRM And MPN Domains 1) and BRCC36 (BRCA1/BRCA2-containing complex subunit 36) are activated in the nucleus to counterbalance H2A and H2B ubiquitination and the corresponding changes in gene transcription and translation [49]. Studies of most GFP-tagged DUBs has revealed that a large portion of DUBs are targeted to specific subcellular compartments, most prominently the nucleus, the ER, endosomes, and mitochondria, likely contributing to the spatial specificity of substrate ubiquitination [47]. Other DUBs dabble in numerous pathways with more widespread roles. USP3, for one, functions in innate immunity by deubiquitinating K63-pUb of retinoic-acid inducible gene I (RIG-1)-like receptors [66], but also functions in cell cycle progression by promoting S-phase progression through remodeling histone ubiquitination [67], and recently has been implicated in modulating p53 stability and hereby cellular dysregulation [68].

As illustrated above, the regulation of protein ubiquitination is orchestrated by an extensive network of enzymes and adaptor proteins continuously surveying their substrate's ubiquitination status and revising the ub chains as needed. The spatiotemporal regulation of substrate ubiquitination and the sophisticated

machinery used to decode the ub signal allows ub to serve numerous roles, and is exploited in most cellular processes, ranging from genomic stability, to signal transduction and cell cycle progression, to innate immunity, highlighting its crucial role in maintaining cellular homeostasis [65].

1.2.4 Ubiquitin-like modifiers and signalling

Following the discovery of the ub signaling pathway, other proteins bearing structural similarity to ub were identified. These peptides are referred to as ubiquitin-like proteins (UbLs) and include the small ubiquitin-like modifier (SUMO), neural precursor cell expressed, developmentally down regulated 8 (NEDD8), Atg8, Atg12, interferon-stimulated gene 15 (ISG15), and FAT10 [69–71]. Comparable to ub, UbLs are covalently conjugated to their target proteins using an E1-E2-E3 ATP-dependent cascade to achieve diverse functions, from regulating catalytic activity and protein-binding, to modulating protein stability and trafficking [70]**.** Atg8 and Atg12 are pivotal players in the process of autophagy and only modify Atg5 and phosphatidylethanolamine (PE), respectively, whereas the other UbLs modify multiple protein targets [70]. The best characterized UbL is SUMO, which is also conjugated via a lysine residue and can be elongated to form a polySUMO chain [70]. SUMO primarily exerts its effects through inducing conformational changes, modulating protein-protein interactions, and recruiting proteins containing SUMO-interacting motifs [72]. While the ub and UbL systems use distinct machinery for conjugation, the crosstalk between both systems is quite apparent. For one, numerous components of the ub-conjugating cascade are modified and regulated by ISG15 and NEDD8 [70,73]. Additionally, the UbLs ISG15 and SUMO can directly compete against ub for substrate lysine modification and may consequently influence protein stability, UbLs NEDD8 and FAT10 can promote ub-independent proteasomal degradation of their substrates, and substrate modification by NEDD8 or SUMO can promote subsequent protein ubiquitination [70,72,73]. Most intriguingly, a feature of UbLs is their ability to modify ub itself, such as by SUMOylation [72] or ISGylation [73], thus contributing to the complexity of the ub code and altering the functional implications of a substrate's ubiquitination [74].

1.3 Degradation pathways

Protein expression and activity is stringently regulated in order to maintain cellular homeostasis [75,76], largely through the targeting of a substrate for degradation [77]. Broadly speaking, three degradation pathways

exist: the ubiquitin proteasomal degradation pathway (UPP), the endolysosomal degradation pathway, and autophagosomal proteolysis [78]. While ub is a hallmark of the UPP, ub is exploited in all three pathways [78], and, indeed, many instances occur within each pathway where ub is not used [79–81]. Each can be further subdivided, and the UPP will be expanded upon to include ERAD.

1.3.1 Ubiquitin Proteasomal Degradation Pathway (UPP)

Revolutionizing the understanding of protein degradation, the UPP demonstrated for the first time how proteins are selectively targeted for degradation in a highly coordinated and complex process [55]. Simplistically speaking, proteins tagged with polyubiquitin chains are recognized and degraded by a large multisubunit complex called the 26S proteasome in an ATP-dependent manner within the cytoplasm or the nucleus [55]. The 26S proteasome is composed of a 20S core, which contains the proteolytic active sites, and two 19S regulatory caps responsible for substrate recognition and substrate unfolding [79]. The 20S core is a barrel-shaped complex comprised of four heteroheptameric rings: two inner rings made of β subunits (proteins PSMB1-PSMB11) bearing caspase-like, trypsin-like, and chymotrypsin-like activity, and two outer rings made of α subunits (proteins PSMA1-PSMA8), marking the entryway into the narrow opening of the catalytic chamber [82,83]. Flanking each end of the 20S core is a 19S regulatory cap composed of scaffolding proteins, AAA ATPases, ubiquitin receptors, DUBs, and other non-ATPase regulatory subunits [82,84]. In mammals, the proteins comprising these subunits are PSMC1-PSMC6 which exhibit AAA ATPase activity, PSMD1-PSMD9, PSMD11, PSMD12, PSMD14/POH1, and ADRM1 [82]. The 19S regulatory particle contains a translocation channel aligned with the pore of the 20S core, and entry into the 19S channel is stringently regulated [84]. Ub-dependent substrate recognition is primarily mediated by PSMD4 and ADRM1 [84]. However, shuttling factors containing ub-like domains which bind the proteasome, and UBA-domains to bind ubiquitinated-substrates, such as RAD23, DDI1 (DNA damage-inducible protein 1), and ubiquilin 2 (UBQLN2; known as Dsk2 in *S. cerevisae*), also act as receptors to recognize substrates targeted for degradation [84]. The large ATPase complex valosin-containg protein (VCP)/p97 is involved in the UPP in several capacities. In the general UPP, it functions as a hub to bring into proximity substrates and their respective adaptor proteins, E3 ligases, DUBs, and shuttling factors to appropriately modify the

substrates and redirect them as needed. Its ATPase activity may also be used to preliminarily unfold proteins in preparation for their proteasomal-mediated degradation [79]. Following docking to recognition subunits, an unstructured segment termed the "initiation site" on the substrate is engaged by the 19S cap, and the AAA ATPases begin the process of unfolding the substrate and translocating it into the catalytic chamber [79,84]. During this process, the 19S DUB PSMD14 cleaves the isopeptide bond connecting the ub chain to the substrate committed for degradation, hereby recycling ub to replenish the free ub pool [49], and permitting passage of the substrate through the narrow pore opening [79,84]. Two other DUBs which are reversibly associated with the lid, USP14 and UCHL5- whose catalytic activity is contingent upon their association with the proteasome- remove ub from the distal end of the chain, and negatively regulate proteasome-mediated degradation by enhancing substrate dissociation from the proteasome [79,84]. Rarely, their editing of substrate ub chains may enhance substrate binding and promote substrate degradation [49]. Juxtaposing these DUBs is the E3 ligase activity of KIAA10, whose extension of a substrate's ub chain allows enhances substrate-proteasome interaction and lengthens the time permitted for the substrate initiation site to be sufficiently engaged for degradation [79,84]. If the ubiquitinated substrate is retained at the proteasome long enough for the 19S cap to latch onto the initiation site, begin the unfolding process, and pull through the substrate to start degradation, then the substrate will undergo complete proteolysis [79]. Thus, it becomes a race of time between initiation of protein degradation, and the opposing activities of the E3 ligase and DUBs, for a protein to be successfully degraded by the proteasome or otherwise liberated [79]. Interestingly, ubiquitination of the substrate protein is not mandatory for substrate degradation [79]. Ubiquitination of another polypeptide pertaining to the same complex as the substrate protein, or alternatively the presence of an adaptor protein capable of binding both the proteasome and substrate, may suffice granted the substrate harbors an adequate initiation site [79].

Although the UPP was once considered to primarily target cytosolic proteins, countless integral membrane and plasma membrane proteins have since been identified as substrates of this pathway. The epithelial sodium channel [85], the CaV2.2 calcium channel [86], the cystic fibrosis transmembrane conductance

regulator [87], and the potassium channel Kv1.5 [88] are all confirmed clients of 26S proteasome. Thus, the UPP is not limited to just soluble proteins, as will also be seen for substrates of ERAD.

1.3.2 Endoplasmic Reticulum Associated Degradation (ERAD)

Utilizing the proteasome is a highly conserved pathway called ERAD. As the central hub for protein biosynthesis and maturation, as well as the point of departure for proteins embarking on the secretory pathway, the ER bears considerable responsibility for maintaining cellular proteostasis [76]. The ER, therefore, implements both quality and quantity control measures to dispose of proteins which fail to achieve their native conformations or to modulate specific protein expression levels (often those of regulatory proteins operating within the ER), respectively [75,89]. These targeted proteins are disposed of through ERAD [89]. The process of ERAD can be loosely arranged into the following steps: 1) substrate identification 2) substrate extraction by ER "dislocons/retrotranslocons" into the cytosol 3) substrate ubiquitination and, finally, 4) proteasome-mediated degradation [75,90]. While comprehensive studies conducted in yeast and mammals have characterized a multitude of components involved in this process, some aspects, such as the identity of the retrotranslocon and the nuances of substrate recognition, remain obscure [89,91]. Substrate recognition factors and the E3 ub ligase complexes employed are often dependent on whether the mutation, or lesion, in a misfolded protein occurs within the cytoplasmic or the luminal/intramembrane region of the protein [75]. By this classification method, ERAD is subdivided into three branches, ERAD-C, ERAD-L, and ERAD-M, indicating cytoplasmic, luminal, and intramembrane lesion positioning, respectively [75]. Proteins which successfully mature their native conformations and are instead targeted for quantity control purposes use the same general pathways, but require additional substrate-specific adaptor proteins [75]. Other times, input from signaling molecules is required, as exemplified by the cholesterol biosynthetic enzyme HMG-CoA reductase, whose conformation is altered upon binding with sterol intermediates, inducing its interaction the adaptor proteins necessary to effectively target it for ERAD when its activities are no longer necessary [91]. To better understand the machinery of ERAD, members of the protein maturation pathway will also be outlined.

The first step, substrate recognition, is a nuanced task as the ER must distinguish terminally misfolded proteins from a wide spectrum of unstable folding intermediates to ensure that the latter are not prematurely eradicated [89]. Orchestrating the folding and modification of proteins are molecular chaperones, some of which play dual roles in mediating both substrate maturation and substrate degradation [89]. Proteins initially entering the ER are structurally unstable, and chaperones, like the ER heat shock protein 70 (Hsp70) enzyme called binding immunoglobulin protein (BiP), and auxiliary factors like Hsp40, stabilize the nascent peptides and use ATP to drive correct folding [89]. Sulfide bridges are introduced by protein disulfide isomerases (PDIs), and glycan chains are constructed by sequential remodeling – oligosaccharyltransferases initially conjugate a $Glc_3Man_9(GlcNAc)_2$ glycan chain to the protein, and subsequent glucose trimming allows for protein recognition by the Ca^{2+}-binding lectin chaperones calnexin (CNX) and calreticulin (CRT) to promote protein maturation [89]. The removal of a final glucose marks completion and allows the protein to dissociate from CNX/CRT [89]. The protein is evaluated by UDP glucose glycosyltransferase, and glucose is re-added if additional rounds of folding are deemed necessary [89].

The presentation of several structural components or signals is often necessary for effective identification and targeting of proteins for ERAD [75]. Frequently, the unmasking of a previously hidden hydrophobic segment indicates a misfolded protein, and these substrates are recognized by BiP, Sel1, the Derlins, Hsp70, and Hsp40 [75,89]. The switch from a pro-folding curriculum to a pro-degratory one may further be actuated by the status of the glycan chain for N-glycosylated proteins [89]. As glycoproteins undergo multiple rounds of folding and are processed by oligosaccharyltransferases, they are simultaneously exposed to slow acting mannosidases, which eventually cleave off mannose from glycoproteins stalled in the ER to disengage the substrate from CNX/CRT and reroute it for ERAD [89]. The mannosylated protein is recognized by ER degradation enhancing mannosidase (EDEM1), and alongside the ERAD PDI ERdj5 (ER DNA J domain-containing protein 5), the substrate is further processed and handed off to the lectins osteosarcoma-9 (OS-9) or XTP3-B [89,91]. These lectins deliver their substrates to ER residing E3 ub ligase complexes, which work in conjunction with dislocons and the p97 segragase to extract the substrate from the ER and ubiquitinate it [89].

In yeast, the two primary ERAD E3 ligase complexes are the Hrd1 and the Doa10 complexes, distinguished by their client population, where Doa10 mediates ERAD-C and Hrd1 processes ERAD-L and ERAD-M [89]. The mammalian orthologs of the Hrd1 complex are the Hrd1 and Gp78 E3 ligases, which work alongside Sel1, the Derlins, and HERP (homocysteine-responsive ER-resident ub-like domain member protein 1) [75,89]. The ortholog of Doa10 is the MARCH6 (membrane-associated RING-CH finger protein 6) ligase, which works in conjunction with the E2 conjugating enzymes Ube2j1/Ube2j2 and Ube2g2[91]. Data indicates that, in yeast, the Ube2j1/Ube2j2 orthologs prime substrates with a K11-linked ub chain, and the Ube2g2 orotholog then extends the chain by transferring K48-linked pUb "en bloc" to the substrate [91]. Interestingly, Ube2j2 is also capable of ubiquitinating serine and threonine residues [91]. Additional mammalian E3 ub ligases have been identified which also contribute to ERAD- TRIM13, RING finger (RNF) protein 5 (Rnf5), Rnf139, Rnf170, and Rnf185- though the extent of their roles is still being elucidated [75,91]. Although the identity of the retrotranslocons remains to be ascertained, the current running candidates are Hrd1, followed the Derlins, and then the Sec61 channel [89]. Regardless of the dislocon employed and the E3 ligases partaking in the process, the p97 multichaperone complex is an indispensable force in ERAD. Complexed with Npl4 and Ufd1 (ubiquitin recognition factor in ERAD protein 1), and possibly Ufd2, p97 uses ATP to extract substrates from the ER lumen/membrane bilayer [89,91]. The following retrotranslocation and ubiquitination model best encompasses the diverse results obtained from studying ERAD when considering that all ERAD substrates require at least partial, if not full, retrotranslocation from the ER, and that E3 ligase complexes are involved both prior to and following protein excision [75]. In the case of ERAD-C, the substrate is first ubiquitinated on its cytoplasmic side prompting the recruitment of the p97 complex. This complex may also bring along DUBs, and the ERAD-C substrate is subject to various rounds of ub modifications coupled with p97-mediated extraction. In ERAD-L, upon binding with the substrate, Hrd1 oligomers self-ubiquitinate thereby recruiting the p97 complex. p97 then uses ATP to induce a conformation change in Hrd1 to promote its capacity for ERAD-L substrate translocation. Once the ERAD-L substrate is exposed to the cytoplasmic milieu, it is ubiquitinated by Hrd1 and the p97 complex completes its extraction from the ER [75]. Once extracted, the ERAD substrates are escorted to the proteasome

by adaptor proteins or shuttle factors, such as Rad23 and Dsk2 [75], and the substrates may be deglycosylated by cytosolic enzymes like PNGase F [89].

In addition to ERAD, branch of ER degradation was uncovered which targets select proteins for ER-to-lysosome-associated degradation (ERLAD) [90]. ERLAD is often resorted to for proteins that have not been accurately recognized by ERAD factors, or for proteins which are too large or form aggregates and therefore cannot be retrotranslocated. These substrates are delivered to endolysosomes by autophagy pathways, whereby ER-residing LC3-binding proteins are important mediators [90]. Thus far, five integral membrane proteins are known to mediate this process: reticulophagy regulator 1 (RETREG1), SEC62, reticulon 3 (RTN3), cell cycle progression protein 1 (CCPG1), and atlasin 3 (ATL3), proteins which are also vital in maintaining general ER homeostasis under specific physiological conditions [90].

1.3.3 Endocytosis and endolysosomal degradation

The plasma membrane serves as a barrier defining the cell as a distinct unit from the extracellular milieu, and is the platform upon which the cell interacts with and is informed of its environment [92]. Thus, modulation of the constituents of the plasma membrane directly impacts the communication between the cell and its environment, and does so through the process of endocytosis [93]. Endocytosis serves multiple purposes – it is a method of interaction with the environment through the uptake of macromolecules, integrins, and adhesion molecules; it allows for selective trafficking of molecules through higher order epithelial barriers; and, finally, it is also used to regulate the abundance and signaling of plasma membrane proteins, which will be the focus of this section [93]. Three pathways mediate the bulk of endocytosis: clathrin-mediated endocytosis (CME), caveolae-mediated endocytosis, and an umbrella category termed clathrin-independent endocytosis which encompasses four lesser characterized pathways – the flotillin-dependent pathway, the Arf6-dependent pathway, the CLIC/GEEC pathway, and a pathway dependent on dynamin, endophilin, and RhoA [93]. All the endocytic pathways converge at the endosomal sorting compartment, which directs cargo proteins either for recycling back to the plasma membrane, or for endolysosomal degradation [93]. Ubiquitin has been implicated in CME and in the subsequent sorting of cargo to their respective destinations [46,94].

CME is mediated by clathrin, the clathrin adaptor protein 2 (AP2) complex, clathrin-associated sorting proteins, dynamin, and other cargo-specific adaptors and scaffolding proteins [93]. The AP2 complex, which is enriched at the plasma membrane by $PI(4,5)P_2$, recruits clathrin to initiate endocytic vesicle budding, and interacts with cargo-specific adaptors to concentrate substrates in the vicitity [93]. Vesicle budding and scission is finalized by the GTPase dynamin, and the clathrin coat is subsequently disassembled by Heat shock cognate 71 kDa protein (HSC70) and auxilin [93]. Ubiquitin, although not necessary, can prompt cargo inclusion at endocytic vesicle nucleation sites through adaptors which simultaneously bind the ubiquitinated cargo alongside clathrin or AP2 [46]. To date, the adaptors known to mediate this role are Epsin, Eps15, and the ankyrin repeat domain-containing protein 13A,B, and D (Ankrd13A,B,D) [46].

Following vesicle budding, multiple endocytic vesicles fuse to create the early endosome, and cargo is sorted to the recycling endosome for re-expression at the cell surface, to the *trans*-Golgi Network for re-inclusion in the secretory pathway, or to the late endosome/MVB for downstream lysosomal degradation [93,94]. It should be stressed that the endomembrane system is dynamic and does not have discrete compartments to which cargo are transferred, but rather endomembrane compartments exist along a spectrum, and their identity is dictated by their composition of membrane proteins, phosphatidylinositol phospholipids (PIPs), and lumenal pH [93]. As endosomes mature, the pH gradually drops with increasing v-type vacuolar H+ ATPase function, specific Rab GTPases are recruited, and the enrichment of differentially phosphorylated PIPs allows for the engagement of specific PIP-binding proteins [93].

Cargo sorting commences in the early endosome, where cargo proteins are concentrated on tubular extensions which bud off into tubule-vesicular transport carriers to transport cargo back to the cell surface [94]. Cargo may alternatively be concentrated in endosomal recycling subdomains by the retriever and retromer complexes through their interaction with the sorting Nexin family of adaptor proteins, which recognize sorting motifs displatyed by cargo proteins [94]. Mechanisms also exist to concentrate cargo lacking sorting motifs into these subdomains: proteins with a propensity to associate with filamentous actin may be marshalled into these regions, as well [94]. Often, the recycling of receptor proteins is dependent on their signaling activity whereby recycling is only possible once signaling is ablated. As signaling is often

contingent on receptor-ligand binding, and dissociation of the ligand is pH dependent, the point at which a receptor is routed for recycling is dictated by the maturation status (and pH) of the endosome [93]. Cargo not rescued by retromer or retriever, or cargo containing a sorting motif designating it for degradation, is concentrated into intraluminal vesicles (ILVs) within MVBs for ensuing lysosomal elimination [94].

The process of cargo sorting into ILVs relies upon the ESCRT machinery which primarily recognizes ub-based sorting motifs [93]. The ESCRT system is composed of four complexes, ESCRT-0, ESCRT-I, ESCRT-II, and ESCRT-III, which recognize ubiquitinated cargo and generate membranous deformations to promote ILV budding [93]. Cargo subject to this degradative pathway, like the epidermal growth factor receptor (EGFR), are often either mono-ubiquitinated or K63-polyubiquitinated [94]. In the early endosome, ESCRT-0 complexes (composed of hepatocyte growth factor-regulated tyrosine kinase substrate (Hrs) and signal transducing adaptor molecule 1 (STAM1)) associate with the membrane through Hrs/PI(3)P interactions, and bind to ubiquitinated cargo with a low affinity. Cargo enrichment is achieved by multimerization of the ESCRT-0 complexes, as well as cargo binding by tumor susceptibility gene 101 (TSG101) and ubiquitin-associated protein 1 (UBAP1) of ESCRT-I, and VPS36 of ESCRT-II [94]. The Eps15 isomer, Eps15b, may also mediate ub-dependent cargo sorting as part of the ESCRT-0 complex [46]. While these early ESCRT complexes foster the enriched degradative subdomain, the late-acting ESCRT-III stimulates ILV budding by remodeling the membrane using SNF7 filaments. Simultaneously, it helps dissolve the early ESCRT complexes using the VPS4 ATPase, and recruits the DUBs AMSH and USP8 to recycle ub from the cargo proteins [94]. Many cargos are deubiquitinated prior to inclusion into ILVs by these DUBs, and, in fact, debuiquitination may be necessary otherwise sorting into ILVs will not proceed [80]. AMSH activity, for one, is critical for targeting EGFR for lysosomal degradation following ub-mediated endocytosis [49]. USP8 can act to promote or inhibit lysosomal degradation of its targets, depending on the substrate [49]. While ubiquitination appears to be the main signal targeting cargo for ESCRT-mediated endolysosomal degradation, ub-independent mechanisms also exist [94] where cargo is bound by the ESCRT accessory protein PDCD6IP (programmed cell death 6-interacting protein) via a YPX_3L motif, or through

ub-independent association with Hrs [80]. Cargo is eventually degraded when MVBs fuse with lysosomes, hereby exposing the ILVs to a slew of proteolytic enzymes and highly acidic environment.

In terms of cargo ubiquitination, mono-ubiquitination has repetitively been shown to regulate protein internalization and subsequent endosomal sorting through studies conducted on mutant fusion proteins expressing an in frame single ub moiety [46]. Additional studies demonstrated that, in addition to monoubiquitination, multi-monoubiquitination and K63-linked polyubiquitination are also sufficient signals for both endocytosis and sorting to lysosomal vesicles, with K63-linked chains being the most effective [46]. For specific proteins, such as the major histocompatibility complex class I, heterotypic K11/K63-linked pUb chains are important mediators of endocytosis [46]. On the flip side, deubiquitination of cargo is equally as important in endocytosis and sorting [95]. Not only is deubiquitination necessary to replenish the free ub pool, but deubiquitination, by AMSH, for example, may also act to salvage a protein from an otherwise degradative fate [95]. Finally, ubiquitination is a dynamic process, and cargos may require deubiquitination following internalization in order to be appropriately re-ubiquitinated, perhaps using an alternative chain linkage or lysine acceptor residue, for subsequent sorting [80].

1.3.4 Autophagosomal degradation

As one of the main cellular degradation pathways, autophagy mediates clearance of proteins, cytoplasmic material, and organelles, by enclosing these substrates in an autophagosome and delivering them to lysosomes for degradation [76]. This process, termed macroautophagy, is constitutively active at basal levels, but may be induced by environmental stimuli such as nutrient deprivation, where it non-specifically degrades cytoplasmic material to provide the cell with nutritional components [76]. While autophagy was once considered to be a predominantly non-selective pathway, findings in the field have long since unveiled its selectivity in its substrates [76]. Autophagy chiefly relies on proteins from the autophagy (Atg) gene family, and the machinery involved in selective and non-selective autophagy are largely the same [76].

In mammalian cells, macroautophagy begins with the formation of the phagophore near ER-mitochondria contact sites [76]. As the phagophore expands through assembly of lipids derived from vesicles, the ER, the mitochondria, the Golgi apparatus, and recycling endosomes, numerous complexes enrich

PI(3)P within the lipid bilayer, allowing for the phagophore to become decorated with the UbL ATG8 via its conjugation to PE (PE-ATG8) [76]. In humans, ATG8 is expressed as six homologous proteins: microtubule-associated protein 1A/1B-light chain 3A (LC3A) , LC3B, LC3C, gamma-aminobutyric acid receptor-associated protein (GABARAP), GABARAP-L1, and GABARAP-L2 [76]. Receptors containing an LC3-interacting motif (LIR) can bind ATG8, and do not discriminate between the six homologs [76]. However, a subset of motifs does promote the interaction of certain receptors with a particular ATG8. NDP52, for example, has an extension of the LIR motif resulting in its preference for the LC3C protein, and PLEKHM1 contains a GABARAP-interacting motif just adjacent to the canonical LIR motif to mediate specificity. More recently, another motif was identified, one homologous to the UIM, which binds to ATG8 in a separate region from the LIR-interacting pockets to mediate interaction with a distinct subset of substrates, such as p97 [76]. Expression of PE-ATG8 on the inner membrane of the phagophore, and substrate receptors containing an ATG8-binding domain, mediate selective autophagy by anchoring their cargo substrates to the expanding phagophore [76]. The ends of the maturing phagophore eventually fuse to form a fully enveloped double membrane structure now called an autophagosome [76]. Through fusion with a late endosome, or through direct amalgamation with a lysosome, the contents of the autophagosome are eventually degraded by lysosomal proteolytic enzymes [76].

Selective autophagy is further classified according to the substrates it targets: aggrephagy (aggresomes), mitophagy (mitochondria), xenophagy (pathogens), ER-phagy (endoplasmic reticulum), and lysophagy (damaged lysosomes) [81,96]. Holding true to the roots of its name, ub is exploited by the autophagy system, too [76]. In addition to its substantive role in modulating autophagic flux through the ub-dependent regulation of autophagic regulatory proteins, ub is directly involved in selective autophagy by mediating recognition of substrates [81]. Mechanisms using ub-independent selective autophagy receptors, such as the mitophagy receptors FUNDC1 (FUN14 domain containing 1 protein), BNIP3 (BCL2/adenovirus E1B 19 kDa protein-interacting protein 3), and NIX (also known as BNIP3L), can be used to promote substrate clearance, but ub-dependent processes are favoured [81]. Ub-dependent autophagy receptors show preference for K63 pUb chains, which partially confers the specificity of this system, such that substrates modified

with K48, K27, and K11 chains are delivered to the proteasome, instead [81]. For aggrephagy, modification of misfolded proteins by multiple UbLs – SUMO1, FAT10, and ISG15 – all promotes their aggregation, and K63 pUb mediates their clearance by the aggrephagy receptors sequestosome 1 (SQSTM1)/p62 and neighbor of BRCA1 gene 1 (NBR1), both of which contain UBDs and LIRs [81]. Interestingly, the DUB USP9X has been implicated in aggrephagy: it targets α-synuclein for autolysosomal clearance, which would otherwise be cleared by the 26S proteasome, through removal of monoubiquitin. Similarly, BCL2 associated athanogene 3 (BAG3) has also been shown to re-direct substrates initially targeted for proteasomal degradation for autolysosomal clearance through chaperone- and BAG1-mediated delivery. BAG3 accomplishes this through its interaction with p62 and its recognition of K48 pUb chains [81]. However, substrate ubiquitination is not always necessary for BAG3 recognition and binding [97]. BAG3 and SQSTM1 were also proposed to mediate the compensatory switch to autophagy when proteasomal degradation is overloaded or impaired [98]. To date, the bridging proteins SQSTM1, Toll-interacting protein (TOLLIP), NBR1, and optineurin, have been identified as autophagy receptors in mammals [99]. ER-phagy characterization is still in its infancy, though five ER-residing proteins with ATG8-interacting domains that are implicated in autophagy-mediated ER-protein degradation have been identified: RETREG1, SEC62, RTN3, CCPG1, and ATL3 [81,90]. Of all the autophagy receptors, SQSTM1 has the most appreciable role in the selective clearance of a broad spectrum of substrates, capable of recognizing both mono- and polyubiquitinated proteins, mediating aggrephagy, and escorting polyubiquitinated proteasome-destined proteins for autophagy-mediated clearance, as needed [100,101].

1.4 ER stress and the unfolded protein response (UPR)

Given the influence that the ER has on maintaining cellular homeostasis, disturbance in the protein maturation pathway can have consequential effects. The ER has therefore developed a measure to address the stress associated with a build-up of unfolded or misfolded proteins, a process termed the unfolded protein response [91,102]. The UPR restores homeostasis by decreasing the protein load on the ER and increasing the ER's capacity to fold and degrade proteins [102]. Perturbations of various forms can precipitate ER stress - as protein folding and maturation is energy and Ca^{2+}-dependent, disruptions in Ca^{2+} homeostasis

or energy metabolism will directly impact ER functioning [102]. Curiously, in cancers, the upregulation of certain oncogenes can saturate the cells leading to protein toxicity and chronic activation of the UPR, or the UPR may be chronically activated as an adaptive survival mechanism [102]. The ER uses three sensory proteins to detect ER stress and invoke the UPR. At resting physiological conditions, BiP associates with ATF6 (activating transcription factor 6), IRE1 (inositol-requiring enzyme 1), and PERK (PRKR-like endoplasmic reticulum kinase), maintaining their inactive state. ER stress recruits BiP to unfolded proteins, leading to the liberation and ensuing activation of these sensors [102]. ATF6 is a transcription factor, which when activated, promotes transcription of ER chaperones and pro-folding enzymes. Likewise, activation of IRE1 and PERK leads to the expression of specific eukaryotic initiation factor species to suppress global protein translational activity, and activates the transcription factor XBP1s to induce transcription of regulatory proteins involved in protein maturation, secretion, and degradation [102]. Autophagy may also be induced as part of the UPR to assist in managing the cellular disruptions, and is further used upon UPR resolution to re-establish ER homeostasis [102]. Prolonged ER stress and an unrelenting UPR eventually leads to apoptosis, through activation of both the intrinsic and extrinsic apoptotic pathways, as well as switching autophagy from a cell survival program to a death promoting one [102].

1.5 Prototypical ubiquitinated substrates

For comparative purposes, the ubiquitination of two model proteins, connexin 43 (Cx43) and tropomyosin-related kinase A (TrkA), will be described. This will serve to illustrate the diverse roles and the dynamic nature of ub on regulating a single protein throughout its entire lifecycle, and may provide some insight into the results divulged in my thesis.

1.5.1 Connexin 43

Literature examining the regulation of Cx43, and specifically its ubiquitination and proteasomal-mediated degradation, is vast [103], and may lend itself to piecing together a narrative with the fragments of PANX1 data included in my thesis. Cx43 is a transmembrane channel protein originating in the ER, and is presented at the cell surface as gap junctions at appositional membranes [104]. Cx43 exhibits a relatively short half-life of 1.5-5 hours, with its abundance intricately regulated by ERAD, endolysosomal degradation, and

autophagosomal degradation, according to the localization of Cx43 and the presence of certain environmental stimuli [103,105]. Cells take advantage of both ub-dependent and ub-independent mechanisms for Cx43 proteasomal degradation and internalization [103–105].

Initial studies found that concurrent treatment of cells with epidermal growth factor (EGF) and 12-O-tetradecanoylphorbol 13-acetate (TPA) induced Cx43 multi-monoubiquitination, seemingly targeting Cx43 to the UPP, as proteasomal inhibition increased its half-life under these conditions [105]. Follow-up studies uncovered that TPA and proteasome inhibitors, rather, indirectly regulate Cx43 through the stabilization of the Cx43 kinase, Akt, as phosphorylation stabilizes Cx43 expression at the cell surface [105]. This led to the discovery of alternate roles for ub on Cx43 regulation, and studies found that, when exposed to TPA, Cx43 is multi-monoubiquitinated and K63 polyubiquitinated, which prompts its association with Eps15 and the ESCRT components Hrs and Tsg101, funneling it down the endolysosomal pathway [103,105].

Multiple E3 ub ligases contributing to Cx43 endocytosis have since been identified [103]. NEDD4, WWP1 (WW domain-containing E3 ubiquitin protein ligase 1), TRIM21, and Smurf2 (SMAD Specific E3 Ubiquitin Protein Ligase 2) all associate with and mediate Cx43 internalization, in different capacities [103]. TRIM21 ubiquitinates Cx43 when the appropriate phosphodegron signal is present, and Smurf2 is involved in TPA-induced internalization of Cx43, albeit its E3 ligase activity is not targeted at Cx43 [103]. The NEDD4 E3 ligase binds to Cx43 by a PY motif expressed by Cx43 to mediate its ubiquitination and promote internalization [103,104]. Coincidentally, this motif overlaps with the YXXΦ tyrosine motif, which is a ub-independent CME sorting signal also used for Cx43 internalization [103,104].

Autophagy also modulates Cx43 stability [105]. NEDD4-mediated ubiquitination promotes Cx43 interaction with autophagy receptors Eps15 and SQSTM1, and the DUB USP8 was found to specifically counteract autophagic degradation through the hydrolysis of both mono- and polyubiquitin Cx43 chains [103,106]. Although the initial conjecture that TPA treatment induced Cx43 UPP-mediated degradation was incorrect, the proteasome does contribute to Cx43 turnover [103]. Under basal conditions, up to 40% of Cx43 is predicted to be degraded by ERAD [103]. Moreover, Cx43 ERAD appears to be mediated by CIP75, a UBA and UbL domain-containing protein [105]. Surprisingly, CIP75 mediates only ub-*independent* proteasomal

clearance of Cx43, further convoluting the narrative between Cx43 ubiquitination and degradation [105]. It may accomplish its role either by mediating Cx43 retrotranslocation across the ER membrane, or by escorting Cx43 to the 26S proteasome as a shuttle factor [103]. Taken together, Cx43 serves as a prime example of a channel whose stability and trafficking is regulated by ubiquitination in a multifaceted manner [103]. Not only is ub used to engage multiple degradation pathways, but ub-independent activity of E3 ligases and ub-independent proteasomal degradation are also involved in regulating Cx43 [103].

1.5.2 Tropomyosin-related kinase A

TrkA is a tyrosine kinase receptor whose signaling promotes cell growth and survival [107]. Ligand binding by neuronal growth factor (NGF) promotes its dimerization and kinase activation, and signaling proceeds until TrkA dissociates from its ligand, at which point TrkA may then be re-expressed at the cell surface, or targeted for degradation [107]. The ubiquitination system is instrumental in regulating TrkA signaling activity, endocytosis, recycling, and degradation, according to the E3 ligase involved, the ub chain topology, and the lysine residues modified [107].

As yet, TrkA is the confirmed target of five ub E3 ligases: c-Cbl, Cbl-b, NEDD4-2, TNF receptor-associated factor 4 (TRAF4), and TRAF6 [107,108]. Following NGF binding, c-Cbl and Cbl-b promote TrkA lysosomal degradation [107]. NGF-binding also promotes TRAF6-mediated K63-linked polyubquitination of TrkA, which is accomplished in collaboration with the E2 conjugating enzyme UBE2L3, to induce TrkA internalization and TrkA kinase signaling [107,109]. In cells where K63-linked pUb of TrkA is inhibited, TrkA internalization is hampered and TrkA accumulates at the cell surface [109]. K63-linked pUb further targets TrkA for endolysosomal degradation [110]. Eloquent time course studies, which found that K63-pUb TrkA associates with the Rpt1 subunit (PSMC2 is the human ortholog) of the 26S proteasome, demonstrated that the SQSTM1 shuttling factor delivers ubiquitinated TrkA to the proteasome for deubiquitination en route to its lysosomal destination [107,110]. By this method, both the proteasomal and the endolysosomal pathways are essential for K63-pUb TrkA degradation, although final clearance of TrkA is carried out by lysosomal proteolysis [107]. In contrast, NEDD4-2 associates with TrkA under basal conditions through its recognition of a PPxY binding motif on TrkA, an interaction which is enhanced by NGF-binding to TrkA, to modulate

TrkA signaling and direct it for lysosomal degradation [107]. NEDD4-2 achieves this by multi-monoubiquitinating TrkA [107]. Impairment of NEDD-4-mediated ubiquitination enhanced TrkA signaling and increased TrkA expression levels. Interestingly, increased TrkA multi-monoubiquitination decreased receptor internalization but increased its downstream lysosomal degradation [111]. More recently, TRAF4-mediated K27 and K29-linked polyubiquitination of TrkA was demonstrated to specifically increase its kinase activity and signaling, hereby promoting the tumorigenicity of prostate cancer [108].

Compounding its modification by E3s, TrkA is also subject to the activity of DUBs in order to be targeted to its appropriate destination [107]. Following NGF-induced ubiquitination and internalization, deubiquitination by USP8 is necessary to subsequently target TrkA for degradation. By promoting its degradation, USP8 also incidentally decreases TrkA signaling [112]. The DUB USP36 also modulates TrkA ubiquitination, however it exerts its effects through competitive binding with TrkA against NEDD4-2, precluding NEDD4-2-mediated ubiquitination and degradation [107].

1.6 Hypothesis and objectives

While PANX1 ubiquitination has been confirmed, the nature of the chains and their implications in the regulation of PANX1 levels, localization, and/or function have yet to be investigated. Our laboratory has also found that treatment with MG132, a proteasome inhibitor, not only allowed for increased ectopic PANX3 in cell lines which otherwise had minimal protein expression, but MG132 also increased PANX1 and PANX3, but not PANX2, levels in cells endogenously expressing these proteins (not published). Taken together, this suggests that ubiquitination may play a multimodal role in regulating pannexins, and that the UPP may be involved in PANX1 and PANX3 protein regulation. Therefore**, I hypothesize that PANX1 and PANX3 are ubiquitinated, and that this post-translational modification regulates their protein levels, subcellular localization, and degradation**. My first aim is to confirm that PANX1 and PANX3 are ubiquitinated and characterize the topology of ubiquitin chains formed. My second aim is to investigate the role of the proteasome on regulating PANX1 and PANX3 protein expression, subcellular localization, and degradation. Finally, my third aim is to identify potential ubiquitination-defective mutants in order to delineate the role of ubiquitination on pannexin regulation.

2.0 MATERIALS AND METHODS

2.1 Cell lines and cell culture

Rh30 cells were obtained from Dr. P. Houghton (St. Jude Children's Hospital, Memphis, TN, USA). HEK293T cells are from the American Type Culture Collection (ATCC). MDA-MB-231 cells were provided by Dr. R. Korneluk (CHEO, Ottawa, ON, Canada). Rh30 were cultured in Roswell Park Memorial Institute (RPMI)-1640 (HyClone, SH30027.01) supplemented with 10% fetal bovine serum (FBS) (Sigma Aldrich, F1051), 100 U/ml Penicillin + 100 μg/ml Streptomycin (Thermo Fisher, sv30010), and 2 mM Glutamine (Thermo Fisher, SH3003401). HEK293T and MDA-MB-231 cells were cultured in Dulbecco Modified Eagle's medium (DMEM) (HyClone, SH30022.01) supplemented with 10% FBS, 100 U/ml Penicillin + 100 μg/ml Streptomycin, and 2 mM Glutamine. All cells were cultured at 37°C in 5% CO_2.

2.2 Plasmids and transfections

cDNA plasmids used for transfection include myc-DDK-PANX1 (Origene, RC204474), myc-DDK-PANX3 (Origene, RC224924), HA-ubiquitin (Addgene, 18712). The untagged PANX1 construct was subcloned into pCDH-CuO-MCS-EF1-GFP lentiviral vector, as described [39] and the untagged PANX3 construct (Origene, RC224924) was subcloned into the pCDH-CuO-MCS-EF1-RFP (System Biosciences, QM516B-2) lentiviral vector by X. Xiang, as above. The Cx43 plasmid and the FLAG-Traf2 construct were generously provided by Dr. D. W. Laird (Western University, London, ON, Canada) and Dr. R. Korneluk (CHEO, Ottawa, ON, Canada), respectively. The empty vector pcDNA3.1 plasmid and the eGFP-pCDNA3.1 plasmid were a gift from Dr. R. Beliveau laboratory (Ste-Justine Hospital, Montreal, QC, Canada). Cells were transfected at 95% confluency using Lipofectamine 2000 (Thermo Fisher, 11668019) following manufacturer's instructions.

2.3 Engineering of the PANX1 and PANX3 ubiquitination-resistant mutants

Ubiquitination-deficient mutants of myc-PANX1 and myc-PANX3 were created by site-directed mutagenesis by introducing lysine to arginine point mutations. The lysine residues targeted in the KR3 myc-PANX1 mutant were chosen according to their identification as confirmed ubiquitinated residues

within literature [113–116]. The lysines included in the KR9 myc-PANX1 and KR8 myc-PANX3 mutants were selected according to predictions by *in silico* analysis using the following prediction softwares: UbPred, UbiProber, iUbiq-Lys, UbiSite, BDM-PUB, UbiPred, and CKSAAP UbSite. Lysine residues with the highest probabilities of ubiquitination, or residues which were identified by multiple softwares, were targeted in the mutants.

All mutants were generated using the QuikChange Multisite-Directed Mutagenesis Kit (Agilent Technologies, 200515). All primers were designed using Agilent's QuikChange® Primer Design Program and synthesized by Thermo Fisher. The primers and their corresponding nucleotide and amino acid mutations are listed in **Table 1**. The KR3 myc-PANX1 mutant was generated in one round. The KR9 myc-PANX1 mutant was created using three rounds of mutagenesis: the first round introduced K307,355, 415R, the second round introduced K18,26,381R, and the third round introduced the remaining K24,204,409R. The KR8 myc-PANX3 mutant was generated by introducing K100,180,379R in round one, K26,108,167R in round two, and K183,381R in round three. The mutagenesis temperature cycling parameters for all the constructs are as follows: one minute at 95°C, followed by 30 cycles of 1 minute at 95°C, 1 minute at 55°C, and 12.36 minutes at 65°C. All the steps were completed according to the manufacture's protocol. Mutant constructs were verified by Sanger sequencing (The Centre for Applied Genomics, Sick Kids Children's Hospital, Toronto).

Table 1. Sequences of the primers used to introduce lysine to arginine mutations by multisite-directed mutagenesis.

Construct	Amino acid change	Nucleotide mutation	Primer sequence (5'-3')
KR3 myc-PANX1	K307R	A920G	tccgacagaagacagatgttctcagagtgtacgaaatc
	K381R	A1142G	ggatgttgttgatggcagaactcccatgtctgcag
	K409R	A1226G	aaggtatgaacatagacagtgaaactagagcaaataatggagagaa
KR9 myc-PANX1	K307R	A920G	tccgacagaagacagatgttctcagagtgtacgaaatc
	K355R	A1064G	gtcttaaggtactggagaatattaggagcagtggtcag
	K415R	A1244G	agcaaataatggagagaggaatgcccgacagagac
	K18R	A53G	tgttctcggatttcttgctgaggggagcccacgg
	K26R	A77G	cacggagcccaagttcagggggctgcg
	K381R	A1142G	ggatgttgttgatggcagaactcccatgtctgcag
	K204R	A611G	gtggagcagtacttgaagacaaagagaaattctaataatttaatcatcaagt
	K409R	A1226G	aaggtatgaacatagacagtgaaactagagcaaataatggagagag

	K24R	A71G	cccacggagcccaggttcagggggctg
KR8 myc-PANX3	K100R	A299G	ggcctggccaggacagaatgaaatctctctgg
	K180R	A539G	tgttctggaatgagctggagagggctcggaaag
	K379R	A1136G	ggctggcttagaaccctcaagacccaaacacctc
	K26R	A77G	aggggaccccgcctcagaggactgcg
	K108R	A323G	ctctctggccccacagggccctcc
	K167R	A500G	gaagatccggcagaggagttccgacccct
	K183R	A548G	agctggagagggctcggagagaacgatactttga
	K381R	A1142G	gcttagaaccctcaagacccagacacctcaccaa

2.4 Pharmacological treatments

For proteasomal inhibition assays, cells were treated with 10 μM MG132 (Sigma Aldrich, M7449), 10 μM lactacystin (Santa Cruz, sc-3575), or DMSO control (Tocris Bioscience, 3176), for 16 hours. Cells were then fixed for immunofluorescence imaging, or the proteins were harvested for western blotting.

For caspase inhibition experiments, cells were treated with 10 μM MG132, 20 μM Z-VAD-FMK (Promega, G723B), both drugs simultaneously, or with DMSO alone, for 16 hours. Proteins were harvested and subjected to western blotting. To verify caspase inhibition (positive control for Z-VAD-FMK), MDA-MB-231 cells were treated with 1 μM LCL-161 (Novartis; supplied by Dr. R. Korneluk) (to induce caspase-dependent apoptosis), 20 μM Z-VAD-FMK, both LCL-161 and Z-VAD-FMK, or DMSO control, and observed by light microscopy to examine LCl-161-induced cell death and rescue by Z-VAD-FMK.

2.5 Cell lysis and western blot analysis

For PANX1 western blots, cells were washed in cold phosphate-buffered saline (PBS) and solubilized in Triton lysis buffer (150 mM NaCl, 10 mM Tris-HCl (pH 7.4), 1 mM EDTA, 1 mM EGTA, 0.5% Nonidet P-40, 1% Triton X-100) containing PhosStop Phosphatase Inhibitor tablets (Sigma Aldrich, 4906837001) and Protease Inhibitor Cocktail tablets (Sigma Aldrich, 4693159001), as previously described [117]. For all PANX3 experiments, proteins were harvested using sodium dodecyl sulfate (SDS) lysis buffer as described previously [118]. Protein concentration was quantified by Pierce BCA protein assay kit (Thermo Fisher, PI23227). Proteins were denatured by boiling in Laemmli buffer and separated by SDS-PAGE gel. Proteins were transferred to polyvinylidene fluoride (PVDF) membranes by semi-dry transfer using the Transblot Turbo (BioRad, 1704150), blocked in Odyssey Blocking Buffer (LI-COR, 927-40003) for one

hour at room temperature, and immunoblotted with the primary antibodies listed in **Table 2**. Membranes were incubated with fluorescently labelled-secondary antibodies (listed in **Table 2**) for one hour at room temperature. Membranes were visualized and protein densities were quantified by Odyssey CLx western blot scanner (Li-Cor, 9140-01).

Table 2. Primary and secondary antibodies used for immunoblotting. Membranes were incubated with all antibodies overnight at 4°C, aside from GAPDH and the secondary antibodies, for which membranes were incubated for one hour at room temperature. BSA, Bovine Serum Albumin.

Antibody (species origin)	Dilution	Dilution buffer	Company	Catalogue number
anti-β-actin	1:2000	Odyssey blocking buffer	Cell Signaling	8457S
anti-Cx43	1:500	Odyssey blocking buffer	Sigma Aldrich	C6219
anti-EGFR	1:500	Odyssey blocking buffer	Santa Cruz	sc-373746
anti-FLAG	1:1000	Odyssey blocking buffer	Sigma Aldrich	F1804
anti-GAPDH	1:2000	Odyssey blocking buffer	Advanced Immunochemical	2RGM2
anti-HA	1:5000	Odyssey blocking buffer	Abcam	ab9110
anti-K48 pUb	1:1000	5% BSA	Cell Signaling	4289S
anti-K63 pUb	1:500	5% BSA	Cell Signaling	5621S
anti-myc (ms)	1:1000	Odyssey blocking buffer	Cell Signaling	2276
anti-myc (rb)	1:1000	Odyssey blocking buffer	Cell Signaling	2278S
anti-myc (ms)	1:5000	Odyssey blocking buffer	GenScript	A00704
anti-PANX1	1:1000	Odyssey blocking buffer	Sigma Aldrich	HPA016930
anti-PANX3	1:500	Odyssey blocking buffer	Santa Cruz	sc-51387
anti-tubulin	1:1000	Odyssey blocking buffer	Santa Cruz	SC-8035
anti-ubiquitin (P4D1)	1:1000	Odyssey blocking buffer	Santa Cruz	SC-8017
anti-vinculin	1:5000	Odyssey blocking buffer	Abcam	ab129002
anti-goat	1:10000	Odyssey blocking buffer	Abcam	ab175776
anti-mouse IRdye800	1:5000	Odyssey blocking buffer	LICOR	925-32210
anti-mouse-HRP	1:10000	5% skim milk	Cell Signaling	7076P2
anti-rabbit Alexa 680	1:5000	Odyssey blocking buffer	Thermo Fisher	A21109
anti-rabbit-HRP	1:10000	5% skim milk	Cell Signaling	7074P2

2.6 *In vivo* ubiquitination assays

To measure global PANX ubiquitination, HEK293T cells were co-transfected with wild-type or mutant KR3 myc-PANX1, wild-type myc-PANX3, HA-tagged ubiquitin, or pcDNA control. The ratio of DNA used for transfection of myc-PANX1:HA-Ub and myc-PANX3:HA-Ub were 1:9 and 1:2. Ratios for myc-PANX to HA-Ub DNA for transfection were chosen following titration of both concentrations to identify the optimal ratio for expression of both proteins in the whole cell lysates, as protein expression

levels between myc-PANX1 and myc-PANX3 varied greatly. For the control conditions, myc-PANX and HA-Ub were substituted with pcDNA at the equivalent ratio for consistent total DNA quantity during transfection. The following day, all cells were treated with 10 μM MG132 for 16 hours. Proteins were harvested under denaturing conditions using SDS lysis buffer, as previously described [118] and supplemented with 1.25 mg/mL N-ethylmaleimide (NEM) (Sigma Aldrich, E3876-5G) . Cell lysates (1 mg) were precleared with 20 μL of Protein A/G Plus Agarose beads (Thermo Fisher, PI20423) then incubated overnight at 4°C on a rotator with either 10 μg of anti-HA antibody (Abcam, ab9110) or anti-myc antibody (Cell Signaling, 2276). Protein A/G Plus Agarose beads (20 μL) were added to the sample and incubated for 2 hours to pulldown the immunocomplexes. Proteins were eluted by boiling in 20 μL of 2x Laemmli buffer prior to loading the samples for SDS-PAGE and immunoblotting analysis.

To assess lysine-48 (K48) and lysine-63 (K63)-linked polyubiquitination, Rh30 cells were transfected with myc-FLAG-PANX1, FLAG-Traf2, or eGFP, as described in **section 2.2**. The following day, cells were treated with 10 μM MG132 for subsequent detection of K48-linked pUb, or were untreated for K63-linked pUb detection, for 16 hours. Proteins were harvested under denaturing conditions using SDS lysis buffer supplemented with 1.25 mg/mL NEM. Cell lysates (1 mg) were precleared and subjected to immunoprecipitation, as described above, using 10 μg anti-FLAG antibody (Sigma Aldrich, F1804). Eluates were separated by SDS-PAGE. For the K48 *in vivo* ubiquitination assays, proteins were transferred to PVDF membranes by overnight wet transfer. Membranes were subsequently boiled in ddH_2O for 30 minutes. For the K63 *in vivo* ubiquitination assays, proteins were transferred to nitrocellulose membranes by overnight wet transfer and membranes were then autoclaved for a total of 50 minutes. For the K48 and K63 *in vivo* ubiquitination assays, membranes were blocked in 5% skim milk, immunoblotted with their respective primary antibodies, and probed with HRP-conjugated secondary antibodies, which are all listed in **Table 2**. Membranes were visualized by enhanced chemiluminescence (Perkin Elmer, NEL103E001EA), except for immunoblotting for FLAG, β-actin, and GAPDH, which were subsequently probed and visualized with fluorescent secondary antibodies (**Table 2**).

2.7 Protein degradation assays

Protein stability was first examined by cycloheximide chase experiments. Rh30 transiently over-expressing myc-PANX1, myc-PANX3, or Cx43 as a control, were incubated with 35 μg/mL of cycloheximide (CHX) (Sigma Aldrich, C7698), supplemented with either 10 μM MG132 or DMSO. Proteins were harvested at 0, 6, and 24 hours of CHX chase using Triton- and SDS-lysis buffers, as described in **section 2.5** and analyzed by western blotting.

Protein stability was validated by radioactive pulse-chase assays. Rh30 cells were transfected with myc-PANX1 or eGFP. Twenty-four hours post transfection, cells were washed twice in room temperature PBS, then incubated for one hour in starvation buffer (methionine & cysteine-free RPMI-1640 (Sigma Aldrich, R7513) containing 10% dialyzed FBS (Thermo Fisher, A3382001), 1% glutamine, and 1% Penicillin/Streptomycin)). The cells were then pulsed for one hour in starvation media containing 100 μCi/mL EasyTag S35 Protein Labeling mix (Perkin Elmer, NEG772007MC). Cells were washed twice with warm PBS and chased in complete RPMI supplemented with 1 mM of each L-cysteine (Sigma Aldrich, C7352) and L-methionine (Sigma Aldrich, M5308), containing either 10 μM MG132 or DMSO. Proteins were harvested using Triton-based lysis buffers, and protein concentration was quantified by BCA. Lysates (100 μg) were precleared with 20 μL of Protein A/G agarose beads then incubated with 1.5 μg anti-myc antibody (GenScript, A00704 (mouse antibody)) overnight. The antibody complexes were incubated with 20 μL of Protein A/G agarose for 2 hours to precipitate the proteins. The immunoprecipitates were washed thrice in Triton-based lysis buffer, followed by a single wash in cold PBS. Myc-PANX1 was eluted by boiling in 2x Laemmli buffer and run on SDS-PAGE, then transferred to PVDF membranes by semi-dry transfer, as described above. Membranes were exposed to autoradiography film at 4°C for visualization of [^{35}S] radioactivity, and the captured radioactivity was then quantified by Image J. Membranes were blocked in 5% skim milk and immunoblotted with their respective primary and HRP-conjugated secondary antibodies (**Table 2**). Membranes were visualized by enhanced chemiluminescence (Perkin Elmer, NEL103E001EA) and protein densities were quantified by Image J.

2.8 Cell surface biotinylation assay

All steps of the cell surface biotinylation assay were completed at 4°C. Transfected Rh30 cells treated with either MG132 or DMSO, as described, were washed twice with cold PBS containing phosphatase PhosStop inhibitors and Protease EDTA-free inhibitors. Cells were incubated in 0.5 mg/mL EZ-Link Sulfo-NHS-LC-LC-Biotin (Thermo Fisher, PI21338) or PBS control for 20 minutes, washed twice with 100 mM cold glycine (in PBS) and incubated in cold glycine for 15 minutes. Cells were lysed in Triton-based lysis buffer, cleared of debris, and protein concentration was measured by BCA assay. Samples (1400 µg of protein) were incubated with 50 µL Neutravidin-agarose beads (Thermo Fisher, PI29200) overnight at 4°C on a rotator. Proteins were eluted in 2x Laemmli buffer by boiling at 100°C prior to running on SDS-PAGE gel for subsequent western blotting and quantification.

For absolute cell surface PANX1 quantification, total PANX1 levels in the pulldown fraction were quantified relative to the EGFR levels in the same fractions. For absolute quantification of each individual species, the same method was used but each band was quantified individually. For assessment of wild type (WT) PANX1 cell surface expression following MG132 treatment, the Gly0, Gly1, Gly2 *and* the lower molecular weight (LMW) species were quantified, whereas only the Gly0, Gly1, and Gly2 species were quantified for comparison of the WT and KR9 mutant cell surface levels. For cell surface PANX1 quantification relative to input, the absolute cell surface PANX1 was divided by the proportion of immunoprecipitates loaded onto the SDS-PAGE to obtain total PANX1 protein in the pulldown fraction. This amount was then divided by the quantity of PANX1 loaded into the Neutravidin bead column (equivalent to the PANX1 levels detected in the input fraction on the SDS-PAGE, relative to their β-actin loading controls, divided by the ratio of sample loaded onto the SDS-PAGE compared to the quantity of protein loaded into the Neutravidin bead column for biotin-pulldown).

2.9 Immunofluorescence staining

Cells grown on glass coverslips were fixed in 3.7% formaldehyde, incubated in permeabilizing blocking buffer (2% Bovine Serum Albumin and 0.1% Triton-X in PBS) for 45 minutes, and immunolabelled with the following primary antibodies diluted in blocking buffer for one hour at room

temperature: calnexin (1:50; Santa Cruz; sc-46669), CoxIV (1:500; Thermo Fisher, 501122859), GM130 (1:150; Abcam; ab169276), LAMP1 (1:50; Santa Cruz, sc-18821), myc (1:100; Cell Signaling, 2278S), myc (1:100; Cell Signaling, 2276), PANX1 (1:100; Sigma Aldrich, HPA016930), and PANX3 (1:50; Santa Cruz, sc-51387). Samples were washed thrice in PBS, then labeled for one hour at room temperature with secondary antibodies conjugated to Alexa Fluor 488 (1:500)(anti-rabbit; Thermo Fisher, A11008)(anti-mouse; Thermo Fisher, A11017)(anti-goat; Abcam, ab150129) or Alexa Fluor 594 (1:500)(anti-rabbit; Thermo Fisher, A11012)(anti-mouse; Thermo Fisher, A11005) and mounted with DAPI Fluoromount-G (Southern Biotech, 0100-20) onto glass slides. Images were taken with Olympus Fluoview FV-1000 Laser Confocal Microscope, and acquisition settings were kept constant between samples in a single replicate.

2.10 Statistical analysis

For each of the assays, experiments were repeated a minimum of three times. For assays where protein densitometry was measured, statistical significance was determined using unpaired two-tailed Student's T-test. Results were considered significant for $P < 0.05$.

2.11 Cross-referencing PANX1 protein interactors

My colleague, X. Xiang, had previously identified PANX1 protein interactors through co-immunoprecipitation (co-IP) and subsequent mass spectrometry of PANX1 in Rh30 and RD rhabdomyosarcoma cell lines ectopically over-expressing PANX1, grown in either suspension or adhesion conditions, with a single replicate for each condition (unpublished). He further identified PANX1 interactors using the BioID method [119] in both Rh30 and RD cells grown in adhesive culture, and completed three replicates for each cell line (unpublished). Any protein interactor for which a single replicate in any cell line of a single growth condition was included for cross-referencing, however only interactors which were identified by either both methods, or by a single method and either in more than one replicate or more than one cell line/growth condition were considered for further interpretation as these were more likely to be true PANX1 interactors.

Ubiquitin pathway and proteasomal-related groups of proteins were selected from HUGO Gene Nomenclature Committee database (https://www.genenames.org/data/genegroup/#!/) using the search term "ubiquitin" and "proteasome." The following lists of proteins were downloaded:

1. HECT and RLD (RCC1-like domain) domain-containing E3 ubiquitin protein ligases
2. Linear ubiquitin chain assembly complex
3. MINDY (motif interacting with ubiquitin-containing novel DUB family) deubiquitinases
4. Pellino E3 ubiquitin protein ligases
5. RBR E3 ubiquitin ligases
6. Ubiquitin C-terminal hydrolases
7. Ubiquitin conjugating enzymes E2
8. Ubiquitin like modifier activating enzymes
9. Ubiquitin protein ligase E3 component n-recognins
10. Ring finger proteins
11. Cullins
12. U-box domain containing proteins
13. Anaphase promoting complex group
14. Membrane associated ring-CH-type fingers (MARCH)
15. Ubiquitin specific peptidases
16. ZUP1 (zinc finger-containing ubiquitin peptidase 1) deubiquitinase
17. Proteasome

The Ubiquilin family was additionally included as these proteins contain ubiquitin-interacting domains and interact with the proteasome to act as receptors of ubiquitinated proteins [120]. The UBX domain-containing proteins was also included as these proteins are predominantly identified as cofactors of the AAA ATPase Cdc48/p97, a complex known to interact with ubiquitinated proteins and mediate their proteolysis [121]. As the E3 ubiquitin ligase list obtained from this database was incomplete, I further complemented this list with one generated by Medvar *et al*. (2016) [122]. Lastly, a most recent list of DUBs

indicated the existence of 91 active DUBs, rather than the 87 listed [123] in the HGNC database, and so the dataset from Table 1 of Coyne & Wing (2016) [49] was included. These proteins were cross-referenced against the putative hits identified by PANX1 co-IP and BioID.

Additional ubiquitin-related proteins, which do not mediate proteasomal degradation, haphazardly found through reading literature were cross-referenced with the PANX1 interactome and briefly mentioned in the discussion.

3.0 RESULTS

3.1 PANX1 is post-translationally modified by ubiquitination

Ubiquitination is a versatile modification, which regulates protein stability, protein-protein interactions, and subcellular localization, according to the extent and structure of the ubiquitin chain(s) tagged onto the target protein [61]. To verify that PANX1 ubiquitination can be detected by *in vivo* ubiquitination assays, as PANX1 ubiquitination has only been demonstrated by high throughput mass spectrometry screens to date [33], and to uncover the fundamental type of ubiquitin chains forms, PANX1 ubiquitination was examined in HEK293T cells. Ectopic myc-DDK-tagged PANX1 (further referred to as myc-PANX1 in this report) was immunoprecipitated from HEK293T cells co-expressing HA-ubiquitin and subjected to western blotting (**Fig. 1A,B**). Both mono-ubiquitinated species (at ~61 kDa) and numerous polyubiquitinated species were detected. These results were validated by reverse immunoprecipitation using myc-tag antibody for the pulldown and then probing for the HA-tag (**Fig. 1C**), which also demonstrated a characteristic higher molecular weight smear.

To characterize the polyubiquitin chain type appended to PANX1 and gain insight with regards to the role ubiquitination plays on regulating PANX1, PANX1 was immunoprecipitated from Rh30 cells transiently over-expressing myc-PANX1 and subsequently probed with linkage-specific antibodies. K48 polyubiquitin immunoblotting revealed a strong higher molecular weight smear in the PANX1 eluates, comparable to the K48 polyubiquitination detected on the Traf2 positive control, which was not visible in the empty vector controls (**Fig. 2A**). Immunoprecipitates were then probed with an anti-K63 chain antibody (**Fig. 2B**). Although the signal is weak, my results suggest that PANX1 can also be modified by K63-linkages *in vivo* in Rh30 cells. Thus, I have shown for the first time that PANX1 is both monoubiquitinated and polyubiquitinated by K48 and K63 linkages, revealing the multifaceted nature by which PANX1 may be regulated by the ubiquitination system.

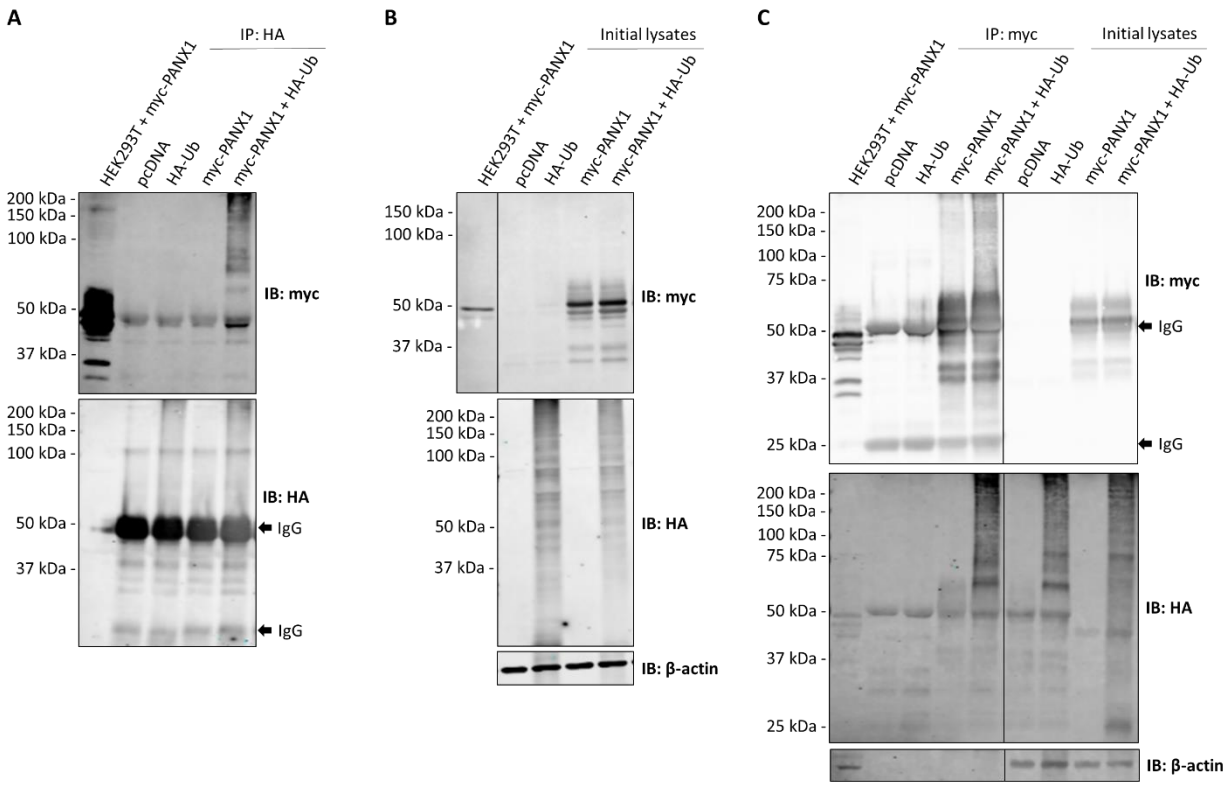

Figure 1. myc-PANX1 is both mono- and polyubiquitinated. HEK293T cells ectopically expressing an empty vector (pcDNA), HA-ubiquitin (HA-Ub) and pcDNA, myc-PANX1 and pcDNA, or both myc-PANX1 and HA-Ub, were treated with 10 μM MG132 for 16 hours. The lysates were subjected to immunoprecipitation (IP) with HA-tag antibody. All of the IP eluates were loaded (**A**), and 30 μg of the initial lysates were loaded per well (**B**). Lysate of HEK293T cells transfected with myc-PANX1 were used as positive control for detection with anti-myc antibodies. β-actin served as the loading control. N=4. The lysates were also subjected to reverse immunoprecipitation with myc-tag antibody (**C**). All of the eluates were loaded, and 30 μg of initial lysates were loaded per well. N=2. IgG bands are indicated by arrows in each of the immunoprecipitations. β-actin served as the loading control.

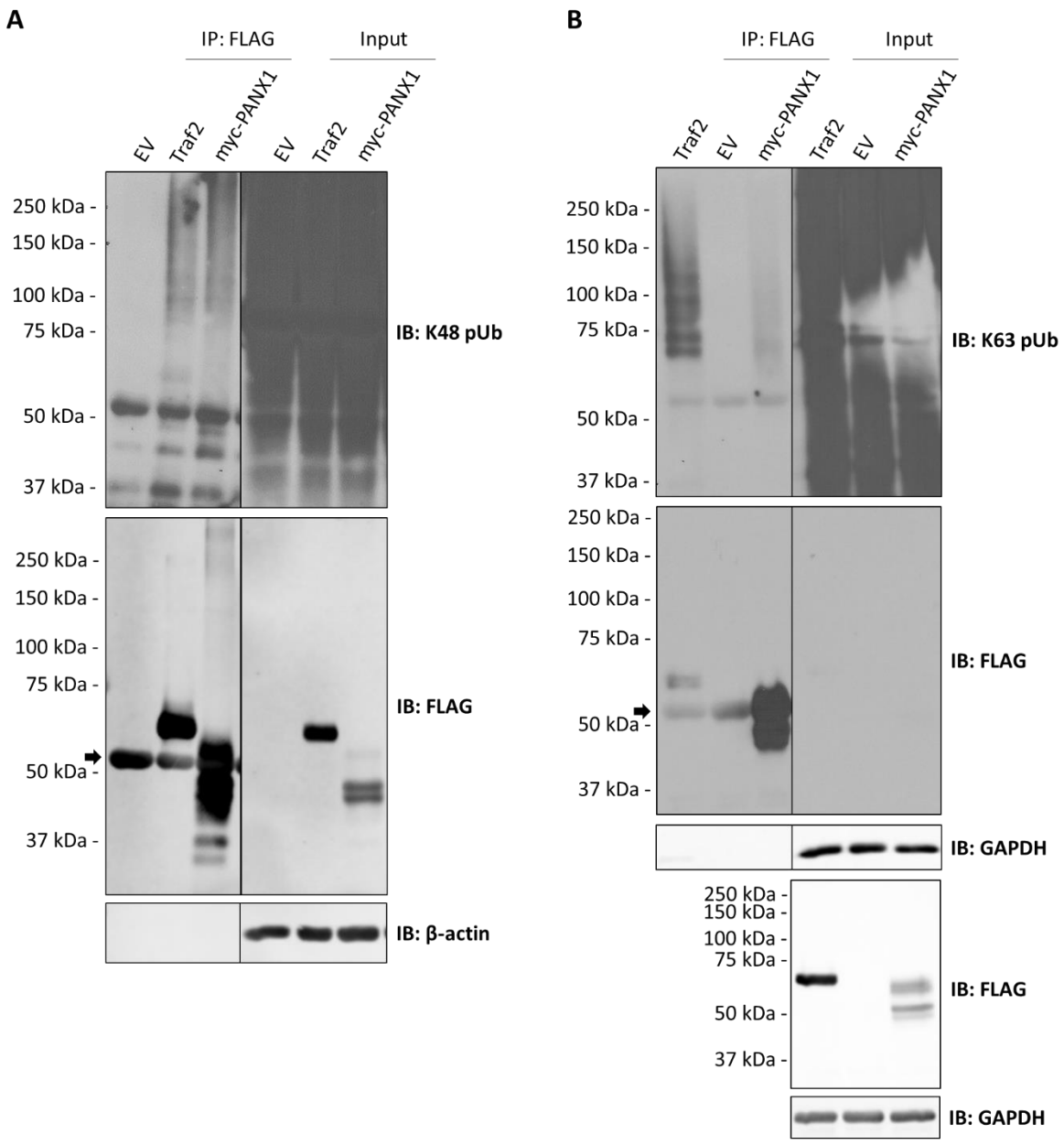

Figure 2. myc-PANX1 is modified by both K48- and K63-linked polyubiquitin chains in Rh30 cells. Rh30 cells transfected with myc-PANX1, FLAG-Traf2 (positive control), or an empty vector control (EV), were treated with 10 μM MG132 (**A**) or untreated (**B**) for 16 hours. Protein lysates were subjected to immunoprecipitation (IP) using FLAG-tag antibody. All of the IP eluates were loaded, and 20 μg of the initial lysates were loaded per well. GAPDH and β-actin serve as the loading controls. The input proteins were re-run on a separate gel for better visualization, shown in the bottom panel (**B**). N=3. IgG bands are indicated by arrows in each of the immunoprecipitations.

3.2 PANX1 interacts with numerous components of the ubiquitin-conjugating system and the proteasomal degradation pathway

As multiple lines of evidence strongly suggest that PANX1 is post-translationally modified with ubiquitin, the next logical course of action is to delineate the modulators of this pathway. I had at my disposal a list of PANX1 interacting proteins identified by my colleague, Xiao Xiang, PhD (c). He generated a list of putative PANX1 interacting proteins using both the BioID method [119] and a mass spectrometry-based co-immunoprecipitation (co-IP) proteomics screen of epitope-tagged PANX1. By cross-referencing these lists with known components of the ubiquitin system and the proteasomal degradation pathway, I identified potential candidates of the ubiquitination pathway that interact with PANX1. While the BioID method was used in both Rh30 and RD RMS cell lines under adherent growth conditions (n=3 each), and the co-IP was used with Rh30 and RD cells, using both suspension and adherent growth conditions, with only a single replicate obtained per cell line per condition, I included all hits identified in at least a single replicate (**Fig. 3**). The interactors identified by both methods include ubiquitin, the UBE2L3 E2 conjugating enzyme, the E3 ligase UBR4, the proteasomal subunits PSMC2 and PSMD2, and the UBX domain-containing protein UBXN4. Interactors that were identified in more than one replicate, in more than one growth condition, or in more than one cell line, include the E2 conjugating enzyme UBE2J1, the E3 ligase TRIM28, the proteasomal subunit PSMA7, and the deubiquitinating enzymes USP3, USP14, and USP48. Finally, the highest confidence PANX1 interactors, which were identified by BioID for Rh30 (n=3) *and* RD (n=3), are ubiquitin, USP14, and UBXN4. While these interactions remain to be validated, they provide a starting point for investigating the mechanistic pathway of PANX1 ubiquitination and may provide some insight into the results obtained from my experiments.

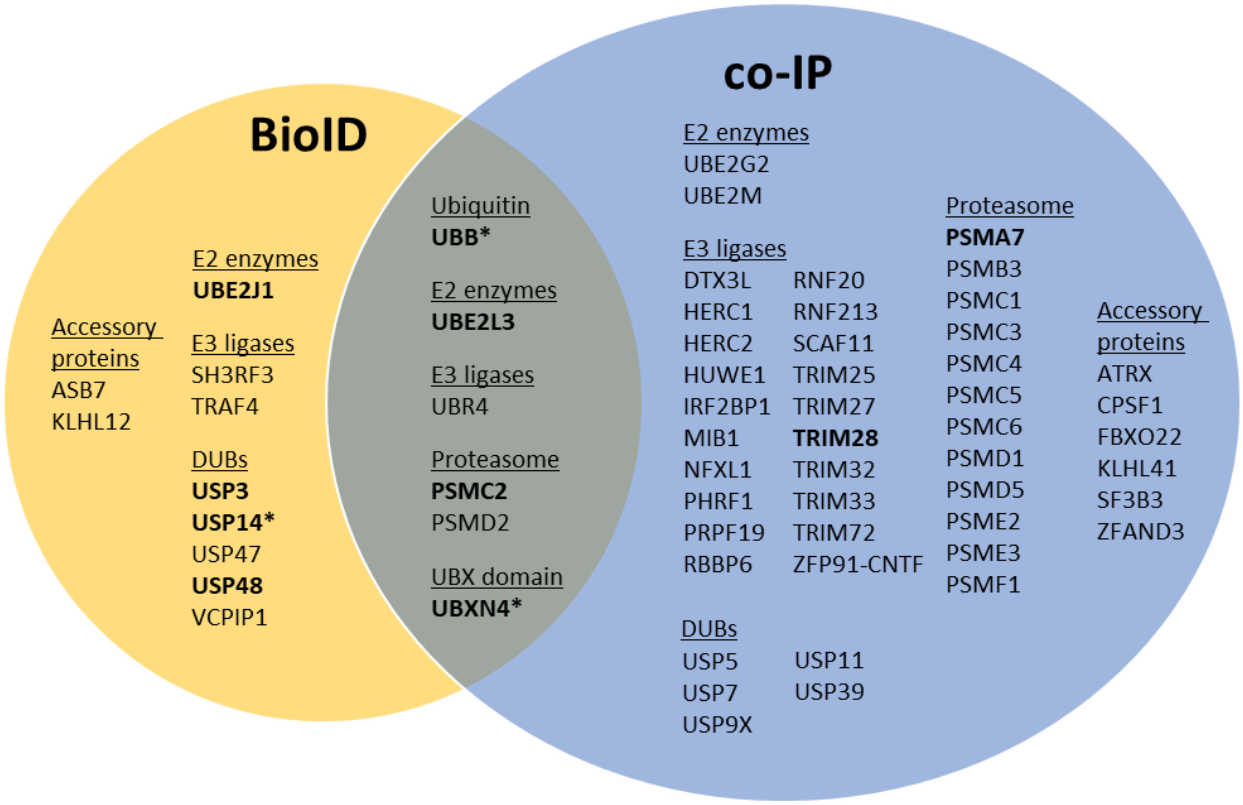

Figure 3. The ubiquitin pathway-related proteins, ubiquitin, UBE2L3, UBR4, PSMC2, PSMD2, and UBXN4 were identified as PANX1 interactors by two proteomic screening methods. BioID and co-immunoprecipitation in Rh30 and RD cell lines ectopically expressing PANX1 were conducted by X. Xiang to identify the PANX1 interactome. Proteins pertaining to the ubiquitin conjugating/deconjugating pathway, the proteasome, or associated accessory proteins, identified within one replicate are listed. Bold, proteins identified in either both cell lines, or in both adherent and suspension growth conditions, or in more than one replicate. *Proteins identified by BioID in both Rh30 and RD cells (n=3, each).

3.3 Proteasomal inhibition regulates PANX1 protein levels

K48 polyubiquitin chains are the most abundant linkages found in cells and serve the primary function of marking proteins for proteasomal degradation [62]. As we discovered that myc-PANX1 is K48 polyubiquitinated, and have also identified various subunits of the 26S proteasome as PANX1 protein-interactors, we wanted to determine if PANX1 levels are regulated by the proteasome. Although the relative contribution of protein synthesis pathways versus degradative pathways cannot be gauged by looking at steady state protein levels at a single time point, evaluating protein abundance following proteasomal inhibition may illuminate whether this pathway participates in regulating protein levels [124]. To this end, Rh30 cells transiently over-expressing either untagged PANX1 or myc-PANX1 were treated

with 10 μM of MG132 to inhibit the 26S proteasome (**Fig. 4A**). Western blots were run on the protein lysates and PANX1 levels were quantified by densitometry. While MG132 treatment did not affect the total untagged (~39-50 kDa) protein, it did significantly increase total myc-tagged PANX1 (~46-57 kDa) protein levels by 1.9 fold (**Fig. 4C**). Interestingly, the banding pattern of PANX1 shifts toward the lesser glycosylated species after MG132 treatment. Specifically, MG132 treatment results in a significant increase in the Gly0 species levels and a decrease in the Gly2 species levels (**Fig. 4D-E**). MG132 also significantly increased the expression of lower molecular weight species (which will hereinafter be referred to the -1, -2, -3, and -4 species) which are detected at ~44.5, 41.5, 36.5 and 34 kDa, respectively, for myc-PANX1, and are detected in the untagged protein at molecular weights of ~38, 35.5, 30, and 27 kDa. The same trend was observed on myc-PANX1 in cells treated with the proteasomal inhibitor lactacystin, confirming that this banding pattern change is a consequence of proteasomal inhibition (**Fig. 4B**). Since the complex glycosylated species Gly2 has been associated with localization at the cell surface, and the un-glycosylated core Gly0 and high mannose Gly1 species are mainly localized in intracellular compartments treatment [1,7], I then examined PANX1 localization following MG132. Immunolabeling of PANX1-transfected Rh30 cells shows that both untagged and myc-tagged PANX1 in DMSO control-treated cells are localized to the plasma membrane with intracellular staining, while MG132 treatment resulted in a large increase in intracellular PANX1 (**Fig. 4F**), paralleling the increase in Gly0 and Gly1 species demonstrated through western blotting in **Fig. 4A**. It should be mentioned that PANX1 distribution patterns were quite heterogeneous in these cells. Ectopic PANX1 had varying levels of localization to intracellular compartments, displaying both diffuse and punctate staining patterns, and presented at the cell surface to varying degrees. Due to the dominating heterogeneity of PANX1 immunofluorescence labelling, changes in PANX1 plasma membrane levels following MG132-treatment could not be visually discerned.

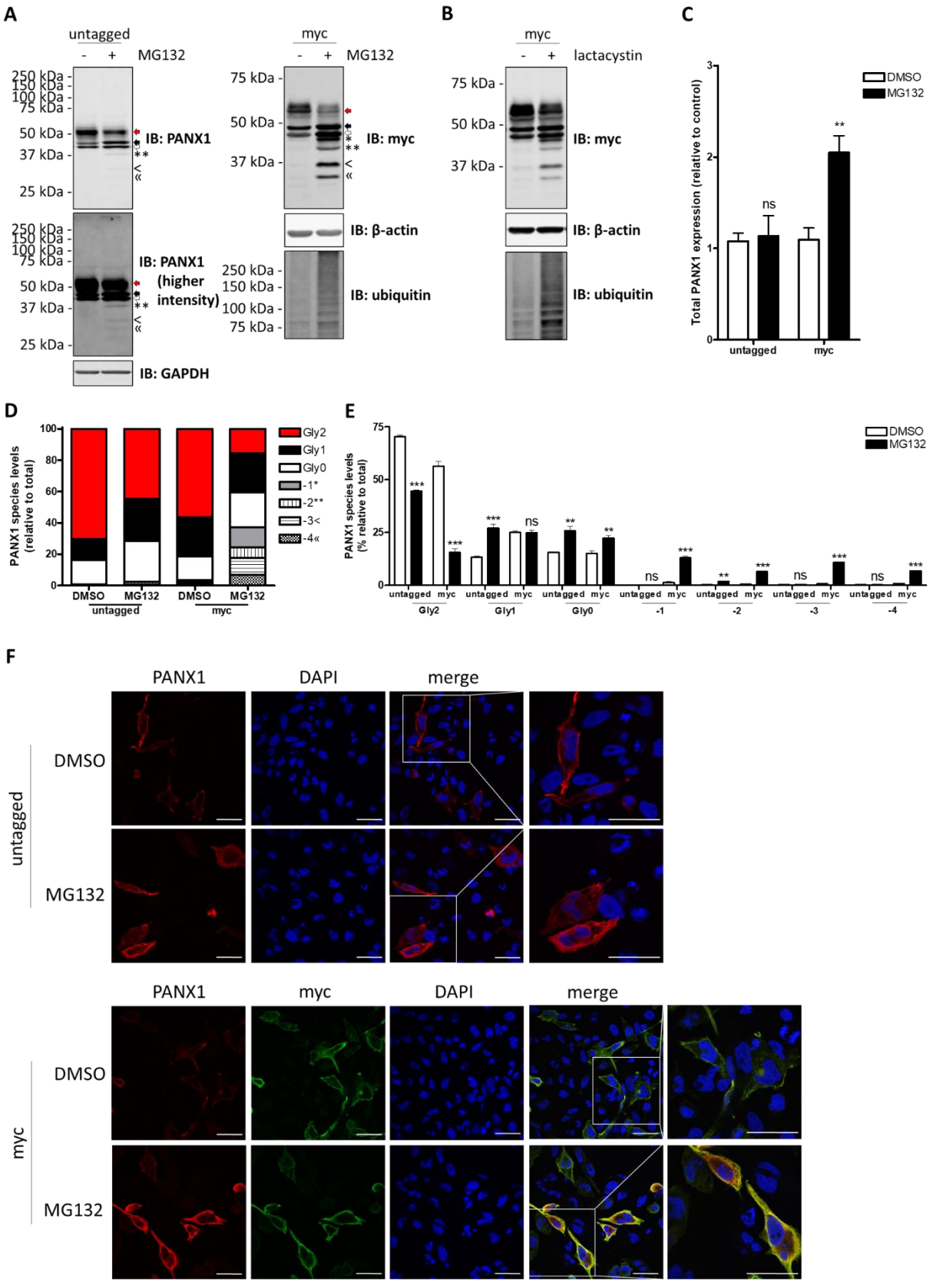
A
untagged
- + MG132
250 kDa
150 kDa
100 kDa
75 kDa
50 kDa
37 kDa
25 kDa
IB: PANX1
IB: PANX1 (higher intensity)
IB: GAPDH
myc
- + MG132
75 kDa
50 kDa
37 kDa
IB: myc
IB: β-actin
250 kDa
150 kDa
100 kDa
75 kDa
IB: ubiquitin
B
myc
- + lactacystin
75 kDa
50 kDa
37 kDa
IB: myc
IB: β-actin
IB: ubiquitin
C
DMSO
MG132
Total PANX1 expression (relative to control)
ns
**
untagged
myc
D
PANX1 species levels (relative to total)
Gly2
Gly1
Gly0
-1*
-2**
-3<
-4«
DMSO
MG132
DMSO
MG132
untagged
myc
E
DMSO
MG132
PANX1 species levels (% relative to total)
***
ns
**
untagged
myc
Gly2
Gly1
Gly0
-1
-2
-3
-4
F
PANX1
DAPI
merge
untagged
DMSO
MG132
PANX1
myc
DAPI
merge
myc
DMSO
MG132

Figure 4. Proteasomal inhibition by MG132 changes the PANX1 banding pattern and induces the expression of lower molecular weight bands in Rh30 cells. Rh30 cells transfected with untagged human PANX1 (PANX1) or with myc-tagged PANX1 were treated with 10 μM MG132 or DMSO (**A**) for 16 hours. myc-PANX1-expressing Rh30 cells were similarly treated with 10 μM lactacystin or H_2O control (**B**). 30 μg of protein lysates were loaded per well for the western blots (**A,B**). GAPDH and β-actin serve as the loading control. N=3. Total protein expression of the MG132-treated samples was quantified by densitometry and statistical significance was analyzed by t-test (**C**). Error bars are standard deviation. **p<0.01; ns, no significance. The individual species (Gly0, white arrow; Gly1, black arrow; Gly2, red arrow) and the lower molecular weight bands (-1 *; -2 **; -3 <; -4 «) were quantified relative to total PANX1 expression (**D**) and its statistical significance determined (**E**). *p<0.05; **p<0.01. N=3. The same samples were labelled for PANX1 in red, myc in green, and DAPI in blue (**F**). N=3. Scale bar represents 40 μm.

To elucidate within which subcellular compartments PANX1 expression is primarily modulated following proteasomal inhibition, Rh30 cells ectopically over-expressing myc-PANX1 were treated with 10 μM of MG132 and co-immunolabeled with various organelle markers for subsequent confocal microscopy imaging. Myc-PANX1 (green) localization overlapped with the ER-marker calnexin (red) in untreated cells, and PANX1 localization to the ER is increased with MG132 treatment in a subset of the transfected cells (**Fig. 5A**). Co-localization with the cis-Golgi network is minimal in untreated cells, and proteasomal inhibition did not noticeably increase co-labelling (data not shown). No localization to the mitochondria was observed under either condition (data not shown). Finally, while myc-PANX1 (green) was notably superimposed with the lysosomal marker LAMP1 (red) under normal conditions in a subpopulation of cells, intriguingly, MG132-treatment decreased their co-localization (**Fig. 5B**). To gauge whether PANX1 expression levels at the plasma membrane are also affected by MG132 treatment, cell surface levels of myc-PANX1 were quantitatively assessed using cell surface biotinylation followed by immunoprecipitation of the biotinylated proteins. Quantification by densitometry demonstrates that absolute levels of myc-PANX1 at the plasma membrane are increased by ~3.6 fold following MG132 treatment, with all three glycosylation species detectable at the cell surface under both conditions (**Fig. 5C,D**). The increase in cell surface myc-PANX1 is primarily achieved through an increase in the presence of the Gly0 and Gly1 species (**Fig. 5E**). The relative proportion of total myc-PANX1 localized to the cell surface is significantly increased from 1.6% in DMSO-treated cells to 3.9% in MG132-treated cells (**Fig. 5F**). We also observed that the change in relative percentage of the individual glycosylation species

compared to the total myc-PANX1 levels at the cell surface is reflective of the change in the species banding profile in the whole cell lysates, with small amounts of the -1, -2, -3, and -4 species also present at the plasma membrane (**Fig. 5G**). Collectively, these results show that the MG132-induced increase in PANX1 protein levels can partially be accounted for by a specific increase in ER and plasma membrane-localized PANX1, suggesting that these pools of PANX1 are being modulated by the proteasome. My data also points to a possible interplay between the lysosomal and proteasomal degradation systems on regulating PANX1 expression.

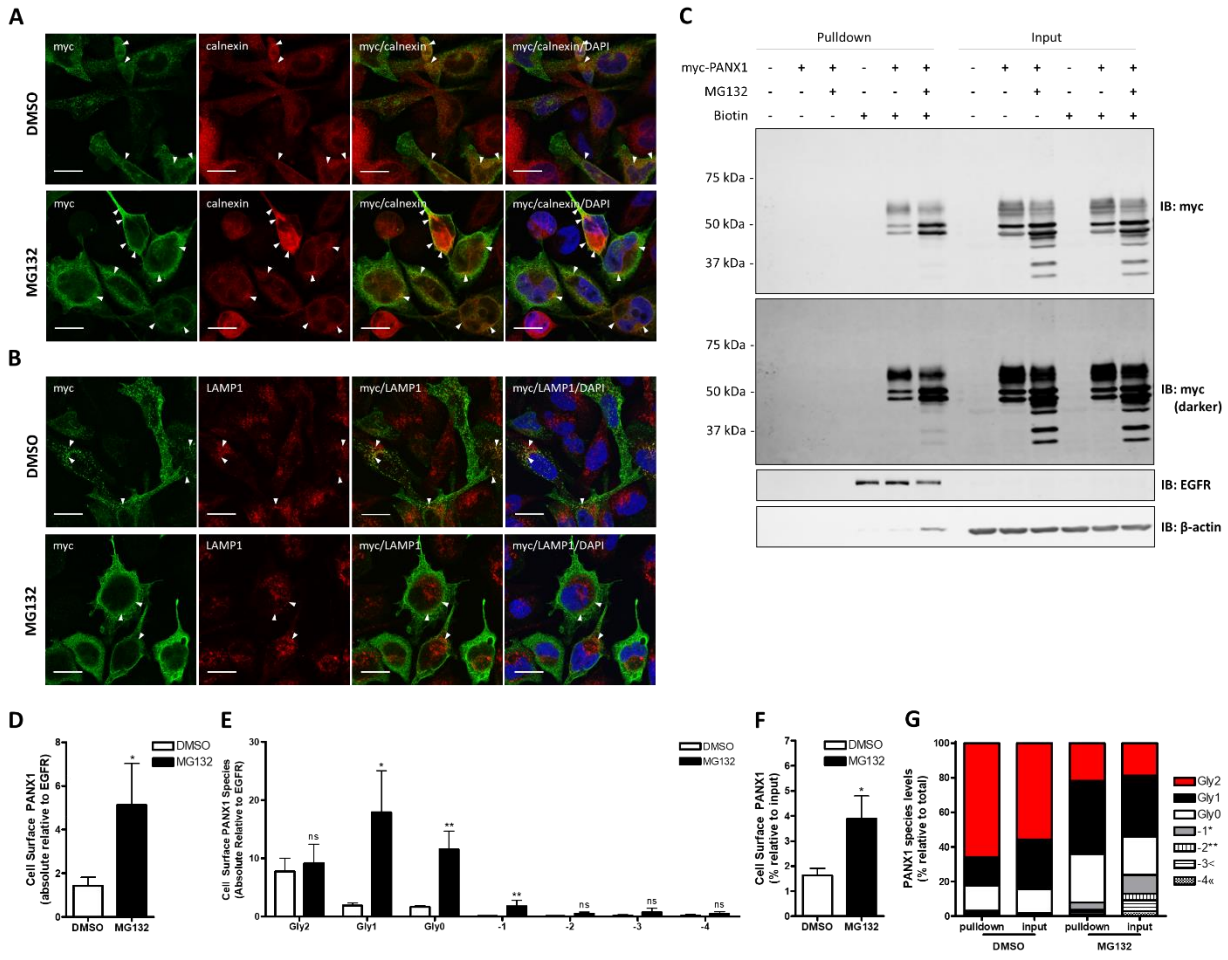

Figure 5. MG132 treatment increases myc-PANX1 localization to the endoplasmic reticulum and plasma membrane, and decreases its co-localization with a lysosomal marker. Rh30 cells ectopically expressing myc-PANX1 were treated with either 10 μM MG132 or DMSO for 16 hours. The cells were co-labelled for myc (PANX1) (green) together with calnexin (ER marker) (**A**) or LAMP1 (lysosomal marker) (**B**) in red. Representative images show co-localization with calnexin and LAMP1 (arrow heads). N=3.

Scale bar = 20 μm. Localization at the plasma membrane was assessed by cell surface biotinylation experiments on Rh30 cells transfected with myc-PANX1 and treated with either 10 μM MG132 or DMSO for 16 hours (**C**). EGFR is the plasma membrane marker. β-actin serves as the cytosolic marker. 50% of the pulldown and 30μg of input was loaded per well. Absolute levels of cell surface myc-PANX1 were quantified by densitometry and normalized to the EGFR pulldown control (**D**). T-test was used to compare the levels between the MG132 and DMSO samples. The absolute levels of the individual myc-PANX1 species were quantified in the same manner (**E**). Cell surface expression was quantified relative to the total protein level in the input lane, which was normalized to the β-actin loading control (**F**). Error bars are standard deviation. *$p<0.05$; **$p<0.01$; ns, no significance. The percentage of each individual myc-PANX1 species relative to total PANX1 detected is shown for the pulldown and input under both conditions (**G**).

PANX1 has been described in literature as three glycosylation species (Gly0, Gly1, Gly2) through western blot analysis, without mention of the -1, -2, -3 and -4 LMW species [7,8]. Therefore, to verify that the myc-PANX1 immunoreactive LMW species which are strongly detected following MG132-treatment are indeed PANX1, lysates of Rh30 cells ectopically over-expressing myc-PANX1, untagged PANX1, or an empty vector control, were treated with MG132 and probed with an anti-PANX1 antibody targeting an epitope on the C-terminus (**Fig. 6A**). These LMW species were detected by both anti-PANX1 and anti-myc tag antibodies. To discount the possibility that these LMW species are an artifact of transient over-expression, the PANX1 banding profile was next examined in the neuroblastoma cell line Sk-N-Be(2), which endogenously expresses PANX1, under the influence of MG132 (**Fig. 6B**). Similar to the ectopically expressed proteins, four lower molecular weight species of endogenous PANX1 were detected in the MG132-treated samples corresponding to the same molecular weights as their ectopically expressed counterparts.

Sustained proteasomal inhibition can lead to apoptosis through the ER-stress-induced unfolded protein response [125], and given that PANX1 is a substrate of caspases 3 and 7 [35], I next assessed whether these LMW species are the result of caspase cleavage. LMW species of PANX1 were still detected in cells concurrently treated with MG132 and the pan-caspase inhibitor Z-VAD-FMK (**Fig. 6C**). All together these data indicate that the lower MW bands detected by anti-PANX1 antibodies following MG132 treatment correspond to PANX1 species and are not the products of caspase cleavage.

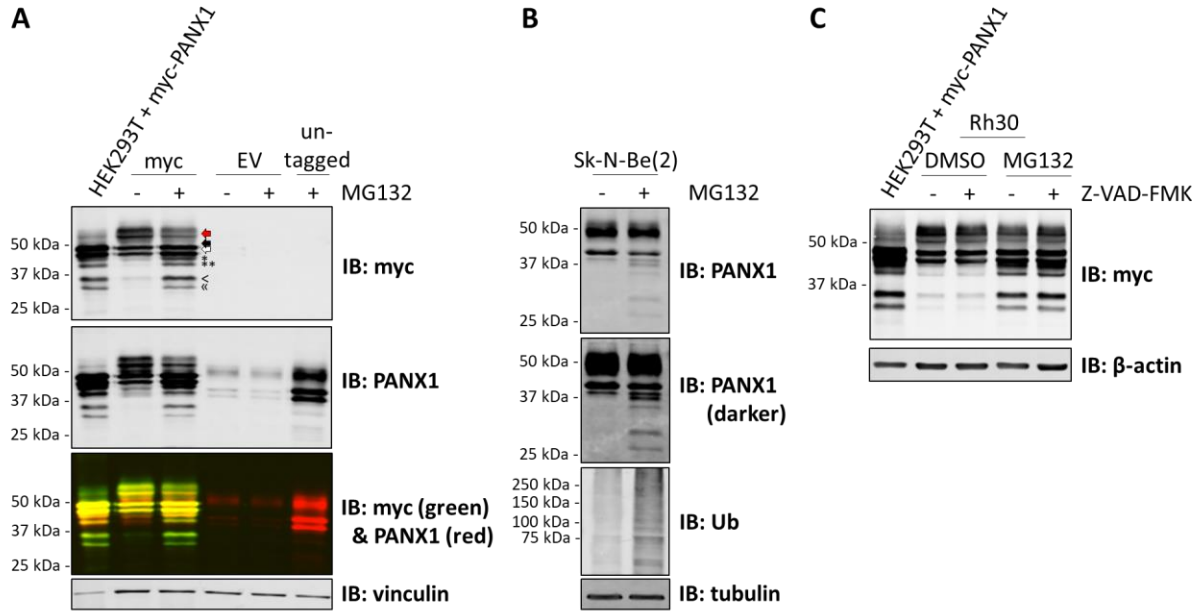

Figure 6. MG132 induces the expression of PANX1 lower molecular weight bands through a process independent of caspase-cleavage. Rh30 cells transfected with empty vector control, untagged and myc-tagged PANX1 were treated with 10 µM MG132 (+) or DMSO (-) for 16 hours (**A**). 40 µg of myc-PANX1 and empty vector protein was loaded per well, and 20µgof untagged PANX1 was loaded per well. The lysates were probed for myc and PANX1 (C-terminus). Vinculin serves as the loading control. HEK293T cells transfected with myc-PANX1 are the antibody control. The glycosylation species (Gly0, white arrow; Gly1, black arrow; Gly2, red arrow) and the lower molecular weight bands (-1 *; -2 **; -3 <; -4 «) are indicated. The lower molecular weight species are also induced by MG132 treatment in the neuroblastoma cell line Sk-N-Be(2) which endogenously express PANX1 (**B**). The lower molecular weight species are not products of caspase cleavage (**C**) as pan-caspase inhibition with 20 µM Z-VAD-FMK in cells concurrently treated with 10 µM MG132 did not diminish the expression of these bands.

3.4 PANX1 is not primarily degraded by the 26S proteasome

As my data indicates that PANX1 is K48-polyubiquitinated and that PANX1 protein expression is altered following proteasomal inhibition, I wanted to establish if PANX1 is directly degraded by the 26S proteasome. To evaluate this prospect, protein stability was examined by cycloheximide (CHX) chase in the presence of MG132, with the expectation that proteasomal inhibition should increase the stability of PANX1 if it is directly degraded by the proteasome [124]. To measure PANX1 protein kinetics, Rh30 cells expressing myc-PANX1 were treated with 35 µg/mL of cycloheximide to inhibit protein synthesis, and either 10 µM of MG132 or DMSO control (**Fig. 7A**). The proteins were harvested at 0, 6, and 24 hours of drug treatment in order to capture the long half-life predicted for PANX1 [27]. Surprisingly, my results showed that MG132 did not significantly increase the half-life of total myc-PANX1, as no

difference in PANX1 protein levels was seen at any time point under either condition (**Fig. 7B**). The respective half-lives of PANX1 when treated with DMSO and MG132 were calculated at 37.9 hours and 25.6 hours.

As treatment with CHX could lead to off-target effects on both PANX1 expression regulation and on the proteolytic degradation systems [77], and the possibility that these systems are further dysregulated due to the simultaneous treatment with two toxic drugs, these results were then corroborated through a radioactive amino acid pulse-chase technique. Rh30 cells transiently expressing myc-PANX1 were pulsed for one hour with [^{35}S]-methionine/cysteine and then chased in complete media containing excess methionine and cysteine (**Fig. 7C**). Proteins were collected at 0, 3, 6 and 24 hours of chase, and PANX1 was purified by immunoprecipitation to measure the amount of radioactive signal relative to total PANX1 emitted at each time point. Unexpectedly, analysis of the 24 hour time course shows that there is a trend for increased myc-PANX1 degradation with proteasomal inhibition (**Fig. 7E**). A possible explanation may be that the cells are increasing autophagy due to the sustained unfolded protein response and precipitant ER stress [102,126]. Alternatively, autophagy can be activated in a manner independent of ER stress to promote increased protein degradation [127]. Therefore, further analysis of the 6 hour time course was conducted and showed no difference in degradation (**Fig. 7F**). The half-lives measured of myc-PANX1 under DMSO and MG132-treated conditions were approximately 4.3 and 5.3 hours, respectively. These results suggest that myc-PANX1 is not primarily degraded by the proteasome despite being modified by K48 polyubiquitin chains.

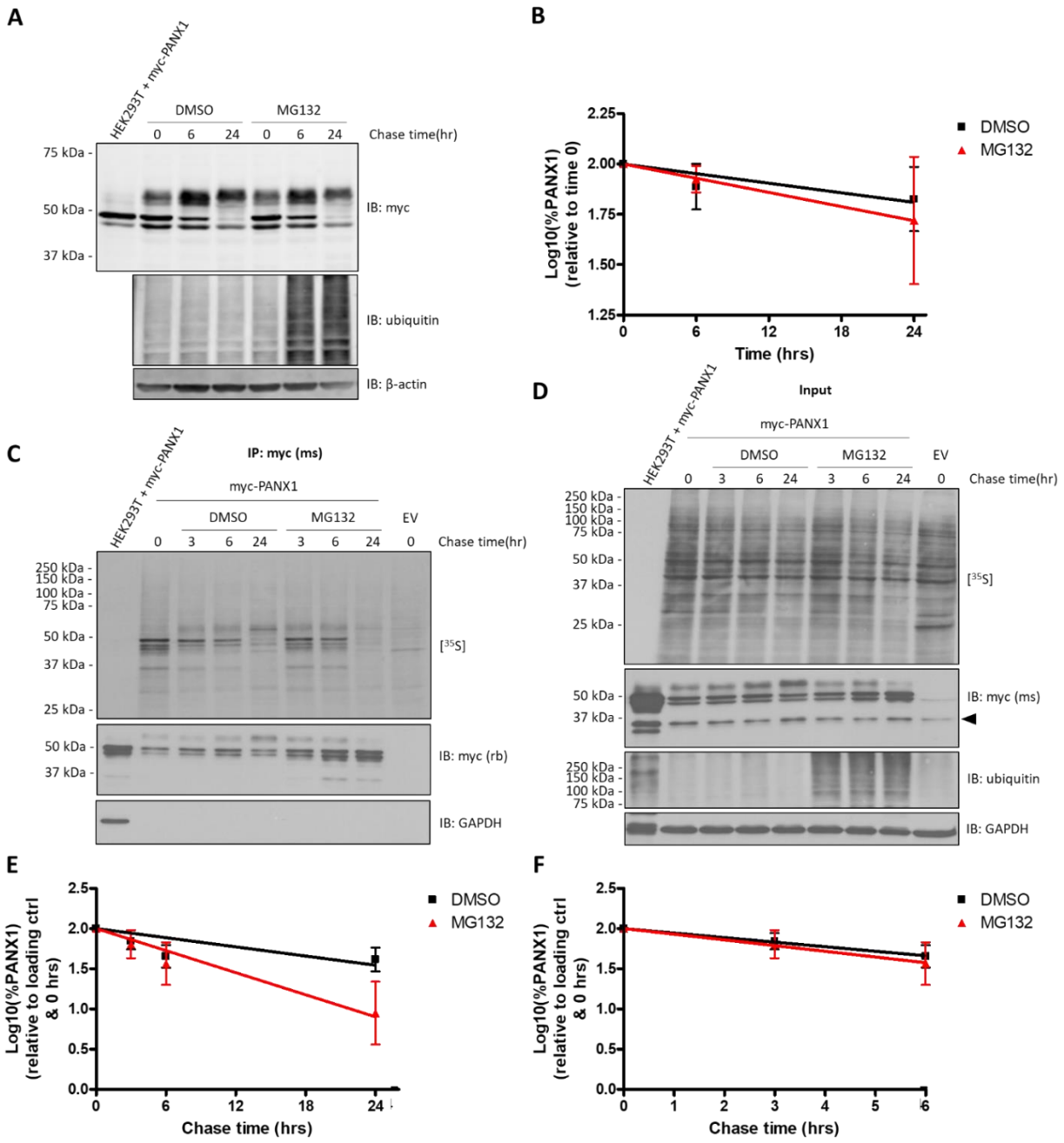

Figure 7. PANX1 is not primarily targeted for degradation by the 26S proteasome. Rh30 cells transfected with myc-PANX1 were treated with 35 µg/mL of cycloheximide and either 10 µM MG132 or DMSO (**A**). The proteins were harvested at 0, 6 and 24 hours. Total myc-PANX1 levels were quantified according to their loading controls, then normalized to their 0-hour controls, where time 0 is 100%. The Log10 of the percentage remaining was plotted on the Y-axis (**B**). The half-life for the DMSO and MG132 treated myc-PANX1 are 37.9 and 25.6 hours, respectively. N=3. Rh30 cells transiently expressing myc-PANX1 were pulsed for 1 hour with 100 µCi/mL of [35S]-labelled methionine/cysteine, then chased for 0, 3, 6, and 24 hours with complete media. 100 µg of initial lysates were subjected to immunoprecipitation with myc-tag antibody of mouse origin (IP: myc) (**C**) with the protein expression of the input indicated, where the arrowhead indicates non-specific bands (**D**). ^{35}S levels were normalized to total

immunoprecipitated myc, and then quantified relative to 0 hours, where time 0 is 100%. The Log10 of the percent of detected radioactive myc-PANX1 was plotted on the Y-axis. A linear regression was applied for either the 24 hour time course (**E**) or the 6 hour time course (**F**). The half-lives are 5.3 and 4.3 hours for DMSO and MG132 treated myc-PANX1 according to the 6 hour time course regression, respectively. N=3. Error bars represent standard deviation.

3.5 Lysine residues 307, 381 and 409 do not mediate PANX1 regulation by ubiquitination and by the proteasome

Equally as important as the ubiquitin chain attributes are in dictating ubiquitin's function, as is the specificity of the acceptor lysine residues within the ubiquitinated protein. While numerous lysine residues can be potentially ubiquitinated in a redundant manner, in many instances, a specific lysine is crucial for ubiquitination to confer its intended regulatory effect [128,129], which may be due to the presence of other competing post-translational modifications either on the same residue or on residues in its immediate proximity [129]. To identify which of PANX1's 28 lysine residues are ubiquitinated and possibly identify additional ubiquitination sites, myc-PANX1 was immunoprecipitated from HEK293T cells and the IP eluate was sent to MSBioworks for mass spectrometry analysis. Only a single putative lysine residue, K409, was identified, which is a known PANX1 ubiquitination site [116]. Interestingly, though, a novel phosphorylation site on T382, and a known phosphorylation site on S385 [33], were identified as well.

As elucidation of the ubiquitinated lysine-residues was unsuccessful by mass-spectrometry, the role of the proteasome and of ubiquitination on regulating PANX1 protein expression, localization, and degradation, was studied by engineering a myc-PANX1 mutant containing lysine to arginine substitutions [130]. At that time, only lysine residues 307, 381, and 409 had been identified as PANX1 ubiquitination sites within literature [113–116]. Site-directed mutagenesis was employed to mutate lysine residues 307, 381 and 409 to arginine in attempt to create a ubiquitination-resistant PANX1 protein (the KR3 mutant) (**Fig. 8A**). Initial characterization showed that a similar banding pattern was observed between the KR3 mutant and wild-type myc-PANX1 when expressed in Rh30 cells, with all three glycosylation species detected (**Fig. 8B**).

To confirm that the KR3 mutant is, indeed, ubiquitination-deficient, the ubiquitination status of the KR3 mutant was assessed by immunoprecipitation. Contrary to expectations, immunoprecipitation of

lysates also expressing HA-Ub showed that the KR3 mutant can still be mono- and polyubiquitinated (**Fig. 8C,D**). KR3 ubiquitination levels were variable and comparable to WT myc-PANX1 in three replicates immunoprecipitating HA (ubiquitin) and probing for myc (PANX1) (**Fig. 8C**), as well as in a single reverse immunoprecipitation where myc (PANX1) was pulled down and subsequently blotted for HA (ubiquitin) (**Fig. 8D**).

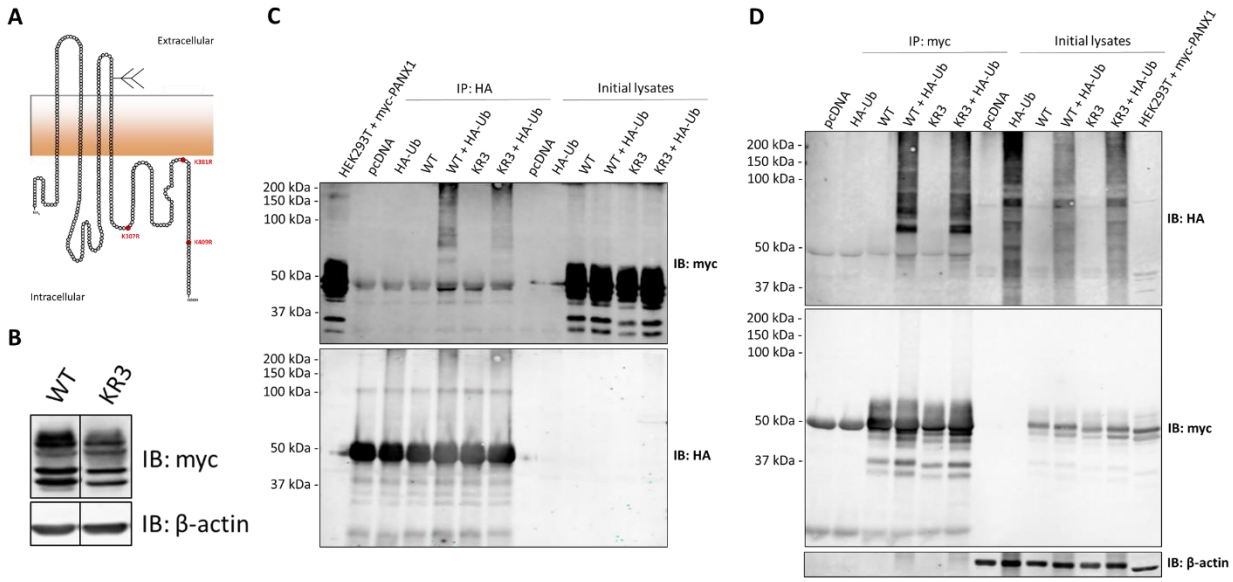

Figure 8. PANX1 construct with lysine to arginine mutations at residues 307, 381, and 409 does not have reduced ubiquitination. A diagram of human PANX1 with the mutated lysine resides indicated in red. Figure modified from Holland, S. (**A**). The wild-type PANX1 (WT) and ubiquitination-resistant mutant (KR3) PANX1 were expressed in Rh30 cells, and 30 µg of protein were loaded per well. β-actin served as the loading control (**B**). 293T cells were transfected with either the empty vector (pcDNA), HA-ubiquitin (HA-Ub) and pcDNA, WT myc-PANX1 and pcDNA, both WT myc-PANX1 and HA-Ub, KR3 myc-PANX1 and pcDNA, or KR3 myc-PANX1 and HA-Ub and treated with 10 µM MG132. The initial lysates were subjected to immunoprecipitation (IP) with HA-tag antibody to pull-down the HA-ubiquitinated-proteins for 3 replicates (n=3) (**C**), or myc-tag antibody to pull down myc-PANX1 (n=1) (**D**). All of the IP eluates were loaded, and 30 µg of the initial lysates were loaded per well. 293T cells transfected with myc-PANX1 were used as antibody controls. β-actin served as the loading control.

To further assess the relevance of these lysines in mediating the effects of MG132 on PANX1, Rh30 cells expressing myc-tagged KR3 were treated with MG132 or DMSO control (**Fig. 9A**). There was no difference in total PANX1 protein expression levels, under both untreated and MG132-treated conditions, between the WT and KR3 mutant proteins (**Fig. 9B**). MG132 induced a statistically significant increase in total protein levels of the KR3 mutant of the same magnitude measured in the WT protein

(**Fig. 9C**). Proteasomal inhibition had similar effects on the banding profile of the glycosylation species and the lower molecular weight species of the mutant compared to the wild-type protein, prompting the expression of the lower molecular weight species, significantly reducing the Gly2 species and favouring the Gly0 and Gly1 species (**Fig. 9D,E**). Altogether, these results suggest that lysine residues 307, 381 and 409 do not exclusively mediate PANX1 global ubiquitination, protein expression, nor sensitivity to MG132 treatment. Most importantly, these results also underscore the existence of alternative ubiquitinated lysine residues within PANX1.

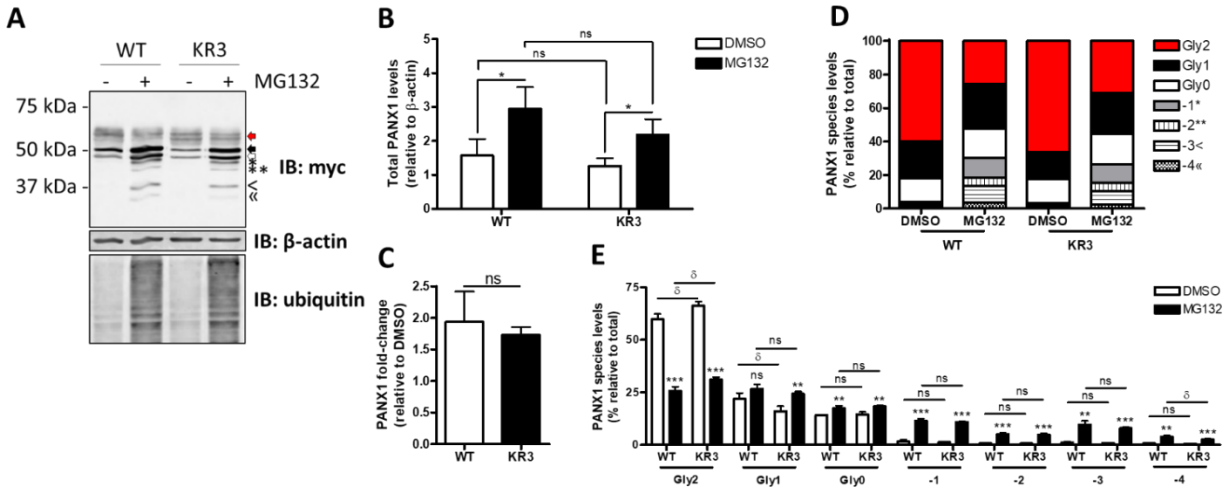

Figure 9. Preventing ubiquitination on lysine residues 307, 381 and 409 does not change the effects of MG132 on PANX1 protein levels. Rh30 cells transiently expressing either wild-type (WT) or mutant myc-PANX1 with 3 lysine-to-arginine substitutions (KR3) were treated with either 10 µM MG132 or DMSO vehicle control for 16 hours (**A**). β-actin serves as the loading control. N=3. Total protein expression (**B**) and the fold increase in total protein expression between the MG132 and DMSO-treated samples (**C**) was quantified by densitometry and analyzed by T-test. Error bars are standard deviation. *p<0.05; ns: not statistically significant. The individual glycosylation species (Gly0, magenta arrow; Gly1, yellow arrow; Gly2, red arrow) and the lower molecular weight bands (-1 *; -2 **; -3 <; -4 «) were quantified relative to total PANX1 expression (**D**) and its statistical significance analyzed (**E**). *p<0.05; **p<0.01; δ p<0.05; ns: not statistically significant. N=3.

3.6 The lysine residues targeted in the KR9 PANX1 mutant regulate PANX1 protein expression

To identify additional putative ubiquitinated lysine residues and evaluate their influence on PANX1 protein regulation, I proceeded to create another myc-PANX1 mutant targeting 9 lysine residues predicted to be ubiquitinated by online prediction softwares (UbPred, UbiProber, iUbiq-Lys, UbiSite, BDM-PUB, UbiPred, CKSAAP UbSite): residues 18, 24, 26, 204, 307, 355, 381, 409 and 415 (**Fig.**

10A). Compared to wild-type myc-PANX1, this KR9 mutant is also detected as numerous species by western blotting, with a distinct enrichment of the Gly1 species and a reduction in the Gly2 species in Rh30 cells, suggesting a possible effect on maturation and corresponding subcellular localization (**Fig. 10B**). Indeed, unlike the KR3 mutant, the lysines within the KR9 mutant may mediate regulation of PANX1 localization: through cell surface biotinylation experiments in Rh30 cells, we observed a dramatic increase in KR9 myc-PANX1 levels at the plasma membrane (**Fig. 10C**). Absolute levels of KR9 myc-PANX1 were approximately 3.5 fold higher than WT PANX1 at the cell surface, which is primarily attributable to an increase in the Gly1 species (**Fig. 10D,E**). When comparing the levels of PANX1 at the plasma membrane relative to total expression within the cell, the increase was more pronounced with 20% of the KR9 mutant detected at the surface compared to 1% of the WT protein (**Fig. 10F**).

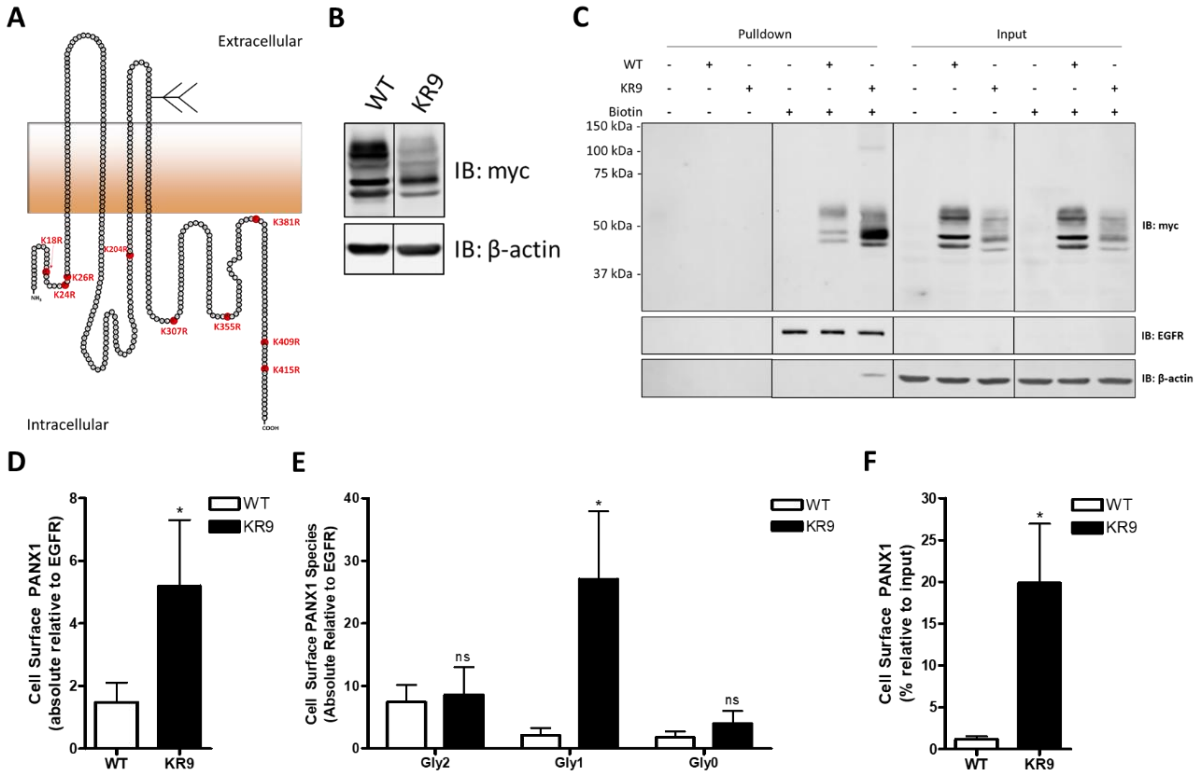

Figure 10. PANX1 construct with 9 lysine to arginine mutations has increased localization at the plasma membrane. A diagram of human PANX1 with lysine residues 18, 24, 26, 204, 307, 355, 381, 409, and 415 mutated to arginine (KR9) in red. Figure modified from Holland, S. (**A**). The wild-type PANX1

(WT) and the KR9 PANX1 mutant were expressed in Rh30 cells, and 30 μg of protein were loaded per well. β-actin served as the loading control (**B**). Mutant myc-PANX1 localization to the plasma membrane was compared to that of the wild-type protein by cell surface biotinylation experiments (**C**). Rh30 cells were transfected with an empty vector control, wild-type myc-PANX1 (WT), or the KR9 myc-PANX1 mutant (KR9). Biotinylated proteins were enriched from the cell surface using Neutravidin beads. EGFR is the plasma membrane marker. β-actin serves as the cytosolic marker. 50% of the pulldown and 30 μg of the input were loaded per well. N=3. Absolute levels of cell surface myc-PANX1 were quantified by densitometry and normalized to the EGFR pulldown control (**D**). T-test was used to compare the levels between the mutant and WT protein. The absolute levels of the individual glycosylation species were quantified in the same manner (**E**). Cell surface expression was quantified relative to the total protein level in the input lane, which was normalized to the β-actin loading control (**F**). Error bars are standard deviation. *$p<0.05$; ns: not statistically significant.

To examine the role of the KR9 mutant in mediating proteasomal regulation of PANX1, the effects of MG132 on steady-state protein expression were assessed in Rh30 cells by Western blotting (**Fig. 11A**). While absolute protein expression of the KR9 mutant was decreased compared to the WT protein (**Fig. 11B**), MG132 treatment still increased the mutant protein levels approximately 2 fold (**Fig. 11C**). However, while similar shifts were seen in the KR9 banding pattern as that of wild-type PANX1 following MG132 treatment with a prominent downward shift in the expression of the Gly2 species (**Fig. 11D**), relative expression levels of the individual glycosylation and LMW species were significantly different between the KR9 mutant and WT PANX1 (**Fig. 11E**). Most evident is the augmented increase in the Gly0 and Gly1 species, and a diminished induction of the -1, -2, -3 and -4 species following MG132 treatment in the KR9 mutant (**Fig. 11E**). In examining cells with strong ectopic PANX1 expression, , no overt differences in staining pattern were observed between the KR9 mutant and WT protein before and after MG132 treatment by immunofluorescence (**Fig. 11F**). For both proteins, Rh30 cells are heterogeneous in their PANX1 expression patterns, and MG132 treatment leads to strong intracellular PANX1 staining. Although the ubiquitination status of the KR9 mutant has yet to be appraised, this data suggests that a subset of these mutated lysine residues do indeed play a role in regulating PANX1 localization at the cell surface, and may also mediate the effects of MG132 on its protein levels.

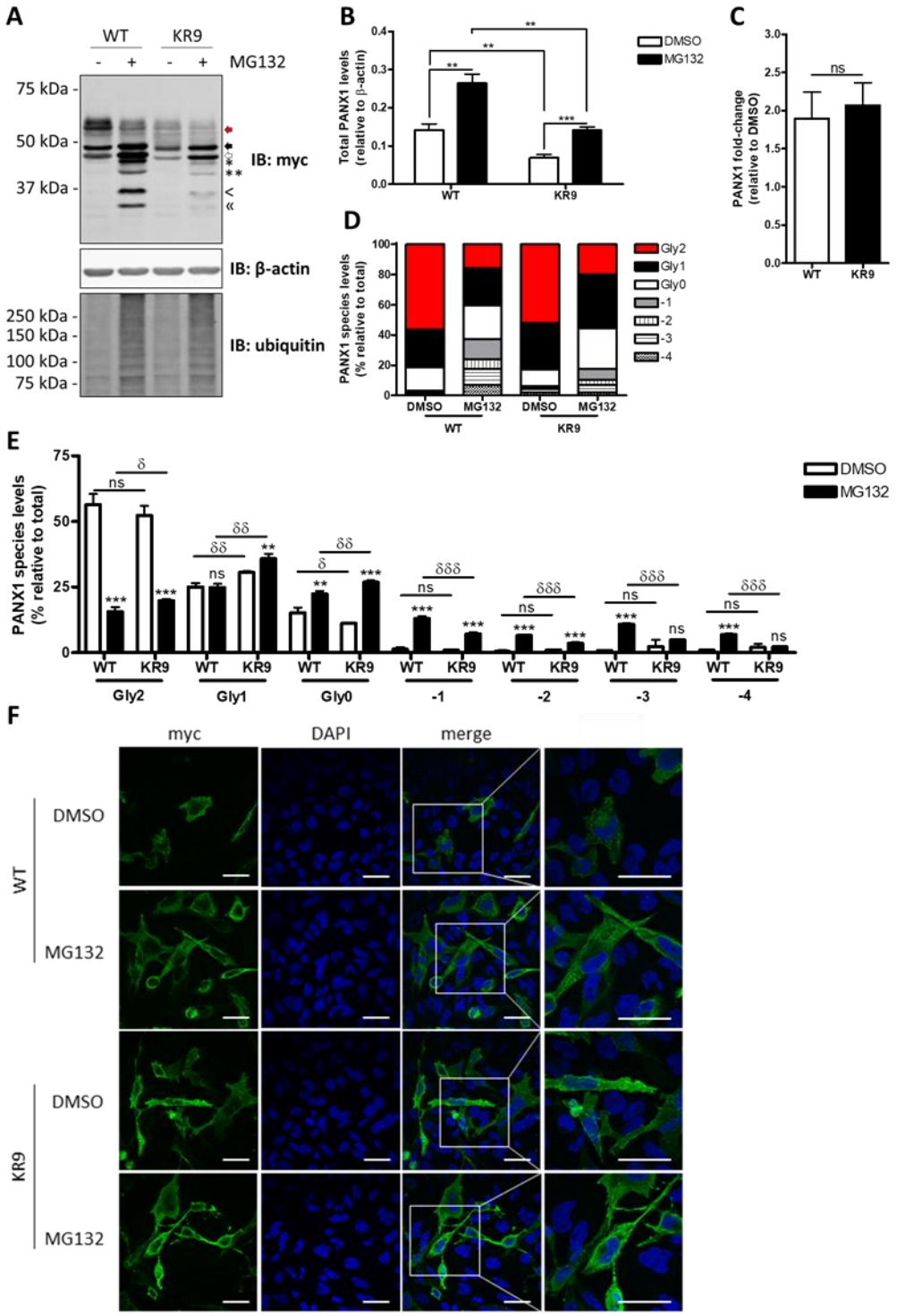

Figure 11. While the increase in total protein levels is unchanged following MG132 in the KR9 mutant compared to the wild-type PANX1, the relative proportion of the individual species levels following MG132 treatment is altered. Rh30 cells transiently expressing either wild-type (WT) or mutant myc-PANX1 with 9 lysine-to-arginine substitutions (KR9) were treated with either 10 μM MG132 or DMSO vehicle control for 16 hours (**A**). β-actin serves as the loading control. N=3. Total protein levels relative to the loading control (**B**) and the fold-increase following MG132 treatment were quantified and analyzed by

T-test (**C**). The individual glycosylation species (Gly0, magenta arrow; Gly1, yellow arrow; Gly2, red arrow) and the lower molecular weight bands (-1 *; -2 **; -3 <; -4 «) were quantified relative to total PANX1 expression quantified (**D**) and the statistical results are indicated (**E**). Error bars are standard deviation. * $p<0.05$; ** $p<0.01$; *** $p<0.001$; δ $p<0.05$; δδ $p<0.01$; δδδ $p<0.001$; ns, no significance. The same samples were labelled for myc in green and and DAPI in blue (**F**). N=3. Scale bar represents 40 μm.

3.7 PANX3 is polyubiquitinated

Data on PANX3 post-translational modifications is limited, and no studies have examined its potential modification with ubiquitin [33,41]. To determine if PANX3 is ubiquitinated, PANX3 tagged with myc-DDK on its C-terminus (referred to myc-PANX3 hereafter) was immunoprecipitated by its myc-tag from HEK293T cells co-expressing HA-tagged ubiquitin (**Fig. 12**). Western blotting demonstrated that PANX3 is polyubiquitinated, indicated by the higher molecular weight smear visible following HA-tag-probing. This provides the first proof of evidence for ubiquitination as a PANX3 post-translational modification.

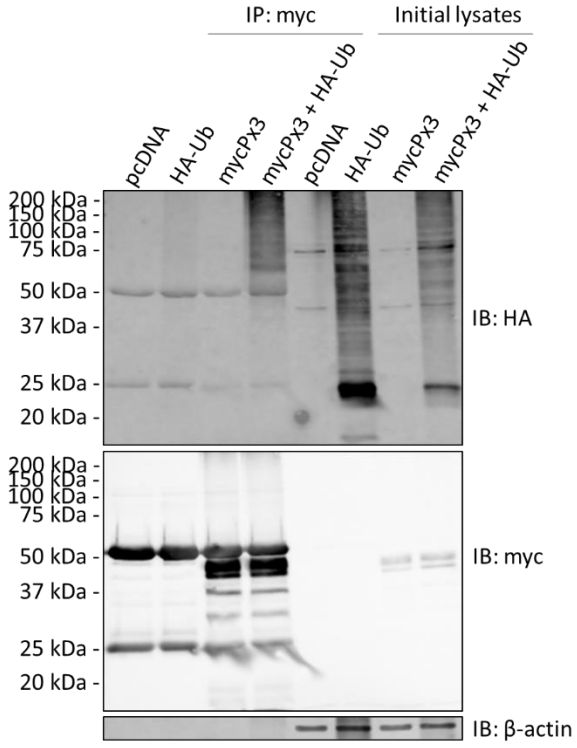

Figure 12. PANX3 is polyubiquitinated. HEK293T cells ectopically expressing an empty vector (pcDNA), HA-ubiquitin (HA-Ub) and pcDNA, myc-PANX3 and HA-Ub, both myc-PANX3 and HA-Ub were treated with 10 μM MG132 for 16 hours. The lysates were subjected to immunoprecipitation (IP)

with myc-tag antibody. All of the IP eluates were loaded, and 30 μg of the initial lysates were loaded per well. β-actin serves as the loading control. N=3.

3.8 Proteasomal inhibition regulates PANX3 protein levels

While PANX3 is presumed to be degraded by lysosomal proteolysis due to its similarities with PANX1, the mechanism of PANX3 degradation has yet to actually be analyzed [9]. As precursory experiments in order to examine the implication of the proteasomal degradation pathway in regulating PANX3, PANX3 protein expression was analyzed by western blot in Rh30 cells transiently over-expressing either untagged or myc-tagged PANX3 following the treatment of either 10 μM MG132 or DMSO control (**Fig. 13A**). Quantification densitometry demonstrates that there is an increase in the total untagged and myc-tagged PANX3 protein levels following MG132 treatment (**Fig. 13C**) of 4.5 and 13 fold, respectively (**Fig. 13D**), with a prominent increase in Gly0 species expression for both (**Fig. 13A**). On the rare occasion that high sensitivity was achieved by western blotting, I observed that, analogous to PANX1, lower molecular weight bands were induced by proteasomal inhibition (**Fig. 13B**). More notably, a higher molecular weight smear was also detected in the myc-PANX3-containing whole cell lysates following MG132 treatment when probing with the myc antibody, which are likely accumulated polyubiquitinated PANX3 species (**Fig. 13B**) [131].

With regards to its subcellular localization, immunofluorescence staining demonstrated that PANX3 is primarily detected in an intracellular punctate pattern in untreated Rh30 cells and MG132 treatment increased the intracellular expression of PANX3 and resulted in a more diffuse staining pattern (**Fig. 13E**). However, likewise to PANX1, PANX3 presented with a pleomorphic profile in the transfected cells with regards to the distribution pattern. Co-labelling with specific organelle markers in untreated conditions showed that myc-PANX3 is partially localized to the endoplasmic reticulum (**Fig. 14A**) and co-localizes with the lysosomal marker LAMP1 (**Fig. 14B**), but not with the mitochondria nor the cis-Golgi network (data not shown). Proteasomal inhibition drastically increases myc-PANX3 localization in the ER in a subpopulation of cells (**Fig. 14A**). Conversely to PANX1, however, the co-localization of PANX3 with LAMP1 may increase or at the very least is unaltered ensuing MG132 treatment (**Fig. 14B**).

Collectively, these data suggest a role of the proteasome in regulating PANX3 protein levels and subcellular localization.

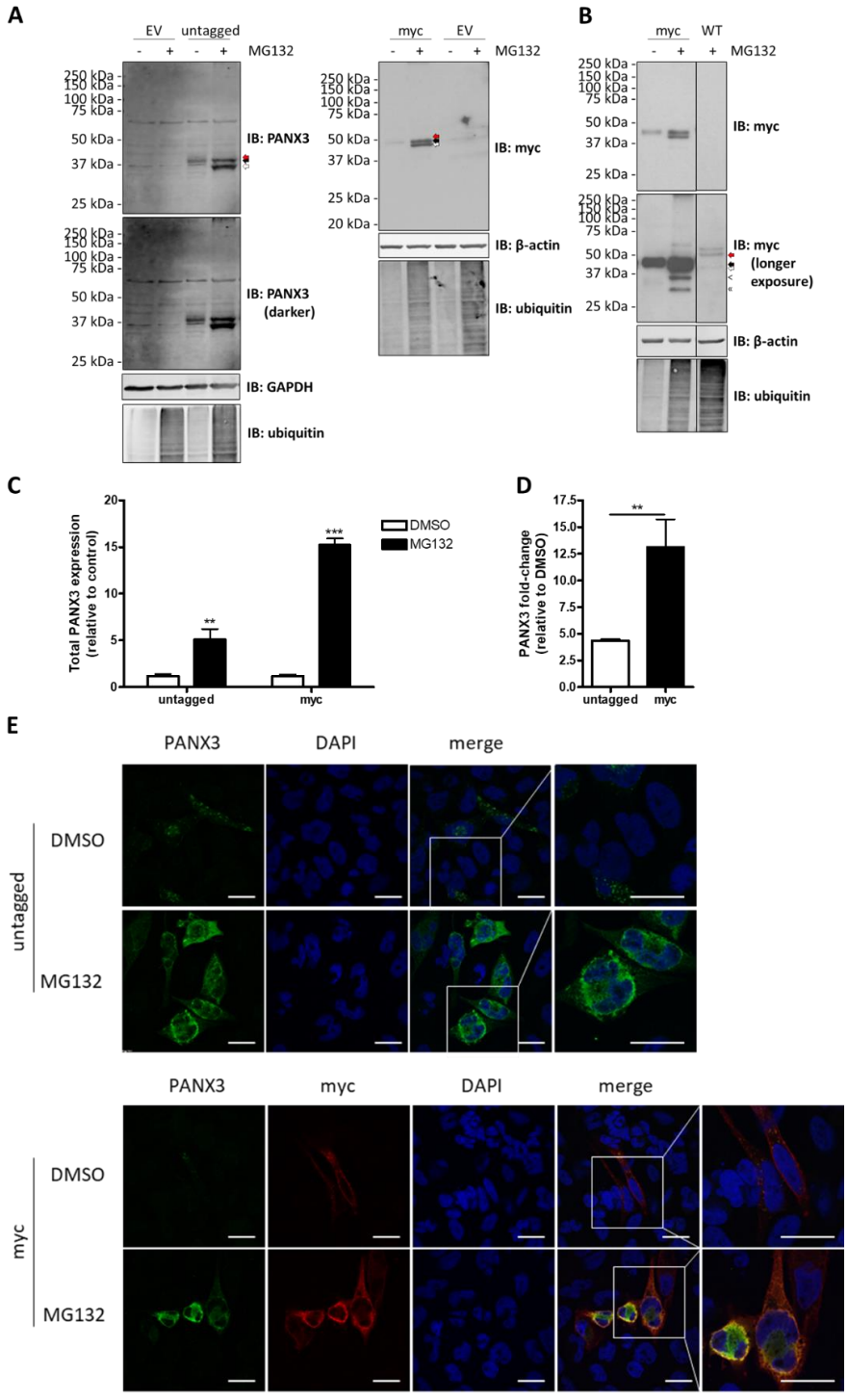

Figure 13. Proteasomal inhibition by MG132 increases PANX3 levels in Rh30 cells. Rh30 cells transfected with untagged human PANX3 (untagged) or with myc-tagged PANX3 (myc) were treated with 10 µM MG132(+) or DMSO control (-) for 16 hours and cell lysates were submitted to Western blot analysis

(**A**). GAPDH and β-actin served as loading controls. A blot with increased myc-PANX3 detection reveals a higher molecular weight smear and two lower molecular weight species (-1 <; -2 «) in addition to the glycosylation species (Gly0, white arrow; Gly1, black arrow; Gly2, red arrow) (**B**), which are not present in wild-type untransfected controls (WT). Total PANX3 levels were quantified (**C**), as was the fold-increase of the MG132-treated samples compared to the DMSO controls (**D**), and analyzed by T-test. **p<0.01; ***p<0.001. N=3. The same samples were labelled for PANX3 in green, myc in red, and DAPI in blue (**E**). N=3. Scale bar = 40 μm.

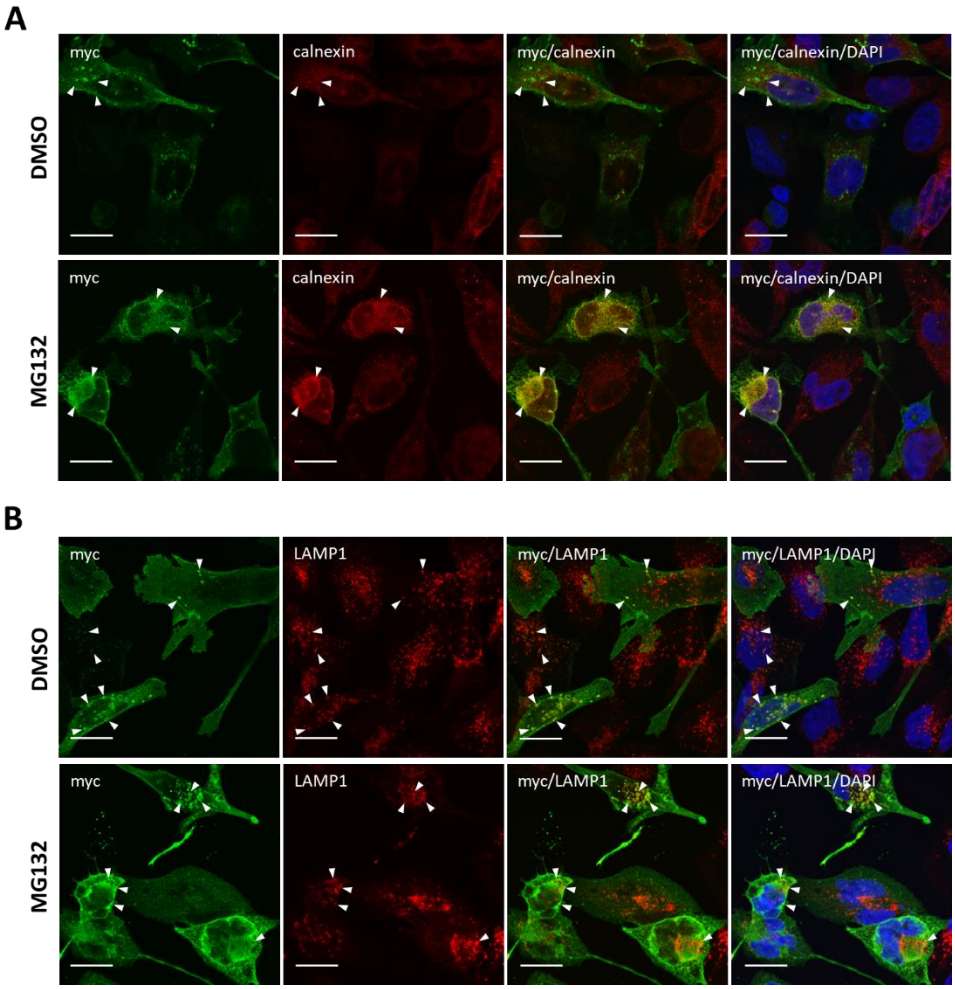

Figure 14. MG132 increases myc-PANX3 co-localization with the endoplasmic reticulum and lysosome markers. Rh30 cells ectopically expressing myc-PANX3 were treated with either 10 μM MG132 or DMSO for 16 hours. The cells were co-labelled for myc (PANX3) (green) together with calnexin (ER marker) (**A**) or LAMP1 (lysosome marker) (**B**) in red. Representative images show co-localization with calnexin and LAMP1 (arrow heads). N=3. Scale bar = 20 μm.

3.9 PANX3 is targeted for ubiquitin-dependent proteasomal degradation

As myc-PANX3 protein levels are responsive to proteasomal inhibition, I next assessed whether PANX3 is degraded by the 26S proteasome. Rh30 cells expressing myc-PANX3 were subjected to CHX

treatment to inhibit protein synthesis, and concurrently treated with either 10 μM MG132 or DMSO for 0, 3 or 24 hours (**Fig. 15A**). Quantification of total PANX3 levels shows that there is a statistically significant increase in protein levels at 24 hours of CHX treatment in the MG132-treated samples compared to the DMSO controls (**Fig. 15B,C**). Linear regression of Log10-transformed data confirmed that the half-life of wild-type PANX3 is lengthened following MG132 treatment, with the half-lives measured at 16 and 70 hours when treated with DMSO and MG132, respectively (**Fig. 15C**). These results suggest that PANX3 is degraded by the 26S proteasome.

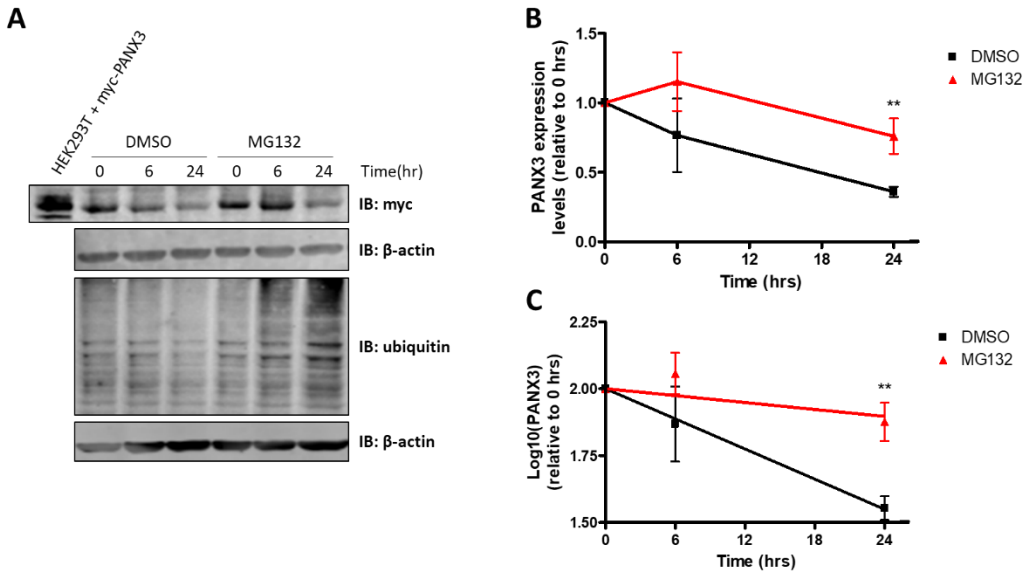

Figure 15. myc-PANX3 is degraded by the 26S proteasome. Rh30 cells transfected with myc-PANX3 were treated with 35 μg/mL of cycloheximide and either 10 μM MG132 or DMSO (**A**). The proteins were harvested at 0, 6 and 24 hours. Total myc-PANX3 levels were quantified according to their loading controls, then normalized to their 0-hour controls (**B**), where time 0 is 1.0. The Log10 of the percentage remaining was plotted on the Y-axis (**C**). The half-lives for the DMSO and MG132 treated myc-PANX3 are 16 and 70 hours, respectively. The difference in protein levels at each harvest time point were compared between the DMSO and MG132-treated cells by T-test. **P<0.01. N=3

In order to specifically examine the role of ubiquitination on PANX3 regulation and identify pertinent ubiquitinated lysine residues, a ubiquitination-resistant myc-tagged PANX3 mutant (KR8 mutant) with 8 lysine to arginine substitutions was created by site-directed mutagenesis. Through *in silico* analysis, the residues predicted to be ubiquitinated of PANX3's 19 lysines were narrowed down to 26, 100, 108, 167, 180, 183, 379, and 381 for evaluation in the KR8 mutant (**Fig. 16A**). Initial characterization

of KR8 myc-PANX3 showed that this mutant has a similar banding profile to wild-type myc-PANX3 in Rh30 cells, with the Gly1 and Gly2 species predominantly being expressed (**Fig. 16B**). To examine the sensitivity of the mutant to proteasomal inhibition, Rh30 cells expressing the KR8 mutant were treated with MG132, and no change was observed compared to WT myc-PANX3 in terms of both the banding profile (**Fig. 17A**), nor the fold increase in total protein expression (**Fig. 17B,C**). These results would suggest that the lysines within the KR8 mutant are not responsible for mediating PANX3 proteasomal regulation.

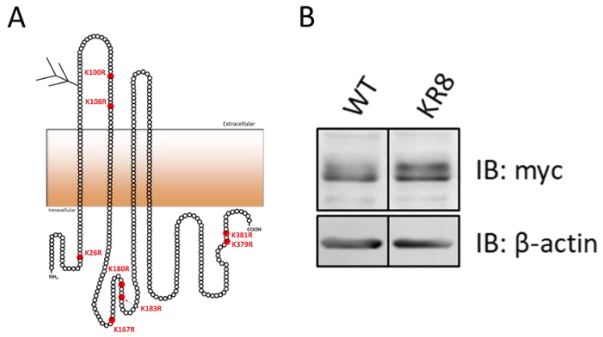

Figure 16. Pannexin 3 construct with 8 lysine to arginine substitutions (KR8). A diagram of human PANX3 with the mutated lysine resides (26, 100, 108, 167, 180, 183, 379, 381) indicated in red. Figure modified from Holland, S. (**A**). Wild-type PANX3 (WT) and the KR8 PANX3 mutant were expressed in Rh30 cells, and 30 μg of protein were loaded per well. β-actin serves as the loading control (**B**).

However, examination of the KR8 mutant protein stability by CHX chase indicates otherwise as MG132 treatment no longer increases stability of the protein in contrast to WT myc-PANX3 degradation, which is delayed with proteasomal inhibition (**Fig. 17D**). No difference was found in total KR8 protein levels at any of the time points up to 24 hours between the MG132 and DMSO-treated cells (**Fig. 17E**). Regression of the data indicates that the half-life of the KR8 mutant is 19 hours when untreated, and 29 hours following proteasomal inhibition, although these values are not statistically significant (**Fig. 17F**). Taken together, these findings provide evidence for myc-PANX3 degradation by the proteasome in a ubiquitination-dependent manner through one or more of the lysine residues targeted within the mutant. However, the combined eight lysine residues included in the mutant do not appear to be the exclusive

mediators of myc-PANX3 sensitivity to MG132 as total protein expression and the banding profile is unchanged in the mutant.

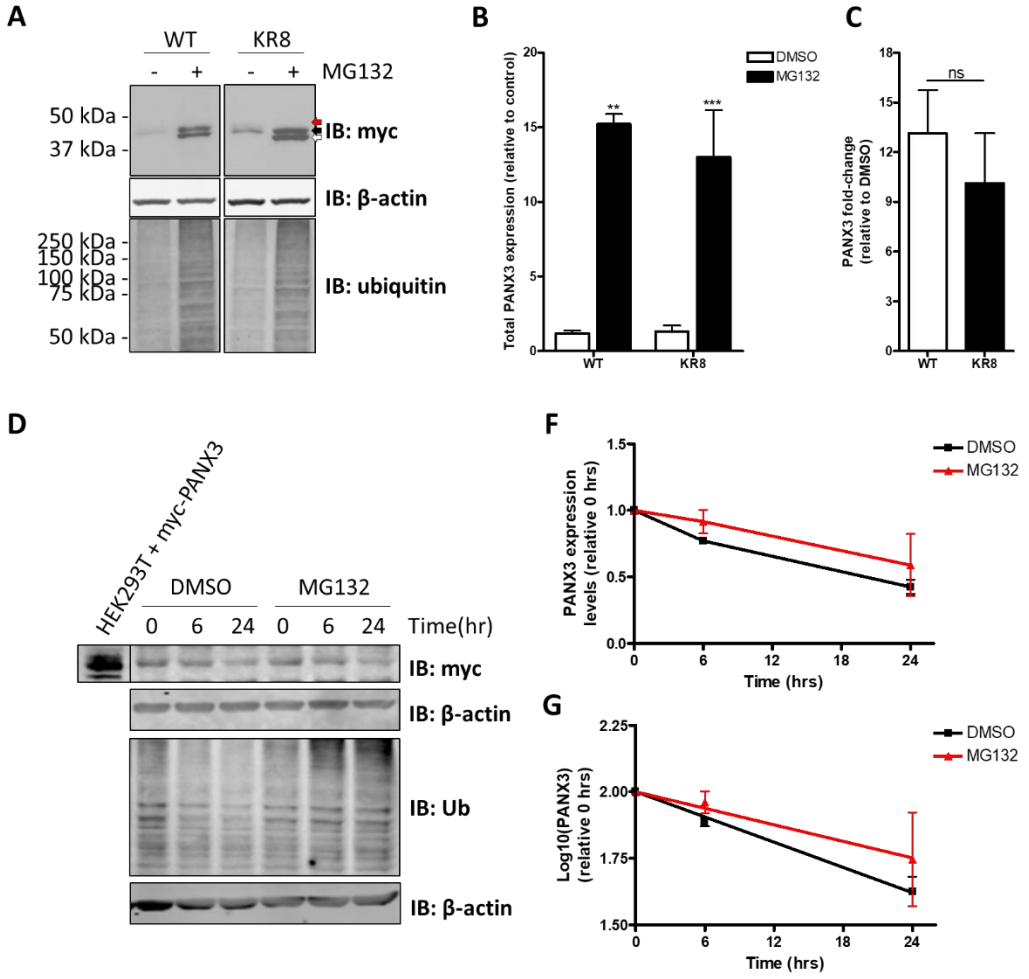

Figure 17. Ubiquitination and sensitivity to MG132 is not reduced in the KR8 mutant compared to WT myc-PANX3, however the mutated lysine residues may mediate myc-PANX3 degradation. Rh30 cells transfected with wild-type (WT) or mutant myc-PANX3 containing 8 lysine to arginine mutations (KR8) were treated with 10 μM of MG132 (+) or DMSO (-) control for 16 hours. 30μgof protein were loaded per well on western blots (**A**). β-actin serves as the loading control. N=3. Total protein expression was quantified by densitometry and the MG132-treated samples were compared to their DMSO controls by T-test (**B**) with the fold increase of the MG132 compared to the DMSO samples indicated (**C**). Error bars are standard deviation. **p<0.01; ***p<0.001; ns, no significance. HEK293T cells ectopically expressing an empty vector (pcDNA), HA-ubiquitin (HA-Ub) and pcDNA, WT myc-PANX3 and HA-Ub, both WT myc-PANX3 and HA-Ub, KR8 myc-PANX3 and pcDNA, or both KR8 myc-PANX3 and HA-Ub were treated with 10 μM MG132 for 16 hours. The lysates were subjected to immunoprecipitation (IP) with myc-tag antibody (**D**). All of the IP eluates were loaded, and 30 μg of the initial lysates were loaded per well. β-actin serves as the loading control. N=1. Rh30 cells transfected with KR8 myc-PANX3 were treated with 35 μg/mL of cycloheximide as well as 10 μM MG132 or DMSO and harvested at 0, 6 and 24 hours (**E**). 30 μg of protein were loaded per well. β-actin serves as the loading control. PANX3 levels were quantified according to their loading controls, then normalized to their time 0 controls (**F**). The Log10 of

the percentage PANX3 remaining was plotted on the Y-axis (**G**). The half-lives for the DMSO and MG132 treated KR8 mutant are 19 and 29 hours, respectively.

4.0 DISCUSSION

I demonstrated that PANX1 is ubiquitinated through various chain topologies by *in vivo* ubiquitination assays, and showed for the first time that PANX1 is modified by mono-ubiquitination, K48- and K63-linkage pUb chains. This suggests a multifaceted approach to PANX1 regulation by ubiquitin, as mono-ubiquitination is generally associated with regulation at the level of endocytosis and endosomal sorting [64,65]. Indeed, K63 ubiquitin linkages have diverse functions ranging from modulating protein binding to endomembrane trafficking to promoting degradation [64,65], whereas K48 polyubiquitin targets proteins for proteasomal degradation [54,64,65]. Given PANX1's important roles in differentiation, proliferation, and apoptosis, and that PANX1 function is closely tied with its subcellular localization and PTM status [7,9], ubiquitination may be one of the mechanisms used by cells to stringently regulate PANX1.

Surprisingly, while some data suggests that PANX1 may be a substrate of the 26S proteasome, my results provide conflicting observations for this hypothesis. Indeed, my data showed that proteasomal inhibition influences PANX1 protein expression, increasing total protein levels of the myc-tagged protein and modifying the glycosylation banding profile. Combined with the detection of K48 ubiquitin linkages, the canonical proteasomal degradation signal [63], and the identification of various candidate PANX1 interactors constituting the 26S proteasome and the proteasome-interacting proteins (PSMA7, PSMC2, PSMD2, USP14) [83], these data would initially point towards a degratory role of the proteasome for PANX1. However, results from CHX chase and radioactive pulse-chase labelling did not support this hypothesis. It is conceivable that only a small subpopulation of PANX1 is degraded by the proteasome, and the degradation assays are not sensitive enough to capture this subpopulation. Indeed, proteins which assemble into higher order oligomeric complexes can exhibit increased stability compared to their nascent monomeric counterparts [132,133]. Increased stability due to glycosylation and surface expression of mature Panx1 was also suggested by Boyce and colleagues [41]. The differential degradation pathways enlisted for PANX1 may, in effect, explain the lesser-than-optimal goodness of fit of the Log10 linear regression applied to the PANX1 pulse-chase data [134]. In keeping with this theory is the heterogeneity I observed in

the PANX1 subcellular distribution by immunofluorescence staining, reflecting PANX1 trafficking throughout the cell during its lifecycle [2], with PANX1 detected in the ER, minimal in the Golgi apparatus, at the plasma membrane, and diffuse staining reminiscent of the cytoplasm. Cells may therefore employ specific degradatory pathways within distinct compartments [135,136]. The population of PANX1 accumulating within the ER following proteasomal inhibition may represent pannexins originally destined for ERAD [137]. This is in accordance with existing literature suggesting that nascent and older Panx1 are differentially degraded, as older Panx1 is selectively targeted to lysosomes [138]. Interestingly, when Rh30 cells ectopically expressing a glycosylation-null (N255A) PANX1 mutant are treated with MG132, the higher molecular weight smear characteristic of ubiquitinated species [131] is observed in the whole cell lysates (data not shown), a phenomenon only observed in *enriched* fractions of wild-type PANX1 by immunoprecipitation. This may be indicative of a subpopulation of PANX1 being modified with polyubiquitin chains for proteasomal degradation, a population not substantive enough to be captured in the whole cell lysates of cells expressing wild-type PANX1. Thus, proteasomal degradation of nascent ER-residing unglycosylated PANX1 by ERAD becomes an enticing hypothesis, especially when taking into account that a very likely PANX1 interactor is UBXN4, which complexes with VCP/p97 and ubiquilin to promote degradation of ERAD substrates [139,140]. Other ERAD effectors [91,141] were also identified by co-IP (UBE2G2, VCP/p97, ERdj5, OS9, and Sec61) and by BioID (AUP1 and UBE2J1). Combined with the knowledge that PANX1 is modified with K48 pUb, and that UBR4 assembles heterotypic K11/K48 ubiquitin chains [58]- a chain topology characteristic of ERAD-destined targets [91]- these suggest a putative PANX1 degradation pathway involving the 26S proteasome warranting further investigation. It would be interesting to assess the effects of the ERAD inhibitor, Eeyarestatin I [142], on PANX1 protein stability, and to specifically examine the degradation of unglycosylated PANX1.

The PANX1 half-lives of ~38 hours and 5 hours identified by CHX and radioactive pulse-chase, respectively, are in keeping with literature which found that PANX1 has a long half-life, in the span of hours to days [27,41,143,144]. The considerable stability of PANX1, and the inherent limitations of the

degradation assays, could explain the disparity in half-life estimated between the CHX chase and the radioactive pulse chase techniques, and may contribute to the lack of observable effect of MG132 on PANX1 stability. For starters, labelling with amino acid radioisotopes can introduce conformational changes, which reduce the protein's antigenicity during immunoprecipitation, giving the impression of higher degradation rate [145]. Relatedly, radioisotope labelling-misfolding, or a protein's inherent susceptibility to aggregating in aggresomes, may decrease solubility again impairing antigenicity during immunoprecipitation [97,145]. This method may, therefore, underestimate protein stability [145]. The CHX chase technique also comes with its shortcomings. For long-lived proteins, target protein stability may seemingly increase with CHX treatment if the proteolytic pathway components have a short half-life themselves, as their synthesis is also being impacted [145]. This is in addition to other off-target effects of CHX, including an increased free amino acid pool, which may inadvertently impact the degratory pathway or regulation of the target protein's life cycle [145] .

Nevertheless, treatment with MG132 had drastic effects on the PANX1 banding pattern by western blotting. It increased intracellular myc-PANX1, which is reflected by an increase in the Gly0 and Gly1 species and a decrease in the Gly2 species, and induced levels of the LMW species. As the degradation experiments do not point to an obvious degradative function of the proteasome for PANX1, this suggests that MG132 may also be regulating PANX1 indirectly, perhaps through modulating the expression of other PANX1 regulatory proteins, as was observed for other proteins. Su and Lau observed that MG132 stabilized Cx43 protein expression indirectly through the stabilization of Akt, a kinase whose phosphorylation of Cx43 stabilizes it at the cell surface [105]. For the membrane-anchored glycoprotein Shadoo (Sho), Kang et al. showed that proteasomal inhibition results in the repartitioning of its glycosylation banding profile with re-localization of Sho from the cytosol to the nucleus [146]. This is presumed to be due to compromised ER import and consequently impaired post-translational processing into its glycosylated species [146] . Interestingly, they further found that expressing Sho, and its related protein, PrpC, under the CMV promoter led to increased total protein levels following both proteasomal

and autophagic inhibition, and considered this to be an artifact of the CMV promoter [146,147]. The vector containing untagged PANX1 uses the CMV5 promoter, whereas the myc-tagged PANX1 is under the control of the CMV6 promoter. However, MG132 treatment of cells highly expressing endogenous PANX1 (such as HSMM) also increases protein levels, suggesting that this may not be an artifact of the CMV-promoter over-expression system, at least in a physiological context. Although, proteasomal inhibition has also been demonstrated to upregulate mRNA transcription and thus subsequent protein levels by regulating promoter activation for another gene (*ULBP1)* [148]. Given the scarcity of evidence supporting a degratory role of the proteasome on PANX1 protein stability, induction through transcription upregulation may provide an alternative explanation.

Not only does MG132 repartition the glycosylation banding profile of PANX1, but it also induces the expression of LMW species, which are detected by antibodies against myc-tag and and against the C-terminal domain of PANX1. However, these species were not detected by an N-terminal PANX1 antibody (data not shown), suggesting that they lack the N-terminus. These species were also detected in the neuroblastoma cell line Sk-N-Be(2) treated with MG132, indicating that this effect is not an artifact of an ectopic overexpression system, but also occurs in a physiological (albeit pathological) context. As the -3 and -4 bands of the PANX1 LMW species migrate at a weight comparable to those of PANX1 caspase cleavage products [35], and the relationship between proteasomal inhibition, ER stress, the unfolded protein response, and eventual apoptosis (activating the caspase cascade) is well established [149,150], it was surprising to find that these immunoreactive species are not products of caspase cleavage. This may, nevertheless, allude to the existence of another cleavage mechanism used to generate these species. Other researchers have also observed the induction of immunoreactive species following proteasomal inhibition: proteasomal inhibition produced faster-migrating Sho species by SDS-PAGE, which were proposed to be cleavage products [146]. Non-degradative proteolytic processing is the specific cleavage of substrates eliciting changes in protein function and/or expression [151]. This processing is employed for various biological purposes: N-terminal methionine excision occurs as part of a protein's maturation, and

is intimately linked with the N-end rule pathway [152]; signal peptide removal is essential for proper protein trafficking, whereby an N-terminal signal sequence demarking a protein towards a specified organelle is cleaved once the protein reaches its destination [152]; in the secretory pathway, cleavage of some substrates (particularly hormones) is required for their biological function or enzymatic activity by proprotein convertases [152]; finally, ectodomain shedding involves the cleavage of membrane-anchored proteins for the regulation of cell signaling and cell adhesion/mobility [152,153]. In fact, two proteases, ADAM9 and HM13, were identified by BioID as putative PANX1 interactors. ADAM9 is a protease which catalyzes ectodomain shedding [153], and HM13 is an ER-resident signal peptide peptidase (SPP) [154], thus these may present two discrete mechanisms by which PANX1 may be processed for distinct purposes to generate the LMW species, mechanisms which necessitate further exploration. Treatment with protease inhibitors, such as ones targeting the ADAM family of metalloproteases [155] or those targeting SPP activity [156], or treatment with protease activators [157], will help to delineate if and which proteases are involved in the production of these LMW species. If not a product of cleavage, then these isoforms may arise from transcriptional or translational, rather than post-translational, mechanisms.

Numerous molecular mechanisms exist which are known to give rise to the vast spectrum of endogenous protein isoforms in existence, from the use of alternative promoters, alternative transcription initiation and termination sites, to the utilization of multiple polyadenylation sites or alternative splicing [158]. The induction of faster migrating protein species following proteasomal inhibition has been observed in various contexts in literature. Numerous splicing regulatory components are substrates of the proteasomal degradation pathway, and proteasomal inhibition was shown to modulate CPT-induced *TAF1* alternative splicing [159]. HER2, a receptor tyrosine kinase highly involved in the tumorigenicity of various cancers, is expressed as C-terminal fragments (CTFs) in many tumors, and arise through alternative translation initiation sites. Interstingly, these CTFs retain their kinase activity and contribute to HER2 pathogenicity [160]. Proteasomal inhibition increased the protein levels of the CTFs, but not the full length protein, which the authors theorized was due to the specific proteasomal degradation of the

CTFs [160]. Examining PANX1 mRNA levels and exon composition with and without proteasomal inhibitor treatment may illuminate whether these truncated PANX1 species are generated at the level of transcription, translation, or post-translation. PANX1 protein isoforms have been predicted and identified in literature. Splice variants have been predicted for human *PANX1*, with the alternative splice site in exon 5 resulting in a 4 amino acid inclusion in the C-terminus [161]. The *PANX1a* variant open-reading frame further contains numerous putative ATG start codons [161]. With regards to protein expression, only rat Panx1 was identified as numerous isoforms corresponding to 3 splice variants, and all contain a complete N-terminus [162]. Unfortunately, neither of these descriptions fit the characteristics of the LMW species observed in my experiments. My data do suggest, however, that the LMW species are primarily expressed intracellularly, as only a margin of the induced LMW species were detected by cell surface biotinylation, compared to the glycosylated species, following proteasomal inhibition. This may further explain the increased PANX1 intracellular staining observed by confocal microscopy. Further, these LMW bands were not detected in the MG132-treated fraction during the CHX chase. If they were cleavage products stimulated by the stabilization of the cognate protease, they would be detected regardless following proteasomal inhibition. Their absence from both untreated and MG132-treated conditions suggests that they may rather be isoforms generated prior to protein translation, as treatment with the protein synthesis inhibitor CHX inhibited their upregulation. With the existing data, one cannot differentiate whether proteasomal inhibition is upregulating a regulatory factor to increase transcript levels, or whether the isoforms generated by alternative transcripts are substrates of the 26S proteasome, and proteasomal inhibition is directly stabilizing the proteins. The latter of these two conceptualizations may better explain the UBR4 E3 ligase identified as a PANX1 interactor. If the LMW species bear an unacetylated destablizing N-terminus, then they could be targets of the N-end rule pathway N-recognin, UBR4 [163]. Of note, N-recognin E3 ligases have been proposed to mediate the clearance of C-terminal fragments of cleaved proteins [52]. Interestingly, in *Drosophila melanogaster*, POE, the homolog of UBR4, was also shown to regulate the steady state levels of MAPK and counteracted the stabilizing effects of USP47 [164], a DUB also identified as a putative PANX1 interactor . However, UBR4 is a large protein

containing a wide range of domains capable of binding microtubules, the ER, calmodulin, Nde11, and mediates many of its roles through direct binding of proteins rather than through substrate ubiquitination [57]. In the cytosol, UBR4 acts alongside clathrin to maintain cytoskeletal organization and may promote target protein degradation through its close association with components of the endomembrane system and its involvement in their formation and development [165,166]. Given the diverse functions of UBR4, it may regulate PANX1 in a different capacity than as an N-recognin. Whether these 4 bands are all distinct isoforms of PANX1, or if they represent 2 isoforms with different glycosylation states, as an example, has yet to be revealed. In Rh30 cells ectopically over-expressing the N255A glycosylation-null mutant of PANX1, the -4 and -2 bands are induced by proteasomal inhibition, supporting the notion that at least 2 of the LMW species are likely unglycosylated forms of the PANX1 LMW species (data not shown). The next step would be to sequence these immunoreactive LMW bands by mass spectrometry to confirm their identity, which may also reveal if these are products of alternative splicing. Furthermore, analysis the N-terminal residue could prove resourceful for identifying putative alternative translation initiation sites or honing in on the potential site(s) of proteolytic cleavage [167]. Mutational studies may be employed to discern which mechanism is generating these LMW species [160,168]. Additionally, information on the identity and/or associated modifications of the N-terminus may give insight into the stability of these protein species, and whether they are earmarked for N-end rule degradation [167]. Afterwards, it will be interesting to determine which proteolytic enzymes are processing PANX1, or which adaptors are promoting alternative translation start sites, and which degradation pathways are involved in their regulation. Most importantantly, assessing whether these LMW species demonstrate any functional activity through ectopic over-expression assays, and gauging under what physiological or pathological conditions their expression is stabilized, will be paramount for determining their biological relevance.

As my results show that PANX1 is mono- and polyubiquitinated, and yet PANX1 is not discernibly degraded by the 26S proteasome, ubiquitination appears to play another role in PANX1 regulation separate from targeting it for proteasomal degradation. To study this end, two mutants were engineered

through site directed mutagenesis - one containing three mutations at confirmed ubiquitinated lysine residues, and the other containing nine lysine mutations at predicted sites. While no overt differences were observed between the myc-tagged KR3 mutant and myc-PANX1 in terms of protein or ubiquitination levels, the KR9 mutant showed decreased sensitivity to MG132treatment with regards to the magnitude of shift in PANX1 banding pattern and increased localization at the cell surface. This suggests that a subset of the mutated lysine residues in the KR9 mutant are key regulators of PANX1 trafficking to and/or cycling from the plasma membrane. Characterizing the ubiquitin chain topology of the KR9 mutant compared to WT PANX1 to distinguish which chain linkage is mediating the differential PANX1 subcellular localization may give insight into the potential E3 ligases and DUBs involved in this process. Additionally, identification of the specific lysines conferring these effects by systematic reintroduction of each lysine residue in the KR9 mutant will help to narrow down the lysines involved to ultimately create a more pertinent mutant to study the implications of ubiquitination on PANX1 while diminishing potential inadvertent consequences of mutating multiple residues. Indeed, mono-, multi-mono-, and K63-linked ubiquitination have all been implicated in the endocytosis of plasma membrane proteins, their subsequent sorting for lysosomal degradation, and/or their recycling back to the plasma membrane [46]. The dynamic process of ubiquitination may also come into play, with an everchanging ubiquitin chain architecture regulating PANX1 according to the complementary activity of E3 ligases and deubiquitinating enzymes orchestrating this process, as is observed for Cx43 [103].

Interestingly, more than four times the amount of KR9 mutant is expressed at the cell surface compared to its WT counterpart, and this is largely achieved by increased Gly1 expression. Ubiquitination regulates protein levels at the plasma membrane at the level of endocytosis, recycling, and lysosomal/proteasomal degradation following internalization [59]**.** Ubiquitination, or the lack therefore, on one of the 9 targeted lysine residues may be modulating PANX1 in this fashion. Epsin and Eps15 were not identified in PANX1's interactome by BioID nor co-IP, suggesting ubiquitin-dependent clathrin-mediated endocytosis is not at play [59]**,** which is in line with studies indicating that a non-canonical

endocytic mechanism mediates Panx1 internalization [41]. However, HGS, STAM1, TSG101, and ALIX/PDCD6IP, all components of the ESCRT machinery, were identified in at least one replicate by either BioID or co-IP, indicating that ubiquitination may be regulating PANX1 in MVBs and sorting into ILVs for endolysosomal degradation [94,169]. Curiously, SQSTM1/p62 [99,170] and BAG3 [171] were also identified as PANX1 interactors by both BioID and co-IP, and NBR1 [99] was identified in a single replicate by co-IP, pointing towards the possible involvement of autophagy [99] in regulating PANX1 protein levels. Without additional information, it is not possible to discern which of the three proteolytic pathways- endolysosomal, autophagosomal, or proteasomal (encompassing ERAD) - is regulating PANX1 expression specifically at the cell surface.

Adding further complexity to the emerging picture of PANX1 regulation by ubiquitination is the disproportional increase of the Gly1 PANX1 species at the plasma membrane. Indeed, glycosylation status has been correlated with PANX1 localization at the cell surface [41]. However, what may also be at play is the nuanced relationship between glycosylation, phosphorylation, and ubiquitination, as all modifications have the ability to influence their target protein's interactome, PTMs, and, consequently, the protein's destiny [60,172]. As such, it is curious that, despite PANX1 being capable of maturing to its complex glycosylation status, it is primarily the high mannose species that accumulates at the plasma membrane. Numerous studies have illustrated the interplay that occurs between these 3 PTMs on target proteins [173–175]. High mannose glycosylation can enhance target protein binding to E3 ligases to promote their degradation in an E3-activity dependent manner [174]. Glycosylation can also impede E3 binding, such that unglycosylated core proteins exhibit enhanced E3 binding, and this interaction can then interfere with non-glycosylated protein maturation and thus promote its degradation [174]. Both instances were demonstrated with the ABCG5/8 transporters and their cognate E3 ligases: HRD1 and RMA1 [174]. Yoshida and colleagues eloquently demonstrated that the SCF^{Fbx2} complex selectively targets cytosolic N-linked glycoproteins modified with high mannose oligosaccharides for proteasomal degradation [175]. Included among its targets are the transmembrane protein integrin β1, which is extracted from the ER during

ERAD, and glycoproteins gathered into aggresomes [175]. With regards to phosphorylation, the phosphodegron is a well established signal to recruit E3 ligases to tag proteins for degradation, whether it be by the 26S proteasome or by lysosomes [60,176]. Li and colleagues found that glycosylation of programmed death ligand 1 (PD-L1) antagonized binding of glycogen synthase kinase 3β (GSK3β), hereby preventing phosphorylation and subsequent ubiquitin-mediated degradation of PD-L1 [173]. Which is to say that *unglycosylated* PD-L1 was more prone to phosphorylation-mediated degradation [173]. As PANX1 is a highly modified protein, it is possible that it is also degraded by a phosphodregon signal. With numerous phosphorylation sites on PANX1 identified by high throughput mass spectrometry screens [33], as well as two addition phosphorylation sites (pT382 and pS385) identified by mass spectrometry located just adjacent to a confirmed ubiquitin-acceptor lysine residue (K381) [33], a relationship may exist between the two modifications. Taken together, the KR9 mutant may be a promising construct for studying PANX1 ubiquitination and its role in regulating PANX1 expression. However, results obtained from studying this mutant must be interpreted with caution, as introducing lysine to arginine mutations may have inadvertent consequences. Lysine residues also have the capacity to be modified by acetylation, methylation, SUMOylation, or NEDDylation [60] - in fact, PANX1 K204 is a confirmed acetylation site [33] - and these modifications could also be impaired in the KR9 mutant, yielding KR9 mutant-specific effects that are unrelated to ubiquitination. Another consideration for future investigations is examining the possibility of PANX1 ubiquitination on N-methionine, serine, threonine, or cysteine residues [49]. Given the various PTMs that can occur on lysine, and the wide selection of residues which may be modified with ubiquitin, a complementary approach to studying PANX1 ubiquitination may be to create a PANX1 fusion protein expressing a DUB catalytic domain to reverse any incidence of PANX1 ubiquitination [130].

Collectively, my experimental data and my analysis of candidate PANX1 interactors from my colleague's BioID and co-IP assays paint a complicated picture for PANX1 regulation by ubiquitin and the proteasomal degradation pathway. A simplified model of the spatiotemporal regulation by ubiquitin

is illustrated in Figure 18. Briefly, PANX1 stability may be regulated in the ER by ERAD to degrade misfolded proteins as a form of ER quality control, or to degrade either the Gly0 or Gly1 species as a form of ER quantity control (**Fig. 18-1**). Supporting evidence for this hypothesis is the K48-linked pUb chains detected on PANX1, accumulation of PANX1 in the ER following proteasomal inhibition, and idenfication of the candidate interactors UBE2G2, UBE2J1, ERdj5, OS9, SEC61, VCP/p97, UBXN4, and UBR4. Following trafficking along the secretory pathway, PANX1 levels may be regulated at the plasma membrane, as suggested by the accumulation of the PANX1 KR9 mutant at the cell surface. PANX1 monoubiquitination and K63-linked polyubiquitination may mediate PANX1 internalization (**Fig. 18-2**). Monoubiquitination and K63-linked polyubiquitination, alongside potential PANX1 association with ESCRT machinery and co-localization with lysosomes, may point towards ubiquitin-dependent sorting within MVBs for endolysosomal proteolysis (**Fig. 18-3**). On the other hand, K63-linked polyubiquitination of PANX1, combined with the putative interacting autophagy receptors SQSTM1, BAG3, NBR1, and the deubiquitinase USP9X, point towards a possible role of autophagy and subsequent lysosomal degradation in mediating PANX1 turnover (**Fig. 18-4**). Finally, the involvement of the 26S proteasome cannot be disregarded in PANX1 regulation as PSMA7 of the 20S core and PSMC2 and PSMD2 of the 19S regulatory caps, as well as the proteasome-interacting deubiquitinase USP14, are putative PANX1 interactors. While the association between PANX1 and the proteasome may be limited to ERAD, another intriguing explanation could also account for these findings. Modification by K48 pUb chains may initially direct PANX1 to the 26S proteasome where the polyubiquitin chain is trimmed by USP14 to disengage PANX1 from the proteasome, hereby allowing PANX1 to be redirected for autophagosomal degradation by BAG3, SQSTM1, and/or other adaptor proteins (**Fig. 18-5**) [177]. Throughout the entire lifecycle of PANX1, ubiquitination may be modulating the PANX1 interactome and activity in addition to its subcellular localization and stability, which is another avenue warranting additional investigation.

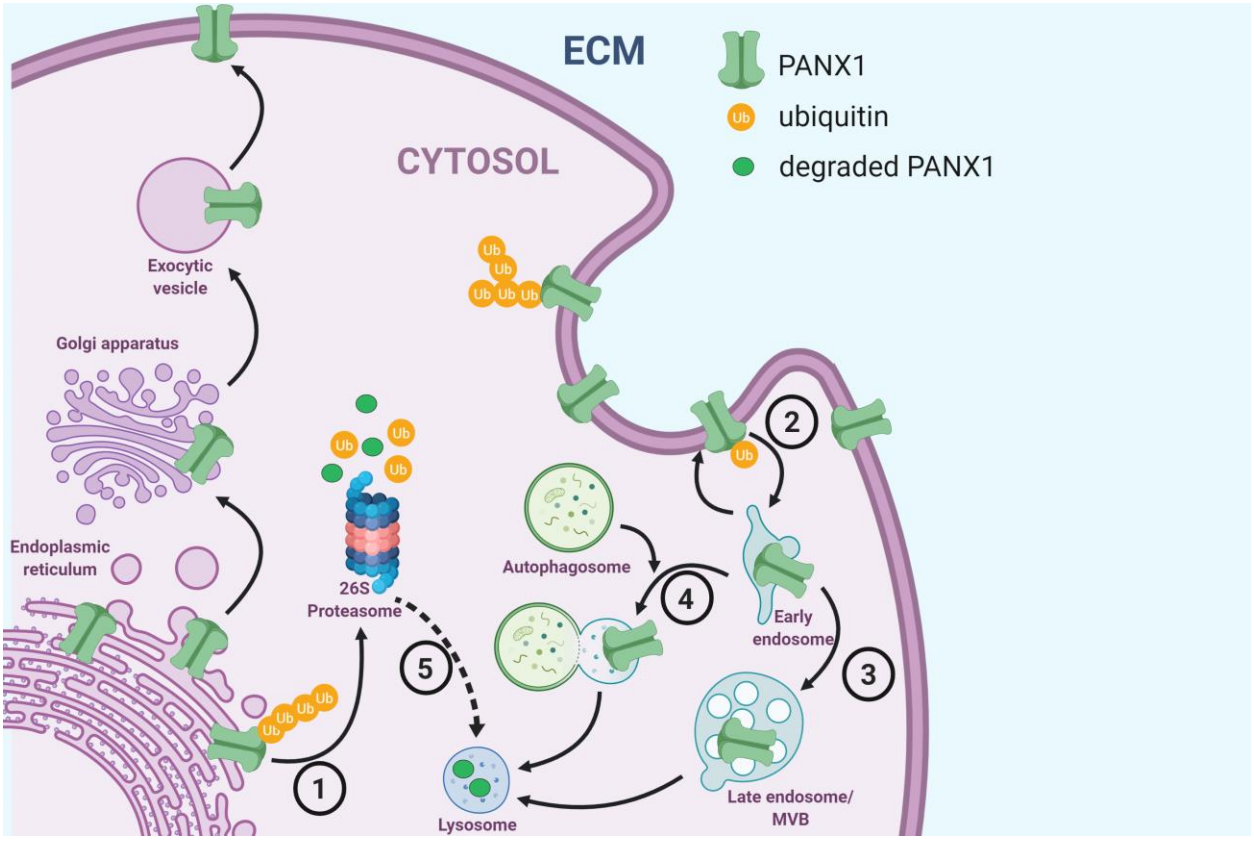

Figure 18. **Potential regulatory roles of ubiquitination on PANX1 trafficking and degradation.** Following translation into the ER, PANX1 may be dislocated and targeted for ERAD by K48-linked polyubiquitination and mediated by UBXN4 (**1**). Mature PANX1 is secreted along the endosomal pathway to the plasma membrane, where monoubiquitination, K48-linked polyubiquitination, or K63-linked polyubiquitination, may mediate internalization into early endosomes (**2**) and/or subsequent sorting into ILVs within the late endosome/MVB (**3**). K63-linked polyubiquitination may alternatively promote autophagosomal degradation (**4**). K48-linked polyubiquitinated PANX1 may be processed by the USP14 hydrolase for release from the 26S proteasome and redirected to lysosomes for degradation (**5**). Figure created with BioRender.com.

Unlike PANX1 for which existing high throughput screens indicated that it is ubiquitinated, my results show for the first time that myc-PANX3 is also ubiquitinated, specifically by polyubiquitin chains. However, the possibility of mono-ubiquitination cannot be discounted from these experiments as mono-ubiquitinated PANX3 may have been obscured by the non-specific band detected after immunoblotting for the HA-tag at ~50 kDa in **Fig. 12**. Additionally, I have shown that proteasomal inhibition significantly increases PANX3 protein levels, notably increasing the expression of the Gly0 species, and specifically results in increased localization in the endoplasmic reticulum and to lysosomes in a subset of cells. In addition, a higher molecular weight smear is occasionally detected in whole cell lysates when probing for

myc-PANX3 in MG132-treated cells is suggestive of the accumulation of ubiquitinated myc-PANX3 proteins, which would otherwise be degraded by the proteasome. Indeed, CHX experiments suggest that PANX3 is degraded by the proteasome in a ubiquitin-dependent manner, and that this process is mediated by one of the lysine residues targeted in the KR8 mutant. Considering that PANX3 is polyubiquitinated and subject to proteasomal degradation, and that MG132 results in the accumulation of PANX3 in the ER, it is conceivable that PANX3 is a target of ERAD.

Interestingly, like PANX1, PANX3 was also found to co-localize with LAMP1, highlighting the role of lysosomal proteolysis on PANX3 stability, which is in agreement with the literature [9]. However, this finding underscores the simultaneous use of at least two degradation pathways to regulate PANX3 expression in Rh30 cells. Under conditions of proteasomal impairment, diverse PANX3 staining patterns are observed: some cells display PANX3 predominantly in a punctate pattern which frequently coincides with LAMP1, some cells primarily exhibit PANX3 in a network-like pattern overlapping with ER staining, and some PANX3 is detected as diffuse staining. The cells in which PANX3 is targeted to lysosomes may demonstrate a population of cells which redirect ubiquitinated PANX3 incapable of proteasomal degradation for autophagy mediated destruction [127]. Indeed, numerous accounts detail the reciprocal relationship between the proteasomal and autophagosomal degradation pathways. In various cell lines, inhibition of one pathway is compensated by upregulation of the alternative pathway [71,102,126,178].

Despite these findings, the KR8 mutant is still responsive to MG132 in terms of total protein expression and its glycosylation banding profile. This implies that, in addition to ub-mediated proteasomal degradation, the proteasome regulates PANX3 in another capacity. A recent publication examining the role of PANX3 in dental pulp inflammation may provide some insight. *In vitro* TNF-α challenge of human dental pulp cells attenuated PANX3 protein levels, a process which was rescued when cells were pre-treated with MG132. These processes acted on the level of *PANX3* mRNA as measured by RT-qPCR, and MG132 had no measurable effects on PANX3 protein expression alone without co-treatment with TNF- α [20]. This research highlights that, while human dental pulp cells may

not use the 26S proteasome to directly degrade PANX3 protein, the proteasome is implicated in PANX3 expression at the level of mRNA expression. Thus, in Rh30 cells, the proteasome may directly degrade PANX3, as evidenced by the CHX chase experiments, but may also be acting upstream of protein translation to accordingly increase protein levels. This would lead to the accumulation of both the WT *and* the KR8 PANX3 proteins following MG132 treatment. Furthermore, similar to PANX1, the untagged and myc-tagged PANX3 cDNA constructs are under the control of the CMV5 and CMV6 promoters. There are multiple accounts in literature demonstrating that proteasomal inhibition increases expression of proteins controlled by CMV promoters [146,147], suggesting that part of the MG132-induced PANX3 expression observed in my experiments may be an artifact of the over-expression system. Repeating these proteasomal inhibition experiments in cells endogenously expressing PANX3 can help to rule out this potential artifact. Determining if K48 or K63-linked polyubiquitin chains mediate PANX3 proteasomal degradation, identifying which lysine residues are participating in this regulation, and also assessing if ubiquitination regulates PANX3 trafficking or degradation by the lysosomal system, are just starting steps to consolidate the unfolding narrative of PANX3 regulation.

5.0 CONCLUSION

In agreement with studies that showed that PANX1 and PANX3 have distinct functions, my results suggest that their ubiquitination and the 26S proteasome may play different roles in regulating both proteins. Although proteasomal inhibition alters the banding profile of both pannexins and increases their localization to the endoplasmic reticulum, the 26S proteasome may only substantially regulate PANX3 degradation in a ubiquitination-dependent manner. MG132 does appear to be modulating both PANX1 and PANX3, indirectly. Therefore, ubiquitination may play other roles in regulating both pannexins. Specifically for PANX1, mono- or polyubiquitination may regulate PANX1 trafficking to the plasma membrane, internalization, or subsequent degradation. For PANX3, polyubiquitination mediates its proteasomal degradation, and future work will be required to unravel in what other capacities ubiquitin may be regulating PANX3. Both pannexins are involved in the development and maintenance of healthy tissue, and their dysregulation has been implicated in the progression of several diseases. Future studies should thus focus on delineating the enzymes and pathways governing PANX1 and PANX3 ubiquitination which may be useful in developing strategies for regulating PANX expression and/or activity, and may ultimately bring insights into development of novel therapies to treat pannexin-related pathologies.

REFERENCES

1. Penuela S, Gehi R, Laird DW. The biochemistry and function of pannexin channels. *Biochim Biophys Acta - Biomembr*. 2013;1828(1):15-22. doi:10.1016/j.bbamem.2012.01.017

2. Bond SR, Naus CC. The pannexins: Past and present. *Front Physiol*. 2014;5(58):1-24. doi:10.3389/fphys.2014.00058

3. Ma W, Compan V, Zheng W, et al. Pannexin 1 forms an anion-selective channel. *Pflugers Arch Eur J Physiol*. 2012;463(4):585-592. doi:10.1007/s00424-012-1077-z

4. Panchin Y, Kelmanson I, Matz M, Lukyanov K, Usman N, Lukyanov S. A ubiquitous family of putative gap junction molecules. *Curr Biol*. 2000;10(13). doi:10.1016/S0960-9822(00)00576-5

5. Sosinsky GE, Boassa D, Dermietzel R, et al. Pannexin channels are not gap junction hemichannels. *Channels*. 2011;5(3). doi:10.4161/chan.5.3.15765

6. Yen MR, Saier MH. Gap junctional proteins of animals: The innexin/pannexin superfamily. *Prog Biophys Mol Biol*. 2007;94(1-2):5-14. doi:10.1016/j.pbiomolbio.2007.03.006

7. Langlois S, Cowan KN. Regulation of skeletal muscle myoblast differentiation and proliferation by pannexins. *Advs Exp Med Biol Respir*. 2016;6:57-66. doi:10.1007/5584

8. Penuela S, Harland L, Simek J, Laird DW. Pannexin channels and their links to human disease. *Biochem J*. 2014;461(3):371-381. doi:10.1042/BJ20140447

9. Penuela S, Laird DW. The cellular life of pannexins. *Wiley Interdiscip Rev Membr Transp Signal*. 2012;1(5):621-632. doi:10.1002/wmts.63

10. Langlois S, Xiang X, Young K, Cowan BJ, Penuela S, Cowan KN. Pannexin 1 and pannexin 3 channels regulate skeletal muscle myoblast proliferation and differentiation. *J Biol Chem*. 2014;289(44):30717-30731. doi:10.1074/jbc.M114.572131

11. Iwamoto T, Nakamura T, Doyle A, et al. Pannexin 3 regulates intracellular ATP/cAMP levels and promotes chondrocyte differentiation. *J Biol Chem*. 2010;285(24):18948-18958. doi:10.1074/jbc.M110.127027

12. Penuela S, Kelly JJ, Churko JM, Barr KJ, Berger AC, Laird DW. Panx1 regulates cellular properties of keratinocytes and dermal fibroblasts in skin development and wound healing. *J Invest Dermatol*. 2014;134(7):2026-2035. doi:10.1038/jid.2014.86

13. Ishikawa M, Iwamoto T, Fukumoto S, Yamada Y. Pannexin 3 inhibits proliferation of osteoprogenitor cells by regulating Wnt and p21 signaling. *J Biol Chem*. 2014;289(5):2839-2851. doi:10.1074/jbc.M113.523241

14. Celetti SJ, Cowan KN, Penuela S, Shao Q, Churko J, Laird DW. Implications of pannexin 1 and pannexin 3 for keratinocyte differentiation. *J Cell Sci*. 2010;123(8):1363-1372. doi:10.1242/jcs.056093

15. Le Vasseur M, Lelowski J, Bechberger JF, Sin WC, Naus CC. Pannexin 2 protein expression is not restricted to the CNS. *Front Cell Neurosci*. 2014;8(392). doi:10.3389/fncel.2014.00392

16. Swayne LA, Sorbara CD, Bennett SAL. Pannexin 2 is expressed by postnatal hippocampal neural progenitors and modulates neuronal commitment. *J Biol Chem*. 2010;285(32):24977-24986. doi:10.1074/jbc.M110.130054

17. Zhou KQ, Green CR, Bennet L, Gunn AJ, Davidson JO. The role of connexin and pannexin channels in perinatal brain injury and inflammation. *Front Physiol*. 2019;10. doi:10.3389/fphys.2019.00141

18. Makarenkova HP, Shestopalov VI. The role of pannexin hemichannels in inflammation and regeneration. *Front Physiol*. 2014;5. doi:10.3389/fphys.2014.00063

19. Li L, He L, Wu D, Chen L, Jiang Z. Pannexin-1 channels and their emerging functions in cardiovascular diseases. *Acta Biochim Biophys Sin (Shanghai)*. 2015;47(6):391-396. doi:10.1093/abbs/gmv028

20. Song F, Sun H, Wang Y, et al. Pannexin3 inhibits TNF-α-induced inflammatory response by suppressing NF-κB signalling pathway in human dental pulp cells. *J Cell Mol Med*. 2017;21(3):444-455. doi:10.1111/jcmm.12988

21. Pham TL, St-Pierre ME, Ravel-Chapuis A, et al. Expression of Pannexin 1 and Pannexin 3 during skeletal muscle development, regeneration, and Duchenne muscular dystrophy. *J Cell Physiol*. 2018;233(10):7057-7070. doi:10.1002/jcp.26629

22. Buvinic S, Almarza G, Bustamante M, et al. ATP released by electrical stimuli elicits calcium transients and gene expression in skeletal muscle. *J Biol Chem*. 2009;284(50):34490-34505. doi:10.1074/jbc.M109.057315

23. Riquelme MA, Cea LA, Vega JL, et al. The ATP required for potentiation of skeletal muscle contraction is released via pannexin hemichannels. *Neuropharmacology*. 2013;75:594-603. doi:10.1016/j.neuropharm.2013.03.022

24. DeLalio LJ, Billaud M, Ruddiman CA, et al. Constitutive SRC-mediated phosphorylation of pannexin 1 at tyrosine 198 occurs at the plasma membrane. *J Biol Chem*. 2019;294(17):6940-6956. doi:10.1074/jbc.RA118.006982

25. Bhalla-Gehi R, Penuela S, Churko JM, Shao Q, Laird DW. Pannexin1 and pannexin3 delivery, cell surface dynamics, and cytoskeletal interactions. *J Biol Chem*. 2010;285(12):9147-9160. doi:10.1074/jbc.M109.082008

26. Penuela S, Bhalla R, Nag K, Laird DW. Glycosylation regulates pannexin intermixing and cellular localization. *Mol Biol Cell*. 2009;20:4313-4323. doi:10.1091/mbc.E09

27. Penuela S, Bhalla R, Gong X-Q, et al. Pannexin 1 and pannexin 3 are glycoproteins that exhibit many distinct characteristics from the connexin family of gap junction proteins. *J Cell Sci*. 2007;120(21):3772-3783. doi:10.1242/jcs.009514

28. Epp AL, Ebert SN, Sanchez-Arias JC, Wicki-Stordeur LE, Boyce AKJ, Swayne LA. A novel motif in the proximal C-terminus of Pannexin 1 regulates cell surface localization. *Sci Rep*. 2019;9(1):1-12. doi:10.1038/s41598-019-46144-5

29. Wicki-Stordeur LE, Swayne LA. Panx1 regulates neural stem and progenitor cell behaviours associated with cytoskeletal dynamics and interacts with multiple cytoskeletal elements. *Cell Commun Signal*. 2013;11(1). doi:10.1186/1478-811X-11-62

30. Bruzzone R, Barbe MT, Jakob NJ, Monyer H. Pharmacological properties of homomeric and heteromeric pannexin hemichannels expressed in Xenopus oocytes. *J Neurochem*. 2005;92(5):1033-1043. doi:10.1111/j.1471-4159.2004.02947.x

31. Ambrosi C, Gassmann O, Pranskevich JN, et al. Pannexin1 and pannexin2 channels show quaternary similarities to connexons and different oligomerization numbers from each other. *J Biol Chem*. 2010;285(32):24420-24431. doi:10.1074/jbc.M110.115444

32. Weilinger NL, Lohman AW, Rakai BD, et al. Metabotropic NMDA receptor signaling couples Src family kinases to pannexin-1 during excitotoxicity. *Nat Neurosci*. 2016;19(3):432-442. doi:10.1038/nn.4236

33. Hornbeck P, Zhang B, Murray B, Kornhauser J, Latham V, Skrzypek E. PhosphoSitePlus, 2014: mutations, PTMs and recalibrations. *Nucleic Acids Res*. 2015;43:D512-20. https://www.phosphosite.org/homeAction.action.

34. Lohman AW, Weaver JL, Billaud M, et al. S-nitrosylation inhibits pannexin 1 channel function. *J Biol Chem*. 2012;287(47):39602-39612. doi:10.1074/jbc.M112.397976

35. Chekeni FB, Elliott MR, Sandilos JK, et al. Pannexin 1 channels mediate "find-me" signal release and membrane permeability during apoptosis. *Nature*. 2010;467(7317):863-867. doi:10.1038/nature09413

36. D'hondt C, Iyyathurai J, Vinken M, et al. Regulation of connexin- and pannexin-based channels by post-translational modifications. *Biol Cell*. 2013;105(9):373-398. doi:10.1111/boc.201200096

37. Penuela S, Lohman AW, Lai W, et al. Diverse post-translational modifications of the pannexin family of channel-forming proteins. *Channels*. 2014;8(2):124-130. doi:10.4161/chan.27422

38. Ishikawa M, Yamada Y. The Role of Pannexin 3 in bone biology. *J Dent Res*. 2017;96(4):372-379. doi:10.1177/0022034516678203

39. Xiang X, Langlois S, St-Pierre ME, et al. Pannexin 1 inhibits rhabdomyosarcoma progression through a mechanism independent of its canonical channel function. *Oncogenesis*. 2018;7(11). doi:10.1038/s41389-018-0100-4

40. Penuela S, Celetti SJ, Bhalla R, Shao Q, Laird DW. Diverse subcellular distribution profiles of pannexin1 and pannexin3. *Cell Commun Adhes*. 2008;15(1-2):133-142. doi:10.1080/15419060802014115

41. Boyce AKJ, Epp AL, Nagarajan A, Swayne LA. Transcriptional and post-translational regulation of pannexins. *Biochim Biophys Acta - Biomembr*. 2018;1860(1):72-82. doi:10.1016/j.bbamem.2017.03.004

42. Johnstone SR, Billaud M, Lohman AW, Taddeo EP, Isakson BE. Posttranslational modifications in connexins and pannexins. *J Membr Biol*. 2012;245(5-6):319-332. doi:10.1007/s00232-012-9453-3

43. Gehi R, Shao Q, Laird DW. Pathways regulating the trafficking and turnover of Pannexin1 protein and the role of the C-terminal domain. *J Biol Chem*. 2011;286(31):27639-27653. doi:10.1074/jbc.M111.260711

44. Jadhav T, Wooten MW. Defining an embedded code for protein ubiquitination. *J Proteomics Bioinforma*. 2009;2(7):316-333. doi:10.4172/jpb.1000091

45. Adhikari A, Chen ZJ. Diversity of polyubiquitin chains. *Dev Cell*. 2009;16(4):485-486. doi:10.1016/j.devcel.2009.04.001

46. Tanno H, Komada M. The ubiquitin code and its decoding machinery in the endocytic pathway. *J Biochem*. 2013;153(6):497-504. doi:10.1093/jb/mvt028

47. Clague MJ, Heride C, Urbé S. The demographics of the ubiquitin system. *Trends Cell Biol*. 2015;25(7):417-426. doi:10.1016/j.tcb.2015.03.002

48. Stewart MD, Ritterhoff T, Klevit RE, Brzovic PS. E2 enzymes: More than just middle men. *Cell Res*. 2016;26(4):423-440. doi:10.1038/cr.2016.35

49. Coyne ES, Wing SS. The business of deubiquitination – location, location, location. *F1000Research*. 2016;5:163. doi:10.12688/f1000research.7220.1

50. Morreale FE, Walden H. Types of ubiquitin ligases. *Cell*. 2016;165(1):248-248.e1. doi:10.1016/j.cell.2016.03.003

51. Ikeda K, Inoue S. Trim proteins as ring finger E3 ubiquitin ligases. *Adv Exp Med Biol*. 2012;770:27-37. doi:10.1007/978-1-4614-5398-7_3

52. Zheng N, Shabek N. Ubiquitin ligases: Structure, function, and regulation. *Annu Rev Biochem*. 2017;86(1):129-157. doi:10.1146/annurev-biochem-060815-014922

53. Akutsu M, Dikic I, Bremm A. Ubiquitin chain diversity at a glance. *J Cell Sci*. 2016;129(5):875-880. doi:10.1242/jcs.183954

54. Ohtake F, Tsuchiya H. JB special review - Recent topics in ubiquitin-proteasome system and autophagy: The emerging complexity of ubiquitin architecture. *J Biochem*. 2017;161(2):125-133. doi:10.1093/jb/mvw088

55. Ciechanover A. The ubiquitin–proteasome pathway on protein. *EMBO J*. 1998;17(24):7151-7160.

56. Tasaki T, Zakrzewska A, Dudgeon DD, Jiang Y, Lazo JS, Kwon YT. The substrate recognition domains of the N-end rule pathway. *J Biol Chem*. 2009;284(3):1884-1895. doi:10.1074/jbc.M803641200

57. Hegazi S, Levine JD, Cheng H-YM. UBR4 (Ubiquitin Ligase E3 Component N-Recognin 4). In: *Encyclopedia of Signaling Molecules*. Springer International Publishing; 2018:5824-5830. doi:10.1007/978-3-319-67199-4_101766

58. Yau RG, Doerner K, Castellanos ER, et al. Assembly and function of heterotypic ubiquitin chains in cell-cycle and protein quality control. *Cell*. 2017;171(4):918-933.e20. doi:10.1016/j.cell.2017.09.040

59. Piper RC, Dikic I, Lukacs GL. Ubiquitin-dependent sorting in endocytosis . PubMed Commons. *Cold Spring Harb Perspect Biol*. 2016;6(1):24384571. doi:10.1101/cshperspect.a016808.Ubiquitin-dependent

60. Hunter T. The age of crosstalk: phosphorylation, ubiquitination, and beyond. *Mol Cell*. 2007;28(5):730-738. doi:10.1016/j.molcel.2007.11.019

61. Komander D, Rape M. The ubiquitin code. *Annu Rev Biochem*. 2012;81(1):203-229. doi:10.1146/annurev-biochem-060310-170328

62. Abdul Rehman SA, Kristariyanto YA, Choi SY, et al. MINDY-1 is a member of an evolutionarily conserved and structurally distinct new family of deubiquitinating enzymes. *Mol Cell*. 2016;63(1):146-155. doi:10.1016/j.molcel.2016.05.009

63. Livneh I, Kravtsova-Ivantsiv Y, Braten O, Kwon YT, Ciechanover A. Monoubiquitination joins polyubiquitination as an esteemed proteasomal targeting signal. *BioEssays*. 2017;39(6):1-7. doi:10.1002/bies.201700027

64. Jacobson AD, Zhang NY, Xu P, et al. The lysine 48 and lysine 63 ubiquitin conjugates are processed differently by the 26 S proteasome. *J Biol Chem*. 2009;284(51):35485-35494. doi:10.1074/jbc.M109.052928

65. Mukhopadhyay D, Riezman H. Proteasome-independent functions of ubiquitin in endocytosis and signaling. *Science (80-)*. 2007;315(5809):201-205. doi:10.1126/science.1127085

66. Liu Q, Wu Y, Qin Y, et al. Broad and diverse mechanisms used by deubiquitinase family members in regulating the type i interferon signaling pathway during antiviral responses. *Sci Adv*. 2018;4(5):1-14. doi:10.1126/sciadv.aar2824

67. Nicassio F, Corrado N, Vissers JHA, et al. Human USP3 is a chromatin modifier required for S phase progression and genome stability. *Curr Biol*. 2007;17(22):1972-1977. doi:10.1016/j.cub.2007.10.034

68. Fu S, Shao S, Wang L, et al. USP3 stabilizes p53 protein through its deubiquitinase activity. *Biochem Biophys Res Commun*. 2017;492(2):178-183. doi:10.1016/j.bbrc.2017.08.036

69. Cappadocia L, Lima CD. Ubiquitin-like protein conjugation: structures, chemistry, and mechanism. *Chem Rev*. 2018;118(3):889-918. doi:10.1021/acs.chemrev.6b00737

70. Lu LS, Yeh ETH. Ubiquitin-like proteins. *Encycl Biol Chem Second Ed*. 2013:467-472. doi:10.1016/B978-0-12-378630-2.00068-2

71. Wang XJ, Yu J, Wong SH, et al. A novel crosstalk between two major protein degradation systems. *Autophagy*. 2013;9(10):1500-1508. doi:10.4161/auto.25573

72. Wang Y, Dasso M. SUMOylation and deSUMOylation at a glance. *J Cell Sci*. 2009;122(23):4249-4252. doi:10.1242/jcs.050542

73. Han HG, Moon HW, Jeon YJ. ISG15 in cancer: Beyond ubiquitin-like protein. *Cancer Lett*. 2018;438:52-62. doi:10.1016/j.canlet.2018.09.007

74. Swatek KN, Komander D. Ubiquitin modifications. *Cell Res*. 2016;26(4):399-422. doi:10.1038/cr.2016.39

75. Ruggiano A, Foresti O, Carvalho P. ER-associated degradation: Protein quality control and beyond. *J Cell Biol*. 2014;204(6):869-879. doi:10.1083/jcb.201312042

76. Wollert T. Autophagy. *Curr Biol*. 2019;29(14):R671-R677. doi:10.1016/j.cub.2019.06.014

77. Alvarez-Castelao B, Ruiz-Rivas C, Castaño JG. A critical appraisal of quantitative studies of protein degradation in the framework of cellular proteostasis. *Biochem Res Int*. 2012;2012(823597):1-11. doi:10.1155/2012/823597

78. Clague MJ, Urbé S. Ubiquitin: Same molecule, different degradation pathways. *Cell*. 2010;143(5):682-685. doi:10.1016/j.cell.2010.11.012

79. Schrader EK, Harstad KG, Matouschek A. Targeting proteins for degradation. *Nat Chem Biol*. 2009;5(11):815-822. doi:10.1038/nchembio.250

80. Frankel EB, Audhya A. ESCRT-dependent cargo sorting at multivesicular endosomes. *Semin Cell Dev Biol*. 2018;74(608):4-10. doi:10.1016/j.semcdb.2017.08.020

81. Grumati P, Dikic I. Ubiquitin signaling and autophagy. *J Biol Chem*. 2018;293(15):5404-5413. doi:10.1074/jbc.TM117.000117

82. Livneh I, Cohen-Kaplan V, Cohen-Rosenzweig C, Avni N, Ciechanover A. The life cycle of the 26S proteasome: From birth, through regulation and function, and onto its death. *Cell Res*. 2016;26(8):869-885. doi:10.1038/cr.2016.86

83. Tanaka K. The proteasome: Overview of structure and functions. *Proc Japan Acad Ser B Phys Biol Sci*. 2009;85(1):12-36. doi:10.2183/pjab.85.12

84. Finley D. Recognition and processing of ubiquitin-protein conjugates by the proteasome. *Annu Rev Biochem*. 2009;78:477-513. doi:10.1146/annurev.biochem.78.081507.101607

85. Staub O, Gautschi I, Ishikawa T, et al. Regulation of stability and function of the epithelial Na+ channel (ENaC) by ubiquitination. *EMBO J*. 1997;16(21):6325-6336. doi:10.1093/emboj/16.21.6325

86. Marangoudakis S, Andrade A, Helton TD, Denome S, Castiglioni AJ, Lipscombe D. Differential ubiquitination and proteasome regulation of Ca v2.2 N-type channel splice isoforms. *J Neurosci*. 2012;32(30):10365-10369. doi:10.1523/JNEUROSCI.0851-11.2012

87. Ward CL, Omura S, Kopito RR. Degradation of CFTR by the ubiquitin-proteasome pathway. *Cell*. 1995;83(1):121-127. doi:10.1016/0092-8674(95)90240-6

88. Boehmer C, Laufer J, Jeyaraj S, et al. Modulation of the voltage-gated potassium channel Kv1.5 by the SGK1 protein kinase involves inhibition of channel ubiquitination. *Cell Physiol Biochem*. 2008;22(5-6):591-600. doi:10.1159/000185543

89. Needham PG, Guerriero CJ, Brodsky JL. Chaperoning endoplasmic reticulum–associated degradation (ERAD) and protein conformational diseases. *Cold Spring Harb Perspect Biol*. 2019;11(8):a033928. doi:10.1101/cshperspect.a033928

90. Fregno I, Molinari M. Proteasomal and lysosomal clearance of faulty secretory proteins: ER-associated degradation (ERAD) and ER-to-lysosome-associated degradation (ERLAD) pathways. *Crit Rev Biochem Mol Biol*. 2019;54(2):153-163. doi:10.1080/10409238.2019.1610351

91. Mehrtash AB, Hochstrasser M. Ubiquitin-dependent protein degradation at the endoplasmic reticulum and nuclear envelope. *Semin Cell Dev Biol*. 2018;(September):0-1. doi:10.1016/j.semcdb.2018.09.013

92. Ellinger I, Ellinger A. Smallest unit of life: Cell biology. In: *Comparative Medicine*. Vienna: Springer Vienna; 2014:19-33. doi:10.1007/978-3-7091-1559-6_2

93. Elkin SR, Lakoduk AM, Schmid SL. Endocytic pathways and endosomal trafficing: a primer. *Wien Med Wochenschr*. 2016;166(7-8):196-204. doi:10.1016/j.physbeh.2017.03.040

94. Cullen PJ, Steinberg F. To degrade or not to degrade: mechanisms and significance of endocytic recycling. *Nat Rev Mol Cell Biol*. 2018;19(11):679-696. doi:10.1038/s41580-018-0053-7

95. Nijman SMB, Luna-Vargas MPA, Velds A, et al. A genomic and functional inventory of deubiquitinating enzymes. *Cell*. 2005;123(5):773-786. doi:10.1016/j.cell.2005.11.007

96. Khaminets A, Behl C, Dikic I. Ubiquitin-dependent and independent signals in selective autophagy. *Trends Cell Biol*. 2016;26(1):6-16. doi:10.1016/j.tcb.2015.08.010

97. Gamerdinger M, Kaya AM, Wolfrum U, Clement AM, Behl C. BAG3 mediates chaperone-based aggresome-targeting and selective autophagy of misfolded proteins. *EMBO Rep*. 2011;12(2):149-156. doi:10.1038/embor.2010.203

98. Minoia M, Boncoraglio A, Vinet J, et al. BAG3 induces the sequestration of proteasomal clients into cytoplasmic puncta Implications for a proteasome-to-autophagy switch. *Autophagy*. 2014;10(9):1603-1621. doi:10.4161/auto.29409

99. Gatica D, Lahiri V, Klionsky DJ. Cargo recognition and degradation by selective autophagy. *Nat Cell Biol*. 2018;20(3):233-242. doi:10.1038/s41556-018-0037-z

100. Demishtein A, Fraiberg M, Berko D, Tirosh B, Elazar Z, Navon A. SQSTM1/p62-mediated

autophagy compensates for loss of proteasome polyubiquitin recruiting capacity. *Autophagy*. 2017;13(10):1697-1708. doi:10.1080/15548627.2017.1356549

101. Shaid S, Brandts CH, Serve H, Dikic I. Ubiquitination and selective autophagy. *Cell Death Differ*. 2013;20(1):21-30. doi:10.1038/cdd.2012.72

102. Sisinni L, Pietrafesa M, Lepore S, et al. Endoplasmic reticulum stress and unfolded protein response in breast cancer: The balance between apoptosis and autophagy and its role in drug resistance. *Int J Mol Sci*. 2019;20(4):857. doi:10.3390/ijms20040857

103. Leithe E. Regulation of connexins by the ubiquitin system: Implications for intercellular communication and cancer. *Biochim Biophys Acta - Rev Cancer*. 2016;1865(2):133-146. doi:10.1016/j.bbcan.2016.02.001

104. Fong JT, Kells RM, Falk MM. Two tyrosine-based sorting signals in the Cx43 C-terminus cooperate to mediate gap junction endocytosis. *Mol Biol Cell*. 2013;24(18):2834-2848. doi:10.1091/mbc.E13-02-0111

105. Su V, Lau AF. Ubiquitination, intracellular trafficking, and degradation of connexins. *Bone*. 2012;23(1):1-7. doi:10.1038/jid.2014.371

106. Sun J, Hu Q, Peng H, et al. The ubiquitin-specific protease USP8 deubiquitinates and stabilizes Cx43. *J Biol Chem*. 2018;293(21):8275-8284. doi:10.1074/jbc.RA117.001315

107. Sánchez-Sánchez J, Arévalo JC. A review on ubiquitination of neurotrophin receptors: Facts and perspectives. *Int J Mol Sci*. 2017;18(3). doi:10.3390/ijms18030630

108. Singh R, Karri D, Shen H, et al. TRAF4-mediated ubiquitination of NGF receptor TrkA regulates prostate cancer metastasis. *J Clin Invest*. 2018;128(7):3129-3143. doi:10.1172/JCI96060

109. Geetha T, Jiang J, Wooten MW. Lysine 63 polyubiquitination of the nerve growth factor receptor TrkA directs internalization and signaling. *Mol Cell*. 2005;20(2):301-312. doi:10.1016/j.molcel.2005.09.014

110. Geetha T, Seibenhener ML, Chen L, Madura K, Wooten MW. p62 serves as a shuttling factor for TrkA interaction with the proteasome. *Biochem Biophys Res Commun*. 2008;374(1):33-37. doi:10.1016/j.bbrc.2008.06.082

111. Georgieva M V., De Pablo Y, Sanchis D, Comella JX, Llovera M. Ubiquitination of TrkA by Nedd4-2 regulates receptor lysosomal targeting and mediates receptor signaling. *J Neurochem*. 2011;117(3):479-493. doi:10.1111/j.1471-4159.2011.07218.x

112. Ceriani M, Amigoni L, D'Aloia A, Berruti G, Martegani E. The deubiquitinating enzyme UBPy/USP8 interacts with TrkA and inhibits neuronal differentiation in PC12 cells. *Exp Cell Res*. 2015;333(1):49-59. doi:10.1016/j.yexcr.2015.01.019

113. Udeshi ND, Svinkina T, Mertins P, et al. Refined preparation and use of anti-diglycine remnant (k-ε-gg) antibody enables routine quantification of 10,000s of ubiquitination sites in single proteomics experiments. *Mol Cell Proteomics*. 2013;12(3):825-831. doi:10.1074/mcp.O112.027094

114. Mertins P, Qiao JW, Patel J, et al. Integrated proteomic analysis of post-translational modifications by serial enrichment. *Nat Methods*. 2013;10(7):634-637. doi:10.1038/nmeth.2518

115. Boeing S, Williamson L, Encheva V, et al. Multiomic analysis of the UV-induced DNA damage response. *Cell Rep*. 2016;15(7):1597-1610. doi:10.1016/j.celrep.2016.04.047

116. Kim W, Bennett EJ, Huttlin EL, et al. Systematic and quantitative assessment of the ubiquitin-

modified proteome. *Mol Cell*. 2011;44(2):325-340. doi:10.1016/j.molcel.2011.08.025

117. Cowan KN, Langlois S, Penuela S, Cowan BJ, Laird DW. Pannexin1 and Pannexin3 exhibit distinct localization patterns in human skin appendages and are regulated during keratinocyte differentiation and carcinogenesis. *Cell Commun Adhes*. 2012;19(3-4):45-53. doi:10.3109/15419061.2012.712575

118. Choo YS, Zhang Z. Detection of protein ubiquitination. *J Vis Exp*. 2009;(30):10-11. doi:10.3791/1293

119. Roux KJ, Kim DI, Burke B. BioID: A screen for protein-protein interactions. *Curr Protoc Protein Sci*. 2013;(SUPPL.74):1-14. doi:10.1002/0471140864.ps1923s74

120. Marín I. The ubiquilin gene family: Evolutionary patterns and functional insights. *BMC Evol Biol*. 2014;14(1):1-22. doi:10.1186/1471-2148-14-63

121. Schuberth C, Buchberger A. UBX domain proteins: Major regulators of the AAA ATPase Cdc48/p97. *Cell Mol Life Sci*. 2008;65(15):2360-2371. doi:10.1007/s00018-008-8072-8

122. Medvar B, Raghuram V, Pisitkun T, Sarkar A, Knepper MA. Comprehensive database of human E3 ubiquitin ligases: application to aquaporin-2 regulation. *Physiol Genomics*. 2016;48(7):502-512. doi:10.1152/physiolgenomics.00031.2016

123. Leznicki P, Kulathu Y. Mechanisms of regulation and diversification of deubiquitylating enzyme function. *J Cell Sci*. 2017;130(12):1997-2006. doi:10.1242/jcs.201855

124. Buchanan BW, Lloyd ME, Engle SM, Rubenstein EM. Cycloheximide chase analysis of protein degradation in Saccharomyces cerevisiae. *J Vis Exp*. 2016;2016(110). doi:10.3791/53975

125. Ding WX, Ni HM, Gao W, et al. Linking of autophagy to ubiquitin-proteasome system is important for the regulation of endoplasmic reticulum stress and cell viability. *Am J Pathol*. 2007;171(2):513-524. doi:10.2353/ajpath.2007.070188

126. Obeng EA, Carlson LM, Gutman DM, Harrington WJ, Lee KP, Boise LH. Proteasome inhibitors induce a terminal unfolded protein response in multiple myeloma cells. *Blood*. 2006;107(12):4907-4916. doi:10.1182/blood-2005-08-3531

127. Wang D, Xu Q, Yuan Q, et al. Proteasome inhibition boosts autophagic degradation of ubiquitinated-AGR2 and enhances the antitumor efficiency of bevacizumab. *Oncogene*. 2019;38(18):3458-3474. doi:10.1038/s41388-019-0675-z

128. Chan WM. Ubiquitination of p53 at multiple sites in the DNA-binding domain. *Mol Cancer Res*. 2006;4(1):15-25. doi:10.1158/1541-7786.mcr-05-0097

129. Bustos D, Bakalarski CE, Yang Y, Peng J, Kirkpatrick DS. Characterizing ubiquitination sites by peptide-based immunoaffinity enrichment. *Mol Cell Proteomics*. 2012;11(12):1529-1540. doi:10.1074/mcp.R112.019117

130. Stringer DK, Piper RC. Terminating protein ubiquitination. *Cell Cycle*. 2011;10(18):3067-3071. doi:10.4161/cc.10.18.17191

131. Nawaz Z, Lonard DM, Dennis AP, Smith CL, O'Malley BW. Proteasome-dependent degradation of the human estrogen receptor. *Proc Natl Acad Sci U S A*. 1999;96(5):1858-1862. doi:10.1073/pnas.96.5.1858

132. Mallik S, Kundu S. Topology and oligomerization of mono- and oligomeric proteins regulate their half-lives in the cell. *Structure*. 2018;26(6):869-878.e3. doi:10.1016/j.str.2018.04.015

133. Buchler NE, Gerland U, Hwa T. Nonlinear protein degradation and the function of genetic circuits. *Proc Natl Acad Sci U S A*. 2005;102(27):9559-9564. doi:10.1073/pnas.0409553102

134. McShane E, Sin C, Zauber H, et al. Kinetic analysis of protein stability Reveals age-dependent degradation. *Cell*. 2016;167(3):803-815.e21. doi:10.1016/j.cell.2016.09.015

135. Jin EJ, Kiral FR, Hiesinger PR. The where, what, and when of membrane protein degradation in neurons. *Dev Neurobiol*. 2018;78(3):283-297. doi:10.1002/dneu.22534

136. Fabre B, Lambour T, Delobel J, et al. Subcellular distribution and dynamics of active proteasome complexes unraveled by a workflow combining in vivo complex cross-linking and quantitative proteomics. *Mol Cell Proteomics*. 2013;12(3):687-699. doi:10.1074/mcp.M112.023317

137. Kato H, Sakaki K, Mihara K. Ubiquitin-proteasome-dependent degradation of mammalian ER stearoyl-CoA desaturase. *J Cell Sci*. 2006;119(11):2342-2353. doi:10.1242/jcs.02951

138. Boassa D, Ambrosi C, Qiu F, et al. Pannexin1 channels contain a glycosylation site that targets the hexamer to the plasma membrane. *J Biol Chem*. 2007;282(43):31733-31743. doi:10.1074/jbc.M702422200

139. Liang J, Yin C, Doong H, et al. Characterization of erasin (UBXD2): A new ER protein that promotes ER-associated protein degradation. *J Cell Sci*. 2006;119(19):4011-4024. doi:10.1242/jcs.03163

140. Lim PJ, Danner R, Liang J, et al. Ubiquilin and p97/VCP bind erasin, forming a complex involved in ERAD. *J Cell Biol*. 2009;187(2):201-217. doi:10.1083/jcb.200903024

141. Klemm EJ, Spooner E, Ploegh HL. Dual role of Ancient Ubiquitous Protein 1 (AUP1) in lipid droplet accumulation and Endoplasmic Reticulum (ER) protein quality control. *J Biol Chem*. 2011;286(43):37602-37614. doi:10.1074/jbc.M111.284794

142. Wang Q, Shinkre BA, Lee J gu, et al. The ERAD inhibitor eeyarestatin I is a bifunctional compound with a membrane-binding domain and a p97/VCP inhibitory group. *PLoS One*. 2010;5(11). doi:10.1371/journal.pone.0015479

143. Dörrbaum AR, Kochen L, Langer JD, Schuman EM. Local and global influences on protein turnover in neurons and glia. *Elife*. 2018;7:1-24. doi:10.7554/eLife.34202

144. Mathieson T, Franken H, Kosinski J, et al. Systematic analysis of protein turnover in primary cells. *Nat Commun*. 2018;9(1):1-10. doi:10.1038/s41467-018-03106-1

145. Yewdell JW, Lacsina JR, Rechsteiner MC, Nicchitta C V. Out with the old, in with the new? Comparing methods for measuring protein degradation. *Cell Biol Int*. 2011;35(5):457-462. doi:10.1042/CBI20110055

146. Kang S, Mays CE, Daude N, Yang J, Kar S, Westaway D. Proteasomal inhibition redirects the PrP-like Shadoo protein to the nucleus. *Mol Neurobiol*. 2019;56(11):7888–7904. doi:10.1007/s12035-019-1623-1

147. Drisaldi B, Stewart RS, Adles C, et al. Mutant PrP is delayed in its exit from the endoplasmic reticulum, but neither wild-type nor mutant PrP undergoes retrotranslocation prior to proteasomal degradation. *J Biol Chem*. 2003;278(24):21732-21743. doi:10.1074/jbc.M213247200

148. Butler JE, Moore MB, Presnell SR, Chan H-W, Chalupny NJ, Lutz CT. Proteasome regulation of ULBP1 transcription. *J Immunol*. 2009;182(10):6600-6609. doi:10.4049/jimmunol.0801214

149. Park HS, Jun DY, Han CR, Woo HJ, Kim YH. Proteasome inhibitor MG132-induced apoptosis via

ER stress-mediated apoptotic pathway and its potentiation by protein tyrosine kinase p56 lck in human Jurkat T cells. *Biochem Pharmacol*. 2011;82(9):1110-1125. doi:10.1016/j.bcp.2011.07.085

150. Bao W, Gu Y, Ta L, Wang K, Xu Z. Induction of autophagy by the MG-132 proteasome inhibitor is associated with endoplasmic reticulum stress in MCF-7 cells. *Mol Med Rep*. 2016;13(1):796-804. doi:10.3892/mmr.2015.4599

151. López-Otín C, Overall CM. Protease degradomics: A new challenge for proteomics. *Nat Rev Mol Cell Biol*. 2002;3(7):509-519. doi:10.1038/nrm858

152. Klein T, Eckhard U, Dufour A, Solis N, Overall CM. Proteolytic cleavage—mechanisms, function, and "omic" approaches for a near-ubiquitous posttranslational modification. *Chem Rev*. 2018;118(3):1137-1168. doi:10.1021/acs.chemrev.7b00120

153. Lichtenthaler SF, Lemberg MK, Fluhrer R. Proteolytic ectodomain shedding of membrane proteins in mammals—hardware, concepts, and recent developments. *EMBO J*. 2018;37(15):1-24. doi:10.15252/embj.201899456

154. Kühnle N, Dederer V, Lemberg MK. Intramembrane proteolysis at a glance: from signalling to protein degradation. *J Cell Sci*. 2019;132(16). doi:10.1242/jcs.217745

155. Seals DF, Courtneidge SA. The ADAMs family of metalloproteases: Multidomain proteins with multiple functions. *Genes Dev*. 2003;17(1):7-30. doi:10.1101/gad.1039703

156. Iben LG, Olson RE, Balanda LA, et al. Signal peptide peptidase and γ-secretase share equivalent inhibitor binding pharmacology. *J Biol Chem*. 2007;282(51):36829-36836. doi:10.1074/jbc.M707002200

157. Molina MA, Codony-Servat J, Albanell J, Rojo F, Arribas J, Baselga J. Trastuzumab (Herceptin), a humanized anti-HER2 receptor monoclonal antibody, inhibits basal and activated HER2 ectodomain cleavage in breast cancer cells. *Cancer Res*. 2001;61(12):4744-4749.

158. Reyes A, Huber W. Alternative start and termination sites of transcription drive most transcript isoform differences across human tissues. *Nucleic Acids Res*. 2018;46(2):582-592. doi:10.1093/nar/gkx1165

159. Katzenberger RJ, Marengo MS, Wassarman DA. Control of alternative splicing by signal-dependent degradation of splicing-regulatory proteins. *J Biol Chem*. 2009;284(16):10737-10746. doi:10.1074/jbc.M809506200

160. Anido J, Scaltriti M, Bech Serra JJ, et al. Biosynthesis of tumorigenic HER2 C-terminal fragments by alternative initiation of translation. *EMBO J*. 2006;25(13):3234-3244. doi:10.1038/sj.emboj.7601191

161. Baranova A, Ivanov D, Petrash N, et al. The mammalian pannexin family is homologous to the invertebrate innexin gap junction proteins. *Genomics*. 2004;83(4):706-716. doi:10.1016/j.ygeno.2003.09.025

162. Li S, Tomić M, Stojilkovic SS. Characterization of novel Pannexin 1 isoforms from rat pituitary cells and their association with ATP-gated P2X channels. *Gen Comp Endocrinol*. 2011;174(2):202-210. doi:10.1016/j.ygcen.2011.08.019

163. Nguyen KT, Mun SH, Lee CS, Hwang CS. Control of protein degradation by N-terminal acetylation and the N-end rule pathway. *Exp Mol Med*. 2018;50(7). doi:10.1038/s12276-018-0097-y

164. Ashton-Beaucage D, Lemieux C, Udell CM, Sahmi M, Rochette S, Therrien M. The deubiquitinase

USP47 stabilizes MAPK by counteracting the function of the N-end rule ligase POE/UBR4 in Drosophila. *PLoS Biol*. 2016;14(8):1-27. doi:10.1371/journal.pbio.1002539

165. Nakatani Y, Konishi H, Vassilev A, et al. P600, a unique protein required for membrane morphogenesis and cell survival. *Proc Natl Acad Sci U S A*. 2005;102(42):15093-15098. doi:10.1073/pnas.0507458102

166. Kim ST, Lee YJ, Tasaki T, et al. The N-recognin UBR4 of the N-end rule pathway is targeted to and required for the biogenesis of the early endosome. *J Cell Sci*. 2018;131(17):1-22. doi:10.1242/jcs.217646

167. Yeom J, Ju S, Choi YJ, Paek E, Lee C. Comprehensive analysis of human protein N-termini enables assessment of various protein forms. *Sci Rep*. 2017;7(1). doi:10.1038/s41598-017-06314-9

168. Ozin AJ, Costa T, Henriques AO, Moran J. Alternative translation initiation produces a short form of a spore coat protein in Bacillus subtilis. *J Bacteriol*. 2001;183(6):2032-2040. doi:10.1128/JB.183.6.2032-2040.2001

169. Leithe E, Kjenseth A, Sirnes S, Stenmark H, Brech A, Rivedal E. Ubiquitylation of the gap junction protein connexin-43 signals its trafficking from early endosomes to lysosomes in a process mediated by Hrs and Tsg101. *J Cell Sci*. 2009;122(21):3883-3893. doi:10.1242/jcs.053801

170. Katsuragi Y, Ichimura Y, Komatsu M. P62/SQSTM1 functions as a signaling hub and an autophagy adaptor. *FEBS J*. 2015;282(24):4672-4678. doi:10.1111/febs.13540

171. Klimek C, Kathage B, Wördehoff J, Höhfeld J. BAG3-mediated proteostasis at a glance. *J Cell Sci*. 2017;130(17):2781-2788. doi:10.1242/jcs.203679

172. Ruggiano A, Foresti O, Carvalho P. ER-associated degradation: Protein quality control and beyond. *J Cell Biol*. 2014;204(6):869-879. doi:10.1083/jcb.201312042

173. Li CW, Lim SO, Xia W, et al. Glycosylation and stabilization of programmed death ligand-1 suppresses T-cell activity. *Nat Commun*. 2016;7. doi:10.1038/ncomms12632

174. Suzuki S, Shuto T, Sato T, et al. Inhibition of post-translational N-glycosylation by HRD1 that controls the fate of ABCG5/8 transporter. *Sci Rep*. 2014;4:1-14. doi:10.1038/srep04258

175. Yoshida Y, Chiba T, Tokunaga F, et al. E3 ubiquitin ligase that recognizes sugar chains. *Nature*. 2002;418(6896):438-442. doi:10.1038/nature00890

176. Cooper JA, Kaneko T, Li SSC. Cell regulation by phosphotyrosine-targeted ubiquitin ligases. *Mol Cell Biol*. 2015;35(11):1886-1897. doi:10.1128/mcb.00098-15

177. Minoia M, Boncoraglio A, Vinet J, et al. BAG3 induces the sequestration of proteasomal clients into cytoplasmic puncta Implications for a proteasome-to-autophagy switch. *Autophagy*. 2014;10(9):1603-1621. doi:10.4161/auto.29409

178. Wu WKK, Wu YC, Yu L, Li ZJ, Sung JJY, Cho CH. Induction of autophagy by proteasome inhibitor is associated with proliferative arrest in colon cancer cells. *Biochem Biophys Res Commun*. 2008;374(2):258-263. doi:10.1016/j.bbrc.2008.07.031